The Role of Ldb1 in ErbB2/Neu-induced Mammary Tumorigenesis

By

Sarra Ahmed

This thesis is submitted as a partial fulfillment of the M.Sc. program in Cellular and Molecular Medicine

Department of Cellular and Molecular Medicine

Faculty of Medicine

University of Ottawa

June 2015

ABSTRACT

The ste-20 like kinase (SLK) is a serine/threonine kinase activated downstream of Neu signaling and functions to mediate efficient migration and invasion of breast cancer cells. Previously, the LIM domain binding protein 1 (Ldb1) has been identified as a negative regulator of SLK kinase activity in MEF3T3 fibroblasts. Ldb1 is a transcriptional cofactor required for normal mouse embryonic development. In the current study we sought to assess the effect of mammary gland-specific Ldb1 deletion on SLK activity and metastasis in a Neu-overexpressing breast cancer model, the MMTV-NIC mouse model. Our results show that Ldb1 deletion does not affect SLK activity in Neu-induced tumors as demonstrated by in-vitro kinase assays. Also, Ldb1 deletion in the mammary epithelium of the MMTV-NIC model does not affect Neu-mediated tumor growth or overall survival. Due to the low incidence of spontaneous metastasis in the model, we performed tail-vein lung colonization assays and found that Ldb1 deletion significantly inhibits the lung colonization capability of primary tumor cells. Taken together, our findings highlight the important implications of understanding Ldb1-mediated transcriptional activity in Neu-overexpressing breast tumors as it could offer therapeutic opportunity to limit the spread of metastatic Neu-induced breast cancers.

TABLE OF CONTENTS

LIST OF TABLES

LIST OF FIGURES

LIST OF ABBREVIATIONS

ATH	AT1-46 homology
Clim	Carboxyl terminal LIM-domain binding protein
Cre	Cre-recombinase
DD	Dimerization domain
DN-Ldb	Dominant negative Ldb mutant
EGFR	Epidermal growth factor receptor
ER	Estrogen receptor
ErbB2	Erythroblastic Leukemia Viral Oncogene Homolog 2
FAK	Focal adhesion kinase
HER2	Human epidermal growth factor receptor 2
HRGβ1	Heregulin β1
IF	Immunofluorescence
IRES	Internal ribosomal entry sequence
LIM-HD	LIM homeodomain
LCCD	Ldb1/Chip conserved domain
LDB	LIM domain binding protein
LID	LIM interaction domain
LMO	LIM only protein
MAPK	Mitogen activated protein kinase
MEK	Mitogen-activated protein kinase kinase
MMTV	Mouse mammary tumor virus
NDL	Neu deletion

NIC	NEU-IRES-CRE
NLS	Nuclear localization sequence
PCR	Polymerase chain reaction
PI3K	Phosphatidylinositol 3-Kinase
PLCγ	Phosphoinositide phospholipase C
PR	Progesterone receptor
SFK	Src Family Kinase
shRNA	Short hairpin RNA
siRNA	Short interfering RNA
SLK	Ste-20 like kinase
TMA	Tissue microarray

ACKNOWLEDGEMENTS

I would like to thank my supervisor Dr. Luc Sabourin for providing me with the opportunity to pursue my master's degree in his laboratory. I started working in the lab with no previous research experience and I feel that I learned a great deal working in your lab. Thanks Luc for your patience and guidance, and most importantly for your words of encouragements. "*Do not despair*" will forever be my motto!

I would like to thank my thesis advisory committee members, Dr. Jim Dimitroulakos, Dr. Douglas Gray and Dr. Barbara Vanderhyden for their valuable scientific inputs. Also, I would like to thank my lab colleagues for their support and help. It's been a pleasure working with you all, I wish you all the best of luck!

Last but definitely not least; I would like to thank my family, my parents Magid and Salma, my siblings Mohamed and Samah, and my uncle Mamoun, for their encouragement and continuous support during the past two years. This M. Sc. is a testament to your faith in me; I hope I have made you proud! Love you all.

1. INTRODUCTION

1.1. Breast cancer histological and molecular classifications

Worldwide cancer statistics reveal that breast cancer is the most common type of malignancy diagnosed in women accounting for 25% of all cancers among the female population. In 2012, approximately 1.7 million new cases of breast cancer were diagnosed in women. Breast cancer takes second place after lung cancer as a cause of cancer death in women, and accounts for about 15% of total cancer deaths (Torre et al. 2012). Breast cancer is a complex heterogeneous disease that can be generally classified into non-invasive in-situ carcinomas and invasive carcinomas. Invasive carcinomas can be further subclassified into different histological subtypes including invasive ductal, invasive lobular, ductal/lobular, mucinous (colloid), tubular, medullary and papillary carcinomas. Of these, invasive ductal carcinomas (IDCs) are the most frequently diagnosed subtype and represent 80% of all invasive carcinomas, followed by invasive lobular carcinoma (ILC) detected in 10-15% of all breast cancer cases (Malhotra et al. 2010).

Breast cancer can also be classified into four major molecular subtypes based on the intrinsic gene expression signature of breast tumors: luminal A, luminal B, HER2-enriched, and basal-like or triple negative (TN) subtypes (**Table 1**). Prognostic and/or therapeutic breast cancer biomarkers include estrogen (ER) and progesterone (PR) hormone receptors, the human epidermal growth factor receptor 2 (HER2), and the Ki67 antigen (Banin Hirata et al. 2014). Luminal -A and -B breast cancers are generally ER+ subtypes with the best clinical outcome. The luminal-B subtype shows higher tumor grade, higher tumor proliferation rate, and a worse prognosis when compared to the

luminal-A subtype (Sotiriou and Pusztai, 2009) (**Table 1**). The luminal subtypes of breast cancer are characterized by the expression of luminal cytokeratin (CK) markers including CK8/18, and are responsive to endocrine therapy such as tamoxifen (Bertucci et al. 2012). HER2-enriched breast cancers overexpress the HER2 receptor and are mostly ER and PR negative (Vallejos et al. 2010). HER2-overexpressing breast cancers exhibit a higher tumor grade when compared to luminal-A and -B subtypes, and are characterized by low overall survival. A targeted therapy for HER2-positive breast cancer involves the use of anti-HER2 treatments including trastuzumab (Herceptin) and lapatinib (Bertucci et al. 2012) (**Table 1**). The basal-like breast tumors do not express ER, PR, or HER2; however, they express basal CK markers such as CK 5/6 and epidermal growth factor receptor (EGFR). The basal-like subtype is characterized by the worst prognosis and is the most difficult subtype to treat (Allison, 2012; Sotiriou and Pusztai, 2009; Bertos and Park, 2011). Targeted therapies for the basal-like breast cancer subtype are currently investigational with chemotherapy being the sole available treatment. One promising treatment exploits the DNA repair defect in TN breast cancer patients with *BRCA1* mutations through the use of poly-ADP ribosepolymerase-1 (PARP-1) inhibitors, which suppress the DNA repair system and sensitize tumors to DNA-damage induced apoptosis (Bertucci et al. 2012).

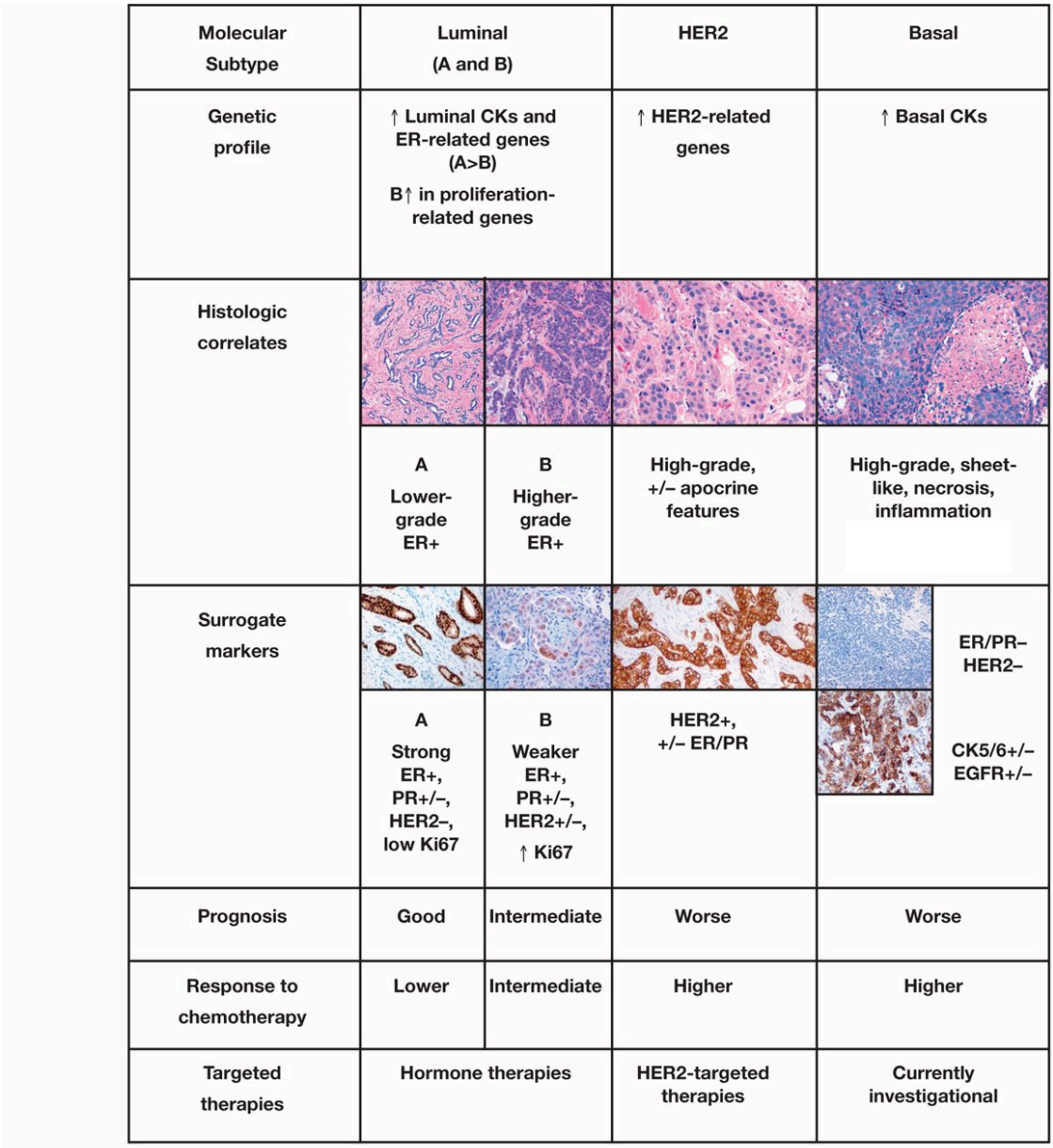

Table 1. Summary of the pathologic features of the major molecular subtypes of breast cancer. There are 4 breast cancer molecular subtypes identified based on tumor gene expression profiling: Luminal A, Luminal B, HER-2 overexpressing, and basal-like subtypes. The features analyzed and compared among the 4 different molecular subtypes are tumor genetic profile, tumor histology, tumor immunohistochemical profile (surrogate markers), prognosis, response to chemotherapy, and targeted therapies. CK: cytokeratin; EGFR: epidermal growth factor receptor; ER: estrogen receptor; PR: progesterone receptor. Reproduced with permission from Allison, 2012.

1.2. The HER2 oncogene

The *HER2* oncogene, also known as erythroblastic leukemia viral oncogene homolog 2 (*erbB-2)* in mouse and *neu* in rat, shares sequence homology with the genes encoding the cellular *EGFR* and avian erythroblastosis viral oncogene (*v-erbB*) (King et al. 1985). Initially, the rat homolog *neu* was identified as a transforming oncogene in an ethyl nitrosourea-induced rat neuroblastoma model (Shih et al. 1981). Subsequently**,** the HER2 oncogene was identified as an amplified gene in MAC117 human mammary carcinoma cell line (King et al. 1985). The HER2 oncogene is located on chromosome 17q21 and it encodes a 1255 amino acid transmembrane glycoprotein receptor that is 185,000 Da in size (Spurr et al. 1984).

HER2 is a member of the EGFR family of type I receptor tyrosine kinases (RTKs). Other members of the HER family receptors include HER1/EGFR/c-erbB-1, HER3/c-erbB-3 and HER4/c-erbB-4 (Yarden, 2001). The structure of each HER receptor is comprised of an extracellular, transmembrane and intracellular tyrosine kinase domain regions (**Figure 1.1**). The extracellular domain contains 4 subdomains: two are cysteine-rich and essential for receptor dimerization, whereas the other two constitute the ligand-binding region (**Figure 1.1**) Members of the HER family, apart from HER2, possess an epidermal growth factor (EGF)-like subdomain within their extracellular domain that confers them the ability to bind to a range of growth factor ligands possessing an EGF-like motif (Yarden, 2001). HER receptor ligands can either bind specifically to a particular HER receptor or may exhibit dual binding specificity (**Figure 1.1**). Following ligand binding, HER receptors undergo homo- or heterodimerization for their activation. HER2 is unlikely to form homodimers in cells expressing normal levels of HER2 due to steric hindrance effects (Yarden and Sliwkowski, 2001; Garrett et al. 2003). HER2

signaling is activated through heterodimerization with other ligand-activated HER receptors (Yarden, 2001). X-ray crystallography analysis of HER2 ectodomain that encompasses the extracellular and transmembrane domains revealed that it adopts an active open conformation similar to ligand-bound activated HER receptors and is prepared to interact with ligand activated HER receptors (Garrett et al. 2003). HER2 is the favored dimerization partner for HER-1, -3, or -4 receptors because of its strong intrinsic tyrosine kinase activity and the strong prolonged activation of its downstream signaling (Tzahar et al. 1996; Graus-Porta et al. 1997; Yarden and Sliwkowski, 2001). Upon dimerization, the intrinsic kinase activity found within the intracellular domain of all HER receptor family members, except for HER3 that is kinase inactive, becomes activated and the receptors transphosphorylate each other on tyrosine residues in the carboxyl terminal tail of the receptor. Specific docking cytoplasmic proteins that bear either src homology 2 (SH2) or phosphotyrosine binding/interacting (PTB/PI) domains recognize and bind to phosphorylated tyrosine residues on the activated HER2 receptor. SH2-containing proteins include phospholipase PLC-γ (PLC-γ), growth factor receptor binding protein 2 (Grb2) and GTPase activating proteins (GAPs), whereas PTB-containing proteins include the adaptor protein Shc (Wagner et al. 2013). The SH2- and PTB-containing proteins activate downstream signaling pathways regulating diverse biological processes including differentiation, proliferation, survival and migration. Examples of signaling pathways stimulated downstream of an activated HER2 receptor include Ras/mitogen-activated protein kinase (MAPK)-, phosphatidylinositol 3-kinase (PI3K)/AKT, and FAK/c-Src-dependent pathways (Yarden, 2001).

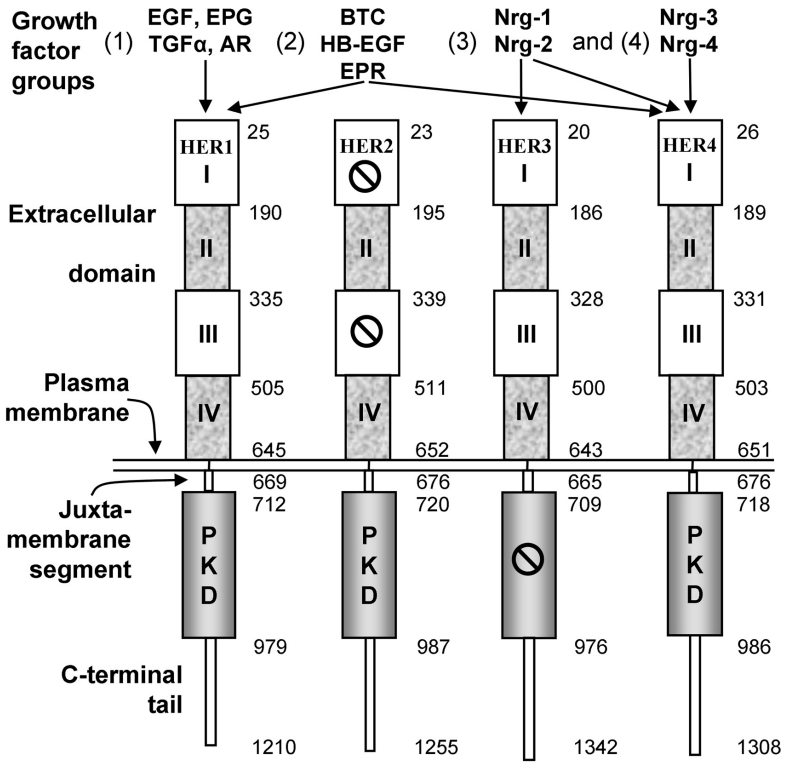

Figure 1.1. Schematic representation of the HER receptor protein structures. Shown are the 4 different HER receptors (HER1, -2, -3, and -4) and the ligands for each HER receptor (Growth factor groups). The extracellular domain of the HER receptor is composed of 4 subdomains (I-IV). Subdomains I and III are essential for ligand binding, whereas subdomains II and IV are cysteine rich and are involved in disulfide bond formation essential for receptor homo- and heterodimerization. Each receptor is composed of a 19-25 amino acid residues transmembrane domain. The intracellular domain is approximately 550 amino acid residues and contains a juxtamembrane segment, a protein kinase domain (PKD), and a carboxyterminal tail that contains the tyrosine residues subjected to transphosphorylation. The HER2 receptor lacks a ligand-binding domain and the HER3 receptor is kinase inactive (stop signs). PKD, protein kinase domain; EGF, epidermal growth factor; EPG, epigen; TGF α, transforming growth factor- α; AR, amphiregulin; BTC, betacellulin; HB-EGF, heparin-binding epidermal growth-factor like growth factor; EPR, epiregulin; Nrg-1/2/3/4, neuregulin-1/2/3/4. Reproduced with permission from Roskoski, 2014.

1.3. HER2-positive breast cancer.

The HER2 oncogene is overexpressed in approximately 20-30% of human breast cancers (Slamon et al. 1989). HER2 overexpression is also reported in other human cancers including ovarian (Slamon et al. 1989), gastric (Falck and Gullick, 1989) and salivary cancers (Stenman et al. 1991). Breast cancers with HER2 gene amplification, about 25 to 50 copies of the *HER2* gene, and the consequent 40 to 100 fold increase in the expression of its encoded protein are known as HER2-positive breast cancers and are characterized by a more aggressive metastatic tumor phenotype (Kallioniemi et al. 1992; Lohrisch and Piccart 2001; Venter et al. 1987). Furthermore, HER2 overexpression is correlated with high tumor grade (Berger et al. 1988) and a poor prognosis of the disease (Ali et al. 1988).

HER2 overexpression activates downstream signaling pathways that promote uncontrolled tumor growth and survival, disrupt the normal breast epithelial cell polarity, and promote tumor invasion (Aranda et al. 2006; Moasser, 2007) (**Figure 1.2**). HER2 receptors can form homodimers when the wildtype *HER2* gene is overexpressed at high levels (Yarden and Sliwkowski, 2001; Garrett et al. 2003). The formation of HER2-containing heterodimers is also favored in HER2-overexpressing breast cancer tumors (Garrett et al. 2003) (**Figure 1.2**). Specifically, HER3 is the preferred biological partner for HER2 in HER2-overexpressing breast tumors. In transgenic mice overexpressing HER2, a significant increase in HER3 expression level was noted in the developed breast tumors, whereas no change in the expression level of HER1 or HER4 was detected. HER2 overexpression resulted in increased HER2-mediated tyrosine phosphorylation of the HER3 receptor. The inhibition of HER3 downstream PI3K/PKB signaling in HER2 overexpressing cells suppressed their proliferation potential (Holbro et al. 2003).

Heregulin-beta 1 (HRG β1) is a ligand for HER3 that stabilizes the HER2/HER3 heterodimer and stimulates tyrosine phosphorylation of HER3 and HER2 (Carraway et al. 1994). Ectopic coexpression of HER2 and HER3 into NIH3T3 cells is necessary for HRG-dependent transformation, suggesting a role for HER2/HER3 heterodimers in the development of breast cancer (Wallasch et al. 1995).

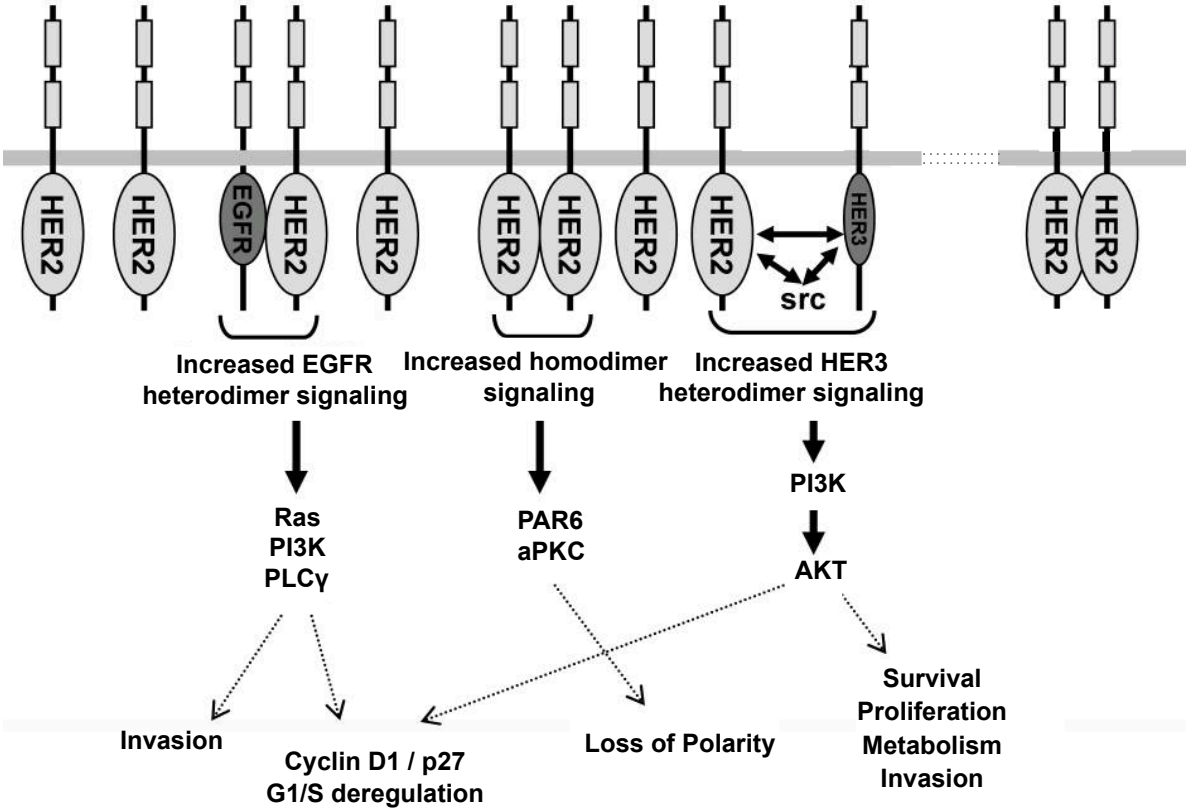

Figure 1.2. HER2 overexpression favors the formation of HER2 homodimers and HER2-containing heterodimers. HER2 overexpression disrupts downstream signaling pathways and promotes tumorigenesis. The activation of the HER2 homodimers promotes the interaction between PAR6 and aPKC; which results in the disruption of the apical-basal polarity of the breast epithelial cells (Aranda et al. 2006). The formation of the HER2/HER3 heterodimer activates the PI3K/Akt pathway that promotes cell proliferation and survival. Also AKT can stimulate downstream pathways that promote glucose metabolism for tumor growth and survival, and tumor invasion (Moasser, 2007). The heterodimerization of HER2 with EGFR stimulates tumor invasion through the activation of pathways including PI3K, Ras, and PLCγ. Reproduced with permission from Moasser, 2007.

The exact mechanisms by which HER2 transforms cells and confers an invasive phenotype remain to be elucidated. HER2-mediated transformation and metastasis is dependent on the phosphorylation of specific tyrosine residues found on the cytoplasmic tail of the receptor (Dankort et al. 2001). One study showed that the HER2 receptor contains functionally redundant tyrosine autophosphorylation sites, termed YA to YE, four of which, YB to YE, are required for the induction of HER2-mediated transformation (Dankort et al. 1997). Phosphorylated tyrosine residues link the activated HER2 receptor to other signaling cascades regulating biological processes involved in HER2-induced tumorigenesis including proliferation, survival and metastasis (Moasser, 2007) (**Figure 1.2**). One example of a signaling cascade that crosstalks with the activated HER2 receptor and is critical for HER2-induced transformation and metastasis is the integrin-mediated focal adhesion kinase (FAK) signaling (Benlimame et al. 2005). Integrins are a family of heterodimer transmembrane receptors that mediate cell-extracellular matrix (ECM) signaling. FAK and Src are non-receptor tyrosine kinases that form an activated complex downstream of integrin receptors to initiate multiple downstream signaling pathways that affect different cellular processes including proliferation, differentiation, survival, and migration (Guo and Giancotti, 2004). One study showed that downstream of HRG-stimulated HER2/3 heterodimer receptor, FAK was phosphorylated at several tyrosine phosphorylation sites including Tyr397, -861 and -925 (Benlimame et al. 2005). FAK knockdown in HER2/3 coverexpressing cells suppressed anchorage independent growth in-vitro and inhibited tumor formation in-vivo. Furthermore, mammary fat pad injection of HER2/3+ but FAK null human cancer cells inhibited the formation of lung metastases (Benlimame et al. 2005). This study

established an important role for the crosstalk between HER2 and Integrin-mediated FAK signaling in HER2-mediated transformation and metastasis.

1.4. HER2-based transgenic mouse models

The role of HER2 in the initiation and progression of breast cancer was established from studies on transgenic animal models overexpressing the *HER2* oncogene. Transgenic studies demonstrated that HER2-mediated transformation is promoted by *HER2* gene overexpression or by acquiring activating mutations within *HER2* that facilitate receptor dimerization and increase HER2 kinase activity in a ligand-independent manner (Siegel and Muller, 1996). Transgenic mice overexpressing wildtype *HER2* in the mammary gland develop metastatic mammary adenocarcinomas after a long latency (Guy et al. 1992). Analysis of established mammary carcinomas in transgenic mice overexpressing the human *HER2* gene showed that the transgene encoding the wildtype *HER2* gene spontaneously acquired sporadic in-frame deletion mutations within the extracellular domain that constitutively stimulated the intrinsic tyrosine kinase activity of the receptor (Finkle et al. 2004). These studies demonstrate that wildtype *HER2* gene amplification is necessary, but not sufficient, for the induction of transformation (Finkle et al. 2004). Mutations in the *HER2* gene promote rapid malignant transformation and progression in transgenic animal models (Siegel et al. 1994). Examples of activating mutations in the *HER2* gene expressed by the genetically engineered transgenic mouse models include a point mutation in the transmembrane domain and in-frame deletion of the extracellular domain (Siegel et al. 1994). To date, there is no evidence for the presence of oncogenic mutations in the *HER2* gene in breast tumors extracted from human patients. Clinical studies have only shown that human breast tumors harbor *HER2* oncogene amplification that results in the overexpression of its encoded protein and the

consequent increase in HER2-associated tyrosine kinase activity (Lemoine et al. 1990). To study the mechanisms that govern HER2-mediated mammary tumor progression, several transgenic mouse models were generated to specifically overexpress the rat homolog of the *HER2* gene in the mammary gland; which will be referred hereafter to as *neu*.

Directing wildtype or activated *neu* oncogene expression in the mammary gland of transgenic animal models involves the use of mammary gland-specific promoter systems. Examples of such promoters are the mouse mammary tumor virus (MMTV), whey acidic protein (WAP) and beta lactoglobulin (BLG) (Menezes et al. 2014). Among these, the MMTV is the most commonly used promoter because it is active in both non-lactating and lactating female transgenic models. The MMTV is a retrovirus that contains a long terminal repeat (LTR) DNA regulatory sequence that promotes steroid hormone-inducible transcription. Specifically, the MMTV-LTR promoter is induced by progesterone and dihydrotestosterone; however, it lacks an estrogen response element and is therefore nonresponsive to estrogen (Otten et al. 1988). The expression pattern of the MMTV-Neu fusion gene in transgenic female and male mice was determined by performing RNase protection assay using total RNA isolated from different tissues of the transgenic mice. In female transgenic mouse carriers, the MMTV-Neu transgene is expressed extensively in the mammary gland and salivary glands, and lower expression levels are detected in the lungs and ovaries. In male carriers, the fusion gene is expressed at high levels in the salivary glands and reproductive organs such as the epididymis, seminal vesicles and testes (Bouchard et al. 1989). Depending on the genomic integration site of the transgene, transcriptional activation of the MMTV-LTR promoter occurs between 6 to 22 days after birth (Ursini-Siegel et al. 2007; Wagner et al. 2001).

Transgenes under the transcriptional control of the MMTV-LTR promoter are expressed in the luminal and myoepithelial cell compartments of the mammary gland throughout all stages of mammary gland differentiation; however, higher expression levels are detected within the luminal compartment (Ursini-Siegel et al. 2007).

1.4.1. MMTV-NDL transgenic mouse models

MMTV-NDL mice express Neu-deletion (NDL) mutants under the transcriptional control of the MMTV-LTR promoter. Specifically, MMTV-NDL mice express *neu* bearing in-frame deletions of cysteine residues within Neu extracellular domain (**Figure 1.3**); which results in Neu receptor constitutive dimerization and activation. In female MMTV-NDL mice, the MMTV-NDL transgene is highly expressed in the mammary gland and in the salivary gland, however, it is expressed at a lower level in the lungs and ovaries. MMTV-NDL mice develop mammary adenocarcinomas with a latency of 3 months as opposed to the 7 months tumor latency observed in mice expressing the wildtype *neu* gene (Guy et al. 1992; Muller et al. 1988). Also, MMTV-NDL mice develop pulmonary metastatic lesions 30-60 days post initial palpation (Siegel et al. 1999) as opposed to wildtype MMTV-Neu mice that develop metastatic lesions 90 days post initial palpations (Guy et al. 1992).

1.4.2. MMTV-NIC transgenic mouse models

MMTV-NIC transgenic mice harbor a bicistronic transgene under the transcriptional control of the MMTV promoter. MMTV-NIC mice express an activated Neu-deletion (NDL 2-5) mutant and the P1 bacteriophage-derived Cre recombinase (Ranger et al. 2009) from the same transcript. An internal ribosome entry sequence (IRES) is placed between the Neu cDNA and the Cre-recombinase cDNA (**Figure 1.4**). The function of the IRES is to couple the expression of Neu and Cre-recombinase within

the same mammary epithelial cell (Ranger et al. 2009). This model is useful as it ensures that the NDL2-5-induced tumors do not escape Cre-mediated recombination as previously encountered when interbreeding MMTV-NDL2-5 mice to different mice strains bearing MMTV-Cre transgene and conditional floxed alleles (Lahlou et al. 2012). MMTV-NIC primary tumors are derived from the luminal layer of the mammary gland. They express the luminal epithelial layer marker cytokeratin-8 and lack expression of basal layer markers such as cytokeratin 14, 5 and 6. Also, the expression profile of genes in the MMTV-NIC tumors is characteristic of the solid/luminal subtype of breast cancer and includes genes that are implicated in protein modification, cell growth and death, metabolism and fibroblast growth factor (FGF) signaling. Furthermore, MMTV-NIC tumors do not show activation of Wnt/β-catenin signaling and express basal levels of β-catenin targets such as cyclin D1, Tcf 7 and Axin2 (Schade et al. 2013).

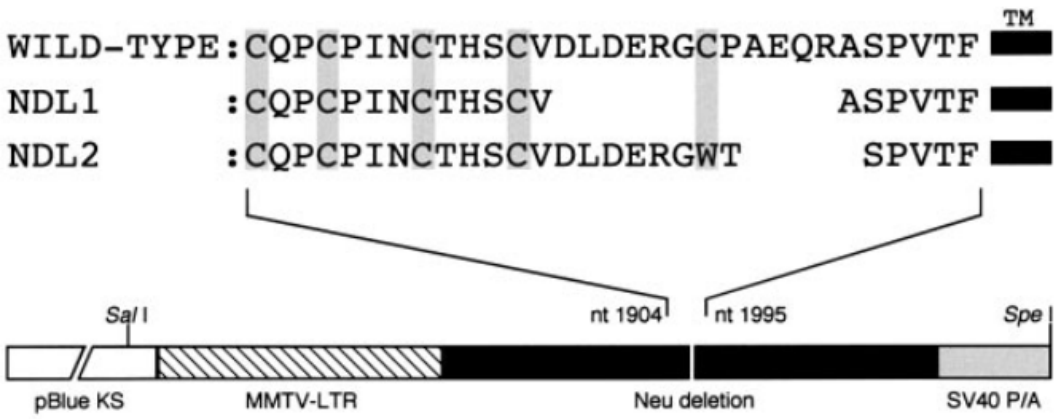

Figure 1.3. Structure of the MMTV-NDL transgene. Shown are three distinct transgenes encoding wildtype, NDL1 and NDL2. The activated transgenes, NDL1 and-2, harbor an in-frame deletion within *neu* extracellular domain, which corresponds to the nucleotide sequence from 1904 to 1995, within *neu* cDNA. Shown is the deleted amino acid sequence in NDL1 and NDL2 transgenes in comparison to the wildtype sequence. A phenylalanine residue (F) is present at the end of each amino acid sequence of the three transcripts, which is directly followed by the sequence that corresponds to the transmembrane domain (TM). (pBluescript KS): vector sequence; MMTV-LTR: mouse mammary tumor virus-Long terminal repeat; SV40 P/A: polyadenylation signals derived from the SV40 early transcription unit. There are two restriction sites: SalI and SpeI, which are used to isolate the deleted fragments for pronuclear microinjection. Reproduced with permission from Siegel et al. 1999.

Figure 1.4. Structure of the MMTV-NIC transgene. It is a bicistronic transcript consisting of two cDNAs; the first cDNA encodes the activated Neu, NDL2-5, (ErbB2/Neu) and the second cDNA encodes cre-recombinase (CRE). The expression of both cDNAs is coupled by the internal ribosomal entry sequence (IRES) inserted between them. The bicistronic transgene is under the transcriptional control of the mouse mammary tumor virus (MMTV) promoter. Reproduced with permission from Huck et al. 2010.

1.5. The Ste-20 like kinase (SLK)

1.5.1. SLK gene expression pattern in adult and embryonic murine tissues

The murine ste-20 like kinase (*slk*) gene is located on chromosome 19 and contains 20 exons (PubMed Gene ID: 20874, 2015). There are three different isoforms transcribed from the murine SLK locus that are 5, 7 and 8.5 kilobases (Pytowski et al. 1998). Among the three SLK isoforms, the most abundant 8.5 kilobases mRNA encodes a 1202 amino acid protein with a predicted molecular weight of 148 kDa (Sabourin and Rudnicki, 1999). The 8.5 kilobases transcript is expressed ubiquitously in all adult tissues except in the testes in which the 5 kilobases isoform is expressed primarily (Pytowski et al. 1998). The SLK protein is expressed as a 220-kDa protein in different adult murine tissues (Zhang et al. 2002); which is different from its predicted size of 148-kDa. This suggests that SLK undergoes post-translational modifications that are yet to be identified (Sabourin et al. 2000). The 220-kDa SLK is preferentially expressed in neuronal and muscle lineages during embryonic development (Zhang et al. 2002).

1.5.2. Murine SLK protein structure

The mammalian Ste20-like kinases are related to *Saccharomyces cerevevisia* Sterile 20 protein (Ste20p) that functions as a mitogen-activated protein kinase kinase kinase kinase (MAP4K) in the mating signaling pathway elicited by the mating pheromone receptor. Ste20-like kinases participate in the MAPK signaling pathway that is implicated in the regulation of various cellular processes including apoptosis, cytoskeletal rearrangements, and cellular motility (Dan et al. 2001). There are two structurally distinct families of Ste-20-related kinases in mammals: the germinal center kinases (GCKs) and p21-activated kinases (PAKs) (Sells et al. 1997). The mammalian SLK is a GCK-related serine/threonine kinase that was originally isolated from a guinea pig liver cDNA library. The nucleotide sequence of murine SLK is 90% identical to human, rat and guinea pig SLK sequences (Itoh et al. 1997).

SLK functional domains include an N-terminal domain (residues 1-338), a central coiled-coil domain (residues 339-788) and a C terminal domain (residues 789-1202) (**Figure 1.5**). The amino-terminal serine/threonine kinase domain of SLK is found to be 74% and 72% homologous to the corresponding domains of the ste20-related lymphocyte oriented kinase (LOK) and Xenopus polo-like kinase kinase 1 (xPlkk1), respectively. The SLK central coiled-coil domain is 70% homologous to microtubule and nuclear associated protein (MNAP). The carboxyl terminal region of SLK is 63% homologous to the AT1-46 protein and has been termed the (ATH) domain. To this date, the function of the central MNAP and carboxyl ATH domains is unknown (Al-Zahrani et al. 2013). SLK contains a putative caspase-3 cleavage site at amino acid residue 436 ($DTQD^{436}$) and a putative SH3 binding domain (PPEPE) at amino acid residue 735 of murine SLK (**Figure 1.5**), which suggests that SLK can interact with SH3 domain-

containing proteins that have yet to be identified (Sabourin et al. 2000). SLK contains an activation segment from amino acids 173 to 222. The activation segment has a magnesium binding-site (DFG motif) at the beginning of the segment and an αEF/αF loop at the end of the segment. Electron density map analysis identified two autophoshorylation sites within the SLK activation loop, Thr-183 and Ser-189. SLK autophoshorylation in its activation loop is a key regulatory element to SLK kinase activity (Luhovy et al. 2012).

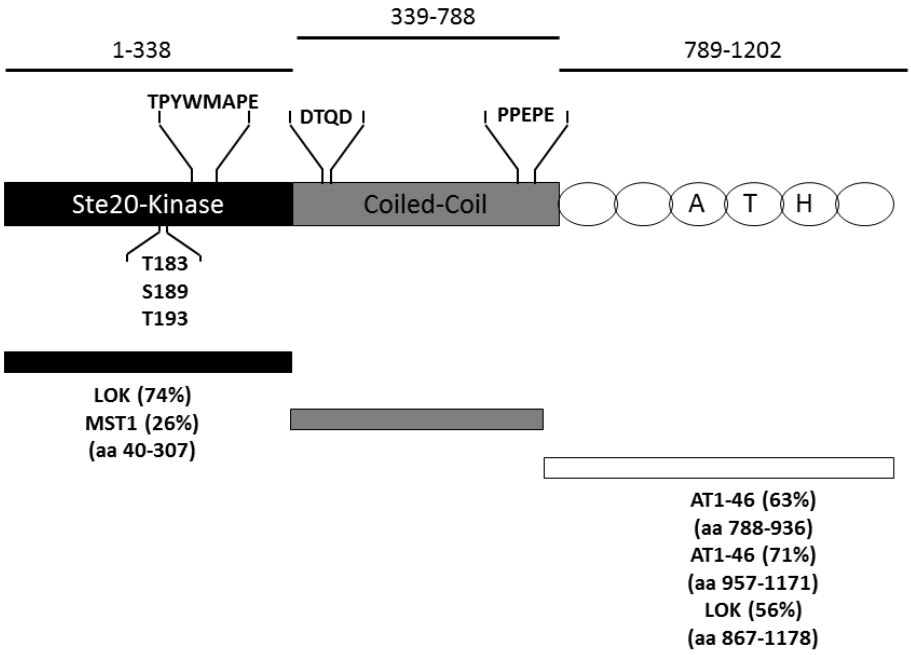

Figure 1.5. Schematic representation of the SLK protein structure. Shown in parentheses are the percent similarities of SLK domains to other proteins. SLK has an N-terminal serine/threonine kinase domain (Ste20-Kinase) similar to two other Ste20-related kinases, LOK and MST1. SLK has a central microtubule and nuclear associated protein homology domain (Coiled-coil) of unknown function. The C-terminal (ATH) domain of SLK shows 63% homology to AT1-46 from amino acids 788-936 and 56% homology to LOK from amino acids 867-1178. Also shown is the Ste20 signature sequence (TPYWMAPE), caspase-3 cleavage site (DTQD), and SH3 binding domain (PPEPE). ATH: AT1-46 homology domain; LOK: lymphocyte oriented kinase; MST1: mammalian sterile twenty kinase 1.

1.5.3. SLK role in murine embryonic development

To elucidate the role of SLK in murine embryogenesis, gene trapping was used to generate a truncated form of SLK protein that lacks the ATH domain due to the insertion of the LacZ cassette. The global expression of the SLK-LacZ fusion protein is embryonic lethal between E12.5 and E14.5. Examples of developmental defects in SLK homozygous mutant animals include small less structured myogenic and neuronal compartments, increased apoptosis in the embryos by E14.5, defective blood vessel formation and reduced proliferation in the placenta that impairs placental growth and development (Al-Zahrani et al. 2014). Overall, this study showed that SLK is required for normal murine development.

1.5.4. SLK protein function

SLK was initially characterized as a promoter of apoptosis. Forced SLK expression in either cultured fibroblasts (Sabourin and Rudnicki, 1999) or C2C12 myoblasts induced apoptosis as evidenced by the presence of TUNEL positive cells exhibiting cellular shrinkage, membrane blebbing and loss of substrate adhesion (Sabourin et al. 2000). In a different study, SLK overexpression in glomerular epithelial cells induced apoptosis by the phosphorylation of p53 on specific serine resides, S-33 and S-315, leading to the activation of the transcriptional activity of p53 (Cybulsky et al. 2009). Also, SLK has been shown to directly phosphorylate signal-regulating kinase-1 (ASK1) and signals via mitogen-activated protein kinase pathway to promote apoptosis (Hao et al. 2006).

SLK kinase activity is also required for progression through the G2/M phase of the cell cycle in fibroblasts. Confocal microscopy showed that SLK colocalizes with α-tubulin at the mitotic spindle during metaphase (O'Reilly et al. 2005). SLK kinase

activity was found to be upregulated during the G2/M phase of the cell cycle. Expression of a kinase inactive SLK results in an arrest in the G2 phase of the cell cycle. Moreover, cultures expressing a kinase inactive SLK failed to upregulate the activity of the maturation promoting factor (MPF) complex, p34/cdc2 kinase. This finding suggests that SLK activity is required upstream of the MPF complex for cell cycle progression into mitosis (O'Reilly et al. 2005).

SLK was also found to mediate actin cytoskeletal remodeling during cell spreading in fibroblasts. In spreading MEF3T3 cells SLK staining is absent in regions where actin stress fibers are dense, and vice versa (Wagner et al. 2002). SLK overexpression in MEF3T3 cells induces cellular retraction, actin stress fibers dissolution and the relocalization of actin to the cell periphery. Stress fiber disassembly can be inhibited in SLK overexpressing cells by introducing a dominant negative mutant of Rac1, which suggests that Rac1 functions downstream of SLK-induced actin remodeling (Wagner et al. 2002). The $SLK^{950\text{-}1202}$ ATH domain is sufficient to induce stress fiber disassembly. C2C12 myoblasts transfected with a vector expressing the ATH domain of SLK resulted in stress fiber disassembly and cellular retraction. The role of SLK in stress fiber dissolution appears to be independent of its kinase activity, since the expression of a kinase inactive SLK^{K63R}, which bears a point mutation (K63R mutation) within its ATP-binding site, in C2C12 cells still resulted in stress fiber dissolution (Sabourin et al. 2000).

Also, SLK mediates focal adhesion turnover during cell spreading in fibroblasts. Specifically, SLK has an important role in microtubule-dependent adhesion turnover (Wagner et al. 2008). Previously, SLK has been shown to indirectly associate with the microtubule network during cellular spreading (Wagner et al. 2002). Also, SLK colocalizes with the adhesion protein vinculin at the cell periphery in fibroblasts during

spreading on fibronectin (FN) (Wagner et al. 2002). SLK knockdown in MEF3T3 cells impairs focal adhesion turnover as evidenced by the sustained levels of phospho-FAK-Tyr397, a marker for stable adhesions (Wagner et al. 2008). Furthermore, MEF3T3 cells expressing an activated truncation of SLK, SLK^{1-373}, show a reduction in the size of peripheral focal adhesions. These findings suggest that SLK mediates focal adhesion turnover during cell spreading in fibroblasts (Wagner et al. 2008). Specifically, SLK mediates focal adhesion disassembly by phosphorylating the adaptor protein paxillin on serine 250. Expression of a S250T paxillin mutant in MEF3T3 cells impairs focal adhesion turnover and significantly decreases cellular migration when compared to wildtype- paxillin expressing cells (Quizi et al. 2013).

SLK activity is also required for efficient migration of MEF3T3 fibroblasts. In a scratch-wounding model, SLK knockdown in MEF3T3 cells using a small interfering RNA (si-RNA) approach resulted in approximately a 60% decrease in migration and a delay in wound closure when compared to controls. The assembly and activation of the Src/FAK complex is important for SLK activation following scratch wounding of fibroblast monolayers (Wagner et al. 2008). Specifically, src is required for SLK recruitment at the leading edge of migrating cells, whereas FAK is required to upregulate SLK kinase activity. The knockdown of FAK or src in MEF3T3 cells significantly inhibited their migration capability. This supports a critical role for SLK in regulating cellular migration in a FAK signaling-dependent manner (Wagner et al. 2008).

1.5.5. SLK activation downstream of Neu signaling

Our lab has shown that SLK kinase activity is upregulated in response to HRGβ1-mediated Neu stimulation in breast cancer cells. On the contrary, no SLK activation was detected following HRGβ1 stimulation of the T47D-5R cell line that is defective in the localization of the Neu receptor from the endoplasmic reticulum to the cell membrane (Roovers et al. 2009). Furthermore, SLK activity is stimulated in cells expressing activated NeuNT. Overexpression of NeuNT in NIH 3T3 cells and Hela cells resulted in a marked SLK activation. Overall, these experiments suggest that Neu stimulation or overexpression activates SLK kinase activity (Roovers et al. 2009). Specifically, Neu activation through the YC and YD autophoshorylation sites is required for SLK activation (Roovers et al. 2009). Ectopic expression of YC or YD into T47D-5R cells followed by HRGβ1 stimulation resulted in SLK activation. Through the use of inhibitors targeting the different intracellular signaling cascades downstream of Neu, HRGβ1-mediated SLK activation was shown to require Src family kinases (SFKs), MEK1, PI3K and PLCγ signaling pathways (Roovers et al. 2009). Furthermore, HRGβ1-induced Neu activation stimulates SLK activation in a FAK dependent manner (**Figure 1.5**). Ectopic expression of NeuNT into FAK-null fibroblasts followed by HRGβ1-stimulation did not result in an upregulation of SLK kinase activity when compared to FAK-expressing cells (Roovers et al. 2009).

1.5.6. SLK mediates adhesion dynamics and breast cancer cell motility downstream of HER2 signaling

SLK mediates focal adhesion turnover downstream of Neu signaling. Expression of a kinase inactive SLK^{K63R} mutant into either NeuNT or Neu-NYPD signaling-deficient *neu* expressing cells resulted in a significant increase in the levels of phospho-FAK Y397, a marker of intact focal adhesion complexes. This indicates that SLK kinase activity is required for efficient focal adhesion turnover downstream of Neu signaling (Roovers et al. 2009). Furthermore, SLK is required in mediating HRGβ1-induced directional cellular migration downstream of Neu signaling. Both, HRGβ1-induced chemotaxis and haptotaxis were markedly inhibited in murine and human breast cancer cell lines expressing a kinase inactive SLK (Roovers et al. 2009). Also, SLK knockdown was accompanied by a significant reduction of the invasion potential of Neu-NT expressing NMUMG cells (Roovers et al. 2009). Taken together, these studies suggest a critical role for SLK activity downstream of Neu signaling in the regulation of efficient migration and invasion of breast cancer cells.

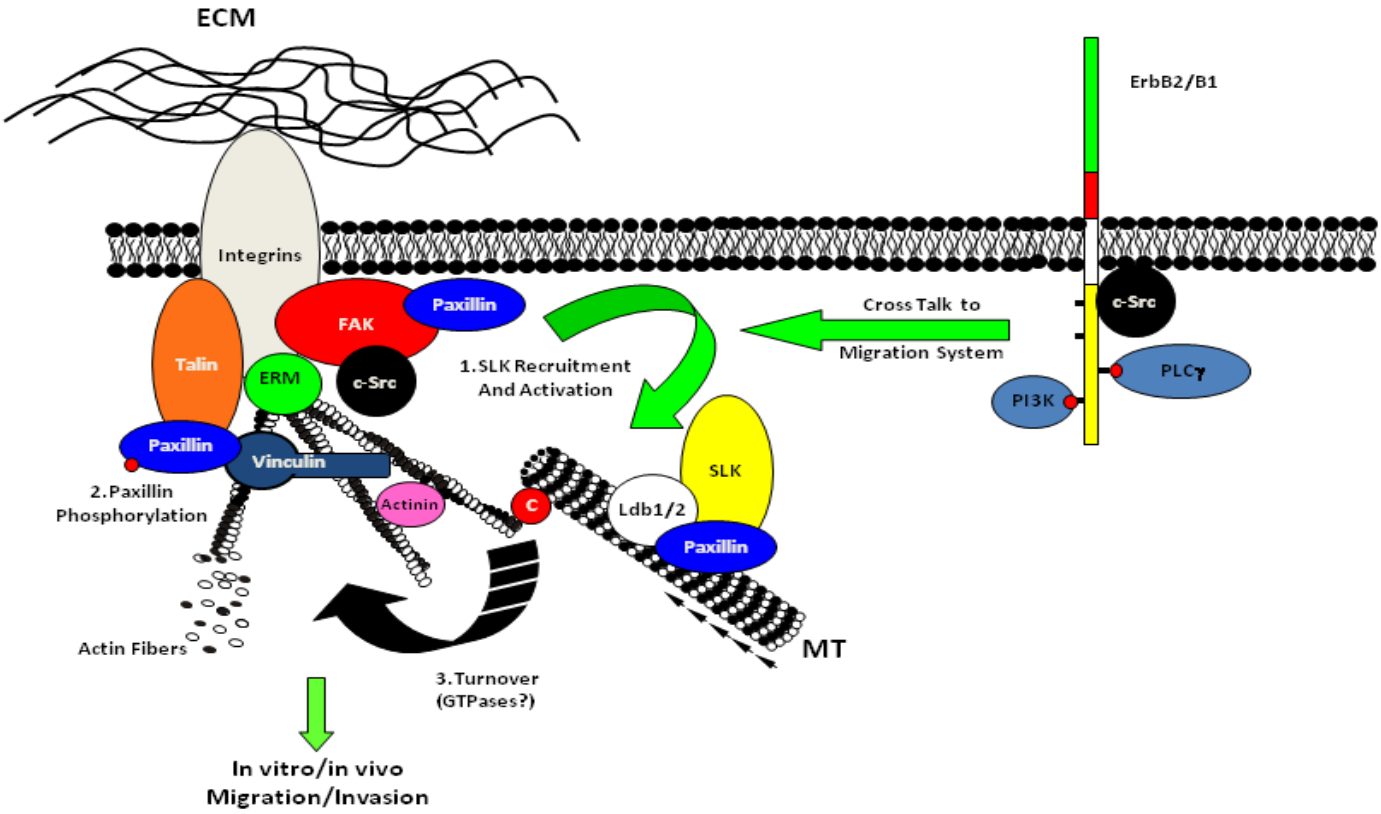

Figure 1.5. SLK activation downstream of the crosstalk between the activated Neu receptor and integrin mediated focal adhesion kinase (FAK) signaling pathway. The activation of Neu signaling through YC and YD autophoshorylation sites stimulates PI3K- and PLCγ- dependent SLK activation. FAK signaling is required for Neu-mediated SLK activation. HRGβ1-mediated ErbB2 stimulation in FAK-null cells inhibited SLK kinase activity upregulation (Roovers et al. 2009). Upon stimulation, SLK becomes recruited to focal adhesion complex sites through its indirect association with the microtubule network to induce microtubule-dependent adhesion turnover. Specifically, SLK phosphorylates microtubule-bound paxillin on serine 250 to induce focal adhesion turnover (Quizi et al. 2013). The dynamic process of focal adhesion complex assembly and disassembly as mediated by SLK kinase activity ensures efficient directional cellular migration downstream of HER2 signaling (Al-Zahrani et al. 2013).

1.6.3. SLK Kinase activity regulation

Previous studies have established a role for SLK in regulating different cellular processes by either knocking down the protein or by introducing a kinase-inactive SLK mutant. To date, no mutations have been identified in the *slk* gene nor has there been a study that addressed a direct association between SLK kinase activity and disease or cancer development. An upregulation in SLK protein level and kinase activity was noted in ischemic acute renal failure and was associated with an increase in apoptosis and cellular damage during renal injury (Cybulsky et al. 2004). Also, SLK kinase activity has been reported to play an antihypertensive role by directly phosphorylating RhoA on serine-188 and inhibiting Rho-mediated vasocontraction in response to angiotensin II type-2 receptor (AT_2R) stimulation (Guilluy et al. 2008). In the context of cancer development, endogenous SLK protein level was found to be upregulated in different types of cancers including thyroid, urothelial, breast, prostate and stomach cancers (The Human Protein Atlas, Uhlen et al. 2005), which suggests a role for SLK in cancer development. Nonetheless, it is still not known whether the increase in SLK protein level in cancer is correlated with an upregulation in its kinase activity. Our studies showed that SLK kinase activity is required for efficient migration and invasion of breast cancer cells downstream of activated HER2 signaling (Roovers et al. 2009). These results highlight the importance of studying the mechanisms by which SLK kinase activity is modulated to gain a better understating of its functional role in physiological and pathological processes including tissue injury, hypertension, cancer development and metastasis.

The SLK ATH domain has an autoinhibitory role on its kinase activity. An activated truncation of SLK, SLK^{1-373}, that only expresses SLK kinase domain rapidly induces apoptosis, whereas expression of SLK ATH domain alone, $SLK^{950-1202}$, induces a

delayed apoptotic response, preceded by actin stress fiber dissolution, cellular retraction and loss of substrate adhesion (Sabourin et al. 2000). Caspase-3 mediated cleavage of murine SLK at amino acid 436 releases an activated SLK kinase domain, which suggests an autoinhibitory role for SLK C-terminal domain on its N-terminal kinase domain. Specifically, amino acids 950 to 1202, and, 552 to 1202, are implicated in the autoregulation of SLK kinase activity (Sabourin et al. 2000).

LIM domain binding proteins (Ldbs) bind to SLK ATH domain and function to negatively regulate SLK kinase activity. A yeast two-hybrid analysis was performed using $SLK^{950-1202}$ ATH domain as a bait to screen a mouse E10.5 cDNA library to identify factors that bind to and therefore contribute to the negative regulation imparted by the ATH domain on SLK kinase domain (Storbeck et al. 2009). Ldb factors were identified as ATH domain interacting proteins that function to negatively regulate SLK kinase activity. In one experiment, recombinant His-tagged $SLK^{950-1202}$ domain has been shown to significantly reduce the kinase activity of GST-SLK^{1-373} domain. When His-tagged Ldbs were added, either separately or together, along with His-tagged $SLK^{950-1202}$ ATH domain, the kinase activity of GST-SLK^{1-373} was decreased even further. This suggests that the Ldb factors function to augment the negative regulation imparted by SLK ATH domain on SLK kinase domain (Storbeck et al. 2009).

1.6. LIM domain binding protein family

LIM domain binding proteins (Ldbs) are transcriptional cofactors that are highly conserved from *Caenorhabditis elegans* to human. In vertebrates, there are two close paralogs of the Ldb family: Ldb1 and Ldb2. Ldb2 shares 75% sequence homology with Ldb1 (Cross et al. 2010). The structure of both Ldb proteins includes an amino-terminal self-association/dimerization domain (DD) critical for their biological function as

transcriptional cofactors (Jurata et sl. 1998); a nuclear localization sequence (NLS) (Jurata et al. 1996); and a carboxyl-terminal LIM-interaction domain (LID) essential for binding LIM domains on LIM domain-containing transcriptional factors and their coregulators (Cassata et al. 2000; Jurata and Gill, 1997; Taira et sl. 1992; Ingolf et al. 1997).

LIM domains are cysteine-rich zinc-binding motifs that mediate protein-protein interactions and are found in a wide range of nuclear and cytoplasmic proteins (Dawid et al. 1998). LIM domain-containing proteins are classified into A-B, C and D subtypes based on the sequence of the LIM domain, the localization of the LIM domain along the protein sequence and the overall structure of LIM-domain containing proteins (Dawid et al. 1998). Both Ldb factors bind with high affinity to the AB-subtype of nuclear LIM domain-containing proteins that include LIM-homeodomain (LIM-HD) and LIM-only (LMO) proteins (LMO1-4), but not to cytoplasmic LIM-domain-containing proteins. In fact, Ldb proteins were initially isolated as interacting partners of nuclear LIM-HD and LMO proteins that have an important role in cell fate determination during embryonic development (Dawid et al. 1998). Several studies have suggested a functional relationship between Ldb factors and LIM-HD or LMO proteins because they exhibit a similar expression pattern during development (Agulnick et al. 1995; Bach et al. 1997; Visvader et al. 1997).

1.6.1. Ldb1 and Ldb2 expression pattern in embryonic and adult mouse tissues.

Ldb1 is widely expressed in different mouse embryonic tissues including fetal liver, lung, kidney, thymus and olfactory epithelium. High Ldb1 levels are detected in the central nervous system and in hematopoietic lineages of the developing mouse embryos.

In adult mice however, high levels of Ldb1 expression are detected in the pituitary gland and skin. Other adult tissues that show low to moderate Ldb1 expression include the heart, brain, liver, kidney, testis, lung and muscle (Agulnick et al. 1995; Bach et al. 1997; Visvader et al. 1997; Tran et al. 2006). Unlike the ubiquitous expression pattern observed for Ldb1, Ldb2 expression is exclusive to specific embryonic and adult tissues. Ldb2 is highly expressed in embryonic neuronal lineages; however, Ldb2 is highly expressed in the brain, trigeminal ganglia and lungs of adult mice (Ingolf et al. 1997).

1.6.2. Murine Ldb1 gene/Ldb1 alternative splice variants

The mouse Ldb1 gene is located on chromosome 19 and consists of 14 exons (PubMed Gene ID: 16825, 2015). There are three different isoforms transcribed from the Ldb1 locus. Isoforms 1 through 3 encode a 411 amino acids protein (46.5 KDa in size), a 319 amino acids protein (36.6 KDa), and a 375 amino acids protein (42.7 KDa in size), respectively (UniProt P70662, 2015). In the current study we will be investigating the protein product encoded from the first isoform, which represents the canonical sequence of Ldb1 protein containing all of its functional domains.

1.6.3. Murine Ldb1 protein structure and isolation

The Ldb1 protein, also known as nuclear LIM-interactor protein (NLI) and carboxyl terminal LIM domain-binding protein 2 (CLIM2), is a transcriptional cofactor with no enzymatic activities. Ldb1 functional domains include a conserved 200 amino acid N-terminal dimerization domain (DD) (Breen et al. 1998), a highly conserved Ldb1/Chip conserved domain (LCCD) covering amino acids 201 to 249 (Van Meyel et al. 2003), and a carboxyl-terminal LIM interaction domain (LID) from amino acid 300 to 338 (Jurata and Gill, 1997). Also, Ldb1 contains a putative nuclear localization signal (NLS) from amino acid 259 to 264 that accounts for the predominant localization of Ldb1

in the nucleus (Jurata et al. 1996). Ldb1 was originally isolated as a LIM-domain binding protein by screening a mouse embryo cDNA expression library with a probe containing the LIM domains of the LIM-homeobox 1 (Lhx1) transcriptional factor (Agulnick et al. 1995).

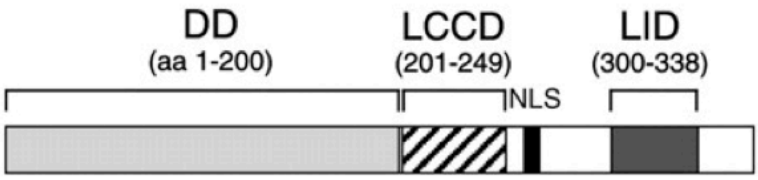

Figure. 1.6. Schematic representation of murine Ldb1 protein structure. Shown are the functional domains of Ldb1. Ldb1 contains a dimerization domain (DD) that spans the first 200 amino acids at the amino terminus, a highly conserved Ldb1/Chip conserved domain (LCCD) from amino acids 201 to 249, a nuclear localization signal (NLS) from amino acid 259 to 264, and a LIM interaction domain (LID) from amino acids 300 to 338. Reproduced with permission from Van Meyel et al. 2003.

1.6.4. Ldb1 function as a transcriptional modulator

The transcriptional cofactor Ldb1 acts as a bridge molecule by bringing distant regulatory elements and promoters of target genes in close proximity for transcriptional regulation. Ldb1 DD and LID domains are essential for Ldb1 function as a facilitator of long-range interactions in transcriptional regulation. Animal cap assays in *Xenopus laevis* demonstrated that the deletion of either the DD or LID domains abrogated Xlim-mediated transcriptional activation of the Spemann organizer and neural genes in-vivo (Breen et al. 1998). In murine erythroleukemia (MEL) cells, Ldb1 DD domain was shown to be necessary in facilitating the interaction between the upstream β-globin locus control region (LCR) and β-globin promoter to activate β-globin transcription during erythroid

differentiation (Song et al. 2007). The recruitment of Ldb1 to transcriptional complexes that occupy cis-regulatory elements of target genes requires Ldb1 interaction with LIM-HD or LMO proteins. Ldb1-containing transcriptional complexes can either activate or repress the expression of target genes. In erythroid progenitor cells, Ldb1 interaction with the LIM domains of LMO2 and its subsequent recruitment to the erythroid complex, Ldb1/LMO2/TAL1/GATA1/E47, is required for augmenting the transcriptional activation of the *P4.2* gene (Xu et al. 2003). On the other hand, Ldb1 negatively regulates the activation of the rat insulin I minienhancer element bound by the LIM homeobox protein (Limx1) and the basic helix loop helix protein (E47) complex. Ldb1 exerts its negative effect on rat insulin I minienhancer by competing with E47 for binding to the LIM domain of Limx1 to form the inhibitory Ldb1/Limx1 transcriptional complex (Jurata and Gill, 1997). Overall, Ldb1 functions as an adaptor protein that facilitates the formation of large multiprotein transcriptional complexes and functions to either enhance or repress the synergistic activation of target gene expression.

1.6.5. Ldb1 role in murine embryonic development

Global Ldb1 knockout is embryonic lethal at E9.5-E10. Ldb1 expression is important for the formation of the anterior-posterior body axis during mouse embryonic development. Ldb1 knockout embryos displayed a number of developmental defects including anterior head truncation, posterior axis duplication, and lack of heart and foregut anlagen (Mukhopadhyay et al. 2003). Interestingly, the dorsalised phenotype observed in Ldb1-null embryos was similar to the phenotype observed in transgenic embryos expressing the Wnt signaling activator, *Wnt8* (Popperl et al. 1997). Ldb1 was specifically shown to negatively regulate Wnt signaling activation during mouse development by upregulating the expression of Wnt inhibitors. In comparison to wildtype

embryos, Ldb1 mutants showed a downregulation in the expression of Wnt inhibitors including *dickkopf1* (*Dkk1*), *Cerberus* (*Cer1*) and the three frizzled-related genes *Sfrp1*, *Sfrp2* and *Frzb*/*Sfrp3*. Overall, the global Ldb1 knockout study showed that Ldb1 deletion results in Wnt signaling overactivation, which contributes to the axial patterning defect observed in Ldb1 mutant embryos (Mukhopadhyay et al. 2003).

1.6.6. Ldb1 role in mammary gland development

Throughout mammary gland development, Ldb1 is expressed preferentially at a higher level within the luminal and basal epithelial layers of the mammary gland (Salmans et al. 2014). Ldb1 overexpression into lactogenic stimulated-SCp2 mammary epithelial cells, isolated from the mammary gland of a midgestation mouse, inhibited the expression of the milk proteins, *β-casein* and whey acidic protein (Wap), suggesting that Ldb1 negatively regulates mammary epithelial differentiation (Visvader et al. 2001). Salmans et al generated a mouse model in which they inhibited Ldb-mediated transcriptional regulation in the basal cell compartment of the mammary gland by expressing a dominant negative Ldb mutant (DN-Ldb) that lacks the DD domain under the transcriptional control of the K-14 promoter (K14-DN-Ldb). They found that the expression of both Ldb factors in the basal compartment of the mammary gland is required for normal branching morphogenesis. The inhibition of the transcriptional activity of both Ldb factors in the basal epithelial cells of the mammary gland resulted in defects that appeared as early as 4 weeks of age including delayed ductal elongation, reduced branching frequency and the generation of smaller terminal end buds (TEB) (Salmans et al. 2014). Pregnant DN-Ldb mice showed a defect in lactation and could not support litters past 2 days of parturition. The defects in branching morphogenesis were attributed to a significant reduction in proliferation in the TEBs and the ducts. Analysis of

the gene expression profile in the TEBs and ducts from wildtype and DN-Ldb mice revealed genes that are differentially expressed (Salmans et al. 2014). In DN-Ldb mammary gland, the expression of *Fgfr2* is downregulated in the basal cells, which results in a significant reduction in the number of basal stem cells and a suppression of their proliferative capacity. Chromatin immunoprecipitation (CHIP) analysis have demonstrated that Ldb1 forms a complex with its interacting partner LMO4 and that Ldb1 expression is required for the recruitment and binding of the complex to a specific region (538 to 708 bp) upstream of Fgfr2 transcriptional start site (TSS) to drive Fgfr2 expression (Salmans et al. 2014).

1.6.7. Ldb1 in cancer development

Several reports in the literature support a role for Ldb1 in cancer development. Ldb1 protein is overexpressed in different types of human cancers including cervical, skin, melanoma, prostate, head and neck, endometrial and breast cancers (Uhlen et al. 2005). In oral squamous cell carcinoma, Ldb1 binds directly to LMO4 to form a nuclear complex that is highly expressed at the invasive front of less differentiated carcinoma cells. Both, Ldb1 and LMO4 are expressed at a higher level in squamous carcinoma cells that have metastasized to the cervical lymph nodes when compared to their low expression level in primary tumors (Mizunuma et al. 2003). Moreover, Ldb1 interacts directly with LMO1 in human T cell lymphoblastic leukemia with the translocation t (11; 14)(p15; q11), suggesting a role for Ldb1 in hematopoietic malignancies (Valge-Archer et al. 1998). In addition, Ldb1 plays a role in the development of hepatocellular carcinoma (HCC). Ldb1 conditional knockout in the liver results in a significant increase in cellular proliferation and increased evasion of apoptosis. Increased cyclin D1 expression is one

underlying genetic mechanism that contributes to the observed increase in cellular proliferation in Ldb1$^{-/-}$ HCC tumors (Teufel et al. 2010).

In the context of breast cancer, Ldb1 is expressed in different human ductal breast epithelial tumor cell lines including T47D, BT-474 and ZR-75B (Visvasder et al. 2001). Among the different molecular subtypes of breast cancer, Ldb1 is highly expressed in the less differentiated claudin-low and basal-like breast cancer subtypes, whereas Ldb2 is highly expressed in the differentiated luminal breast cancer subtypes (Salmans et al. 2014). Breast cancer tissue microarray (TMA) analysis shows that Ldb1 protein is highly expressed in advanced tumor stages and in less differentiated tumors (Johnsen et al. 2009). Ldb1 is also expressed in estrogen receptor (ER) positive human primary breast tumors. Co-immunoprecipitation analysis of protein extracts from primary breast tumors showed that Ldb1 directly interacts with estrogen receptor α (ERα). Specifically, Ldb1 negatively regulates ERα activity by decreasing estrogen response element (ERE)-dependent transcription of estrogen-regulated genes including *PS2 (TFF1), cathepsin D,* and *WISP2*. Also, ER+ and/or PR+ tumor microarrays show strong Ldb1 positive staining when compared to ER- and/or PR- TMAs (Johnsen et al. 2009); suggesting a role for Ldb1 in estrogen positive breast cancers.

1.6.8. Ldb1 role in the regulation of SLK activity and cellular migration in MEF3T3 fibroblasts

Ldb1 interacts directly with SLK to negatively regulate its kinase activity in MEF3T3 fibroblasts (Storbeck et al. 2009). In-vitro binding assays demonstrated that both Ldb factors use a 186 amino acid portion of their dimerization domain (DD) and a 100 amino acid portion of their nuclear localization sequence (NLS) to specifically bind

SLK in the ATH domain (Storbeck et al. 2009). Ldb1 has been shown to enhance the interaction between the two functional domains of SLK, the ATH domain and the kinase domain, thereby augmenting the inhibition imparted by the ATH domain on SLK kinase activity (Storbeck et al. 2009). Ldb1 knockdown in MEF3T3 cells using si-RNA resulted in a 5.5 fold increase in SLK kinase activity. Furthermore, Ldb1 knockdown was associated with a 2-fold increase in focal adhesion turnover rate and a 2-fold increase in MEF3T3 cellular migration (Storbeck et al. 2009). Overall, these results suggest a role for Ldb1 in negatively regulating SLK activity, focal adhesion turnover and motility in MEF3T3 fibroblasts.

2. Statement of hypothesis and objectives

SLK kinase activity is upregulated by Neu overexpression in breast cancer cells (Roovers et al. 2009). Our lab has shown that downstream of Neu signaling, SLK kinase activity is essential for efficient cellular migration and invasion. During the course of a yeast two-hybrid screen using the SLK ATH autoregulatory domain as a bait to screen a mouse E10.5 cDNA library, Ldb1 was identified as an ATH-interacting protein that functions to negatively regulate SLK kinase activity. Ldb1 and SLK are both expressed in human breast cancer tissues (The Human Protein Atlas, Uhlen et al. 2005) and in transformed breast cancer cell lines (Visvader et al. 2001; Salmans et al. 2014; Johnsen et al. 2009; Roovers et al. 2009). This suggests a role for both proteins in the development of breast cancer. The purpose of this thesis is to investigate the effect of Ldb1 deletion on SLK kinase activity in a breast cancer animal model. Since Ldb1 global knockout is embryonic lethal (Mukhopadhyay et al. 2003), we used a conditional Ldb1 knockout mouse model. In the current study we hypothesize that *conditional deletion of the Ldb1*

gene in the mammary gland results in an increase in SLK kinase activity that may enhance Neu-driven tumorigenesis.

Before studying the *role of Ldb1 in Neu-overexpressing breast cancer in-vivo*, we will analyze the *effect of Ldb1 deletion on mammary gland development* as defects in the tissue may affect the interpretation of the tumorigenesis studies. This is important to address as previously published reports have established a role for Ldb1 in mammary gland development (Salmans et al. 2014; Visvader et al. 2001). Preliminary data from our lab have showed that Ldb1 is involved in the negative regulation of SLK activity in MEF3T3 fibroblasts (Storbeck et al. 2009). Accordingly, we will be assessing the *effect of Ldb1 deletion on SLK kinase activity in Neu-overexpressing tumors*. Furthermore, a previous study done in MEF3T3 fibroblasts outlined a potential role for Ldb1 in the regulation of cellular motility (Storbeck et al. 2009). For this reason, we will be studying the *effect of Ldb1 deletion on the metastatic potential of Neu-overexpressing breast cancer cells*.

3. MATERIALS AND METHODS

3.1. Mouse model under study

Through the use of a homologous recombination technique, a *loxP*-flanked neomycin-resistance gene (*Neo*) cassette (*loxP–Neo–loxP*) and a loxP site were inserted into the ninth intron and an upstream region of the *ldb1* gene, respectively, to generate a floxed Ldb1 conditional mutant allele ($Ldb1^{fl/fl}$) in embryonic stem cells as previously described by Zhao et al. 2007 (**Figure 3.1**). Homozygous Ldb1 floxed conditional mutant ($Ldb1^{fl/fl}$) mice provided by Heiner Westphal (Eunice Kennedy Shriver National Institute of Child Health and Human Development, National Institute of Health, U.S.A) were crossed with MMTV-NIC mice provided by William J. Muller (McGill University, Montreal) to generate mammary gland-specific Ldb1 knockout mice (MMTV-NIC^{+} $Ldb1^{-/-}$, hereafter referred to as NIC^{+} $Ldb1^{-/-}$).

Three different cohorts were generated for this study: wildtype (NIC^{+} $Ldb1^{wt/wt}$), heterozygote (NIC^{+} $Ldb1^{wt/-}$) and Ldb1-null (NIC^{+} $Ldb1^{-/-}$). Primary mammary tumor formation was assessed by biweekly physical palpations and mice were sacrificed when the total tumor volume was about 1.7 cm^3 as determined by caliper measurements.

3.2. Genotyping

Genomic DNA was extracted from ear clips taken from 3 weeks old mice at the time of weaning. Polymerase chain reaction (PCR) was used to genotype the floxed Ldb1 conditional mutant allele ($Ldb1^{fl/fl}$) using a pair of primers that flank the loxP site that was inserted into the upstream region of the Ldb1 gene. The sequence of the primers used is as follows: Ldb1-sense, 5′-CAGCAAACGGAGGAAACGGAAGATGTCAG-3′; and Ldb1G, 5′-CTTATGTGACCACAGCCATGCATGCATGTG-3′. Wildtype Ldb1 allele

(Ldb1$^{wt/wt}$) generated a 350 bp band, whereas floxed Ldb1 allele (Ldb1$^{fl/fl}$) generated a 400 bp band. The primer pairs used to amplify the *cre* gene were obtained from eurofins mwg/operon and their sequence was as follows: Cre-1S, 5'GGGATTGCTTATAACACCCTGTTACG3'; and Cre-2AS, 5' TATTCGGATCATCAGCTACACCAGAG3' The PCR amplified a 240 bp fragment for the *cre* allele.

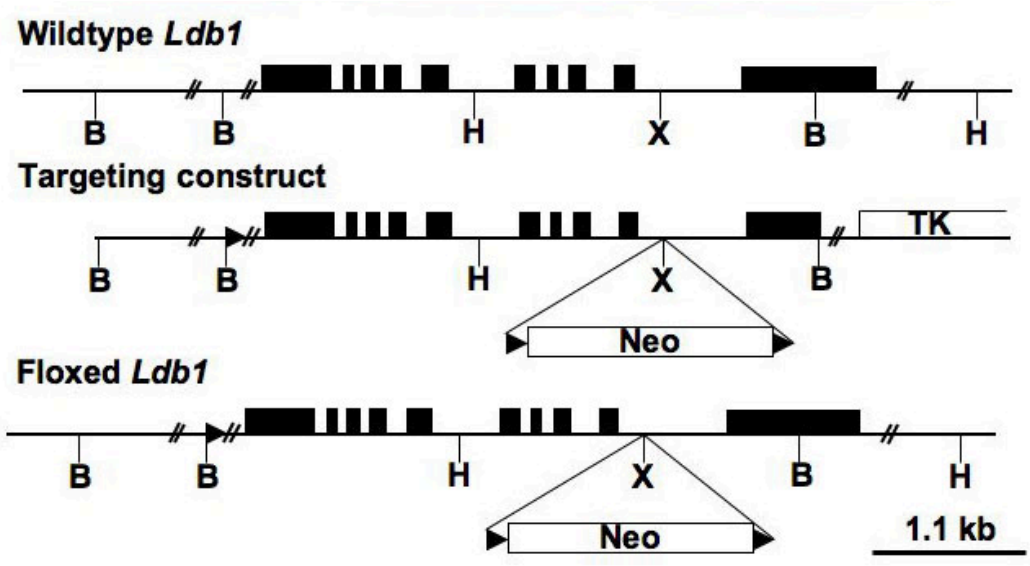

Figure. 3.1. Diagram illustrating the generation of an Ldb1 conditional mutant allele in embryonic stem cells. Ldb1 wild type allele, the targeting construct, and the Ldb1 conditional mutant allele are shown in the diagram. Black bars represent the exons of the Ldb1 gene, arrowheads represent loxP sites inserted into the Ldb1 locus. To generate an Ldb1 conditional mutant allele, a *loxP*-flanked neomycin-resistance gene (*Neo*) cassette (*loxP–Neo–loxP*) and a loxP site were inserted into the ninth intron and an upstream region of the ldb1 gene, respectively, through the use of homologous recombination. Neo, neomycin-resistance gene; TK, thymidine kinase gene; B, BamHI; H, HindII and X, Xbal. Reproduced with permission from Zhao et al. 2007.

3.3. Neu-induced primary tumor cell culture

Primary tumors were extracted from wildtype and Ldb1-null mice at endpoint and washed 3 times with Dulbecco's phosphate buffered saline 1X (DPBS 1X)(Corning, Cellgro, USA). After washing, the extracted tumors were chopped into small pieces using a scalpel and then collagenase type II was added to dissociate/disaggregate the tumor fragments. Collagenase type II (Gibco Life Technologies Inc, USA, Catalog No: 17101-015) was dissolved in serum free Dulbecco's Modification of Eagle's Medium 1X [DMEM 1X] (Corning Cellgro, USA) to a final concentration of 3mg/ml. Dispersed tumor cells were incubated with collagenase type II at 37°C in 5% CO_2 for 45 minutes. Following incubation with collagenase type II, the dispersed cells were washed 5 times using DMEM1X with 10% fetal bovine serum (FBS) and centrifuged after each wash for 1 minute at 300rcp. After the final wash, the tumor cell pellet was resuspended in tumor media and cultured at 37°C and 5% CO_2. Tumor media contains a 1:1 ratio of DMEM1X to F-12 (1X) Nutrient Mixture (Ham) (Gibco Life Technologies Inc, USA); 10% FBS (Sigma, USA), 1% mammary epithelial growth supplements (MEGS) (Gibco Life Technologies, Catalog No: S-015-5), and 1% penicillin streptomycin (Pen strep) (Gibco Life Technologies Inc, USA). Tumor media (described above) is used for culturing primary mammary tumor cells on collagen-coated plates [Collagen type I Rat Tail, Corning, REF: 354236, diluted 1 in 10 in sterile double distilled water (ddH_2O)]. When cells were 80-90% confluent, the cultures were split 1 in 2 and cultured for 2-5 days until they were 80-90% confluent again and ready for splitting.

3.4. In-vitro Boyden Chamber migration and Matrigel invasion assays

The isolated wildtype and Ldb1-null Neu-induced tumor cells were used to conduct in-vitro Boyden Chamber Chemotaxis and Haptotaxis migration assays. Tumor cells (1 x 10^5 cells) were suspended in a serum free DMEM1X media (Corning Cellgro, USA) and added to the top well of the chamber, whereas complete tumor media was added to the bottom well of the chamber. DMEM 1X serum free media contains penicillin streptomycin (Pen strep), but does not contain FBS. For Haptotaxis migration assay, the porous membrane in Boyden chamber was coated with fibronectin (Sigma-Aldrich, USA. Product Number: F1141) diluted in sterile DPBS 1X to a final concentration of 10 μg/ml. To coat the porous membrane, diluted fibronectin was added to the bottom well of the Boyden Chamber and the chamber was left in the incubator at 37°C and 5% CO_2 for 45 minutes. DPBS 1X was then added to the bottom well of the Boyden chamber to wash off excess fibronectin. Tumor cells (1 x 10^5 cells) were suspended in complete tumor media and added to the top well of the chamber, and complete tumor media was added to the bottom well of the chamber. The Boyden chamber for both migration assays was maintained at 37°C and 5% CO_2 for 17 hours. For the matrigel invasion assays, 1 x 10^5 tumor cells were suspended in complete tumor media and added to the top well of a matrigel invasion chamber and complete tumor media was added to the bottom well. The chamber was then maintained in the incubator at 37°C and 5% CO_2 for 24 hours. At the end of the incubation period for either the migration or invasion assays, the porous membrane was rinsed in DPBS 1X and Q-tips were used to remove residual cells from the top of the membrane. The porous membrane was then fixed in 4% paraformaldehyde (PFA) for 10 minutes, and stained with 4,6-diamidino-2-phenylindole (DAPI) (Life Technologies Inc, USA. REF: P36931). DAPI fluorescence was used to visualize the cells

that have migrated from the top to the underside of the porous membrane. Cell counts were then performed in triplicates for wildtype and Ldb1-null primary tumor cells, and 5 random fields were counted in each porous membrane for statistical analysis.

3.5. Antibodies

The primary antibodies used for this study were: rabbit polyclonal Ldb1 antibody (Origene Technologies Inc, USA [Catalog No: TA308742]); rabbit polyclonal Ldb2 antibody (Abcam Inc, USA [Catalog No: ab90315]); rabbit polyclonal SLK antibody, described previously (Sabourin et al. 2000); mouse monoclonal α-tubulin antibody (Sigma Aldrich); E-cadherin (BD Transduction Laboratories [Catalog No: 610181]); N-cadherin (BD Transduction Laboratories [Catalog No: 610920]); cyclin D1 (Santa Cruz [Catalog No: sc-20044]); cytokeratin 8 (Abcam [Catalog No: ab7800]); cytokeratin 14 (Abcam [Catalog No: ab53280]); Ki-67 (Millipore [Catalog No: AB9260]); rabbit monoclonal cleaved-caspase 3 (Cell signaling [Catalog No: 9664]); β-actin (Sigma-Aldrich [Catalog No: A2228]); and mouse anti-c-ErbB2/c-Neu (Ab-3) (3B5) monoclonal antibody (EMD Millipore, USA [Catalog No: OP15).

3.6. Immunofluorescence

For the scratch wound induced migration assay, wildtype (NIC^{+} $Ldb1^{wt/wt}$) tumor cells were plated on coverslips coated with fibronectin (Sigma-Aldrich, USA. Product Number: F1141, diluted in sterile DPBS 1X to a final concentration of 10 μg/ml). Confluent monolayers were serum starved overnight. A pipette tip was then used to scrape across the monoconfluent cell layer. The scratched confluent monolayer of primary tumor cells on the coverslip was then washed with PBS, refed by adding tumor media, and then put in the incubator at 37°C and 5% CO_2 for collection at various time points (0, 15, 30, 45 and 60 minutes). After that, the cells were rinsed with 1X (DPBS) 3

times, fixed in 4% PFA for 10 minutes and blocked in 1X (DPBS) containing 7% goat serum for an hour. Anti-Ldb1 or Anti-SLK primary antibody diluted in 5% goat serum in 1X (DPBS) was then added to the fixed cells and incubated overnight at 4°C. The following day, primary antibodies were washed and detected with an anti-rabbit secondary antibody conjugated to either fluorescein isothiocyanate or tetramethyl rhodamine isothiocyanate (Sigma-Aldrich). The coverslips containing the scratched monolayer of cells were then visualized and photographed with AxioCam digital camera using a Zeiss fluorescence microscope.

For immunofluorescence analysis on fixed paraffin embedded tissues, the sections were deparaffinized, subjected to antigen retrieval in 10 mM citrate buffer (pH 6.0) and permeabilized with 0.3% Triton X-100 for 20 minutes at room temperature. The sections were blocked with 7% goat serum in 1X StoPBS for an hour. Primary antibody (cytokeratin 8 or 14) was then added to 5% goat serum in 1X DPBS. Antibodies were detected with either anti-mouse or anti-rabbit secondary antibodies conjugated to either fluorescein isothiocyanate or tetramethyl rhodamine isothiocyanate (Sigma-Aldrich). The sections were then incubated with 5mM $CuSO_4.5H_2O$/50 mM NH4 acetate (pH 5.0) for two hours at room temperature. Finally, samples were visualized and photographed with AxioCam digital camera as described above.

3.7. Immunohistochemistry

Mammary gland and primary tumors were extracted from wildtype and Ldb1-null mice at endpoint. The tissues were fixed overnight in 10% formalin and then transferred to 70% ethanol the following day. The tissues were then paraffin embedded, sectioned at 4 μm and then mounted on glass slides. Sections were deparaffinized, subjected to antigen retrieval in 10 mM citrate buffer (pH 6.0), and quenched in 3% H_2O_2. Triton X-100

(0.3%) was used for improving antibody penetration for IHC. The sections were then incubated with primary antibodies overnight at 4 °C, followed by 30 minutes incubation with horseradish peroxidase (HRP)-conjugated secondary antibodies at room temperature, and then the sections were incubated with 3, 3'-diaminobenzidine (DAB) substrate. After that, the sections were subjected to Hematoxylin staining, dehydrated in ethanol and cleared in xylene before mounting. Finally, the sections were scanned using a Scanscope XT Digital Slide Scanner (Aperio) and analyzed using Imagescope software (Aperio) and ImageJ software.

3.8. Western blot

RIPA lysis buffer [5% 1M Tris pH8, 150 mM NaCl, 1% NP-40, 1% Triton-X, 12 mM NaDeoxycholate, 20%SDS and 0.4% 0.5M ethylenediaminetetraacetic acid (EDTA)] was used for protein extraction from wildtype and Ldb1-null mammary tumors and the established primary tumor cells in culture. Fifty micrograms (50µg) of total tumor lysate was subjected to SDS-polyacrylamide gel electrophoresis (PAGE) and the gels were then transferred to polyvinylidene difluoride (PVDF) membranes. Blots were probed with primary antibodies for 1 hour at room temperature. The PVDF membrane was incubated with Ldb1 primary antibody overnight at 4°C in 5% bovine serum albumin (BSA) or skim milk in 0.1% Tris-Buffered Saline and Tween 20 (TBST). 0.1% TBST washing buffer was used to wash the PVDF membrane (500ml of 0.1% TBST is made by mixing 50 ml of 10X Tris-Buffered Saline (TBS) pH 7.5, 450ml of dH_2O and 500 µL of Tween 20). Secondary horseradish peroxidase (HRP)-conjugated anti-rabbit or anti-mouse secondary antibodies (BIO-RAD) were then added to the probed membrane for 1 hour at room temperature. The reactions were detected by chemiluminescence (Perkin Elmer, Waltham, MA, USA) and exposure to X-ray film.

3.9. Immunoprecipitation

For SLK immunoprecipitations, 600 µg of total tumor lysate was immunoprecipitated with 2-3 µg of rabbit polyclonal anti- SLK antibody and 20 µL of protein-A-sepharose (GE Healthcare) for 2 hours at 4 °C. The resulting immunocomplexes were then subjected to 5 consecutive cycles of washing with NETN (2% 1M Tris pH 8, 0.2% 0.5M EDTA pH 8, 4.3% 5M NaCl, 0.5% NP-40) and centrifugation (3000 rcf, at 4 °C for 5 minutes), and then loaded on to SDS-polyacrylamide gels for western blot analysis using anti-SLK antibody.

4.0 In-vitro kinase assay

For in-vitro autophosphorylation and Histone H1 kinase assays, SLK protein was immunoprecipitated from total tumor lysates as described above in *Immunoprecipitation*. Kinase assays were performed as described previously (O'Reilly et al. 2005). To stop the kinase reactions, 7 µL of 4X SDS sample buffer was added and the reaction mix was then electrophoresed on SDS gels. For Histone H1 kinase assay, Histone H1 was added to the master mix as a substrate for SLK to phosphorylate [Master mix contains: 1X Kinase Buffer (0.1% 10X kinase buffer [33% 1M Tris pH 7.4, 1.6% 1M NaF, 16.6% 1M β-gly, 1.6% 1M DTT, 12% 2M $MgCl^2$], 0.001% 200 mM $NaVO_3$) and ^{32}P-γATP (5 uCi)]. The Gels were transferred to PVDF membranes and subjected to autoradiography at -80 °C for 2-5 hours.

For the scratch wound induced migration assay, in-vitro kinase assays were performed to assess SLK activity at different time points from 0 to 60 minutes post scratch wounding. In these experiments, wildtype tumor cells were plated on 10 cm dishes, about 4 dishes per time point, and then the plates were scratched using a pipette tip to remove approximately 50% of the monoconfluent layer. The cells were then washed

with PBS to remove non-adherent cells, then complete tumor media was added to the cells and incubated at 37°C and 5% CO_2. The cells were then collected at the different time points for western blot analysis and in-vitro kinase assays.

4.1. Experimental lung colonization assay

Wildtype and Ldb1-null tumor cells were grown to confluency in an incubator at 37°C and 5% CO_2. In-vivo lung colonization assay was performed by injecting 5 x 10^5 cells/100μL (Wildtype vs. Ldb1-null) into the lateral tail vein of CD1 nude mice that were 6 weeks old (Charles River Laboratories) (5 mice per group). All mice were sacrificed 6 weeks post injection and the lungs were isolated for analysis. Specifically, 2 vs. 3 lungs were isolated from mice injected with wildtype and Ldb1-null primary tumor cells, respectively. Pulmonary metastatic lesions on the lung surface were analyzed by inflation with Indian ink, thus allowing easier visual observation and quantification. The rest of the isolated lungs were analyzed by hematoxylin and eosin (H&E) analysis for the presence of pulmonary metastatic lesions. Lung paraffin sections of 4 μm were stained with H&E and the sections were scanned using a Scanscope XT Digital Slide Scanner (Aperio). Specifically, the stained sections were analyzed using Imagescope software (Aperio) to quantify and compare the total number of metastatic foci per lung in the mice injected with wildtype vs. Ldb1-null tumor cells.

4. RESULTS

4.1. Ldb1 is expressed within the mammary ductal epithelium and in the surrounding adipocytes

Prior to analyzing the effect of Ldb1 knockout on mammary gland development, we investigated its expression pattern in wildtype and Ldb1-null mice. IHC was performed for Ldb1 expression on paraffin-embedded sections of mammary glands collected from wildtype (NIC^{+} $Ldb1^{wt/wt}$) and Ldb1-null (NIC^{+} $Ldb1^{-/-}$) adult virgin mice that were 8- 12 weeks old. In wildtype mammary glands, Ldb1 shows nuclear expression within the cuboidal epithelium layer of the lactiferous duct (**Figure 4.1A**). Conversely, Ldb1 expression is absent within the ductal epithelium of Ldb1-null mammary glands (**Figure 4.1B**). Interestingly, when analyzing Ldb1-null mammary gland sections we observed nuclear Ldb1 staining in some of the ducts (**Figure 4.2A)**; which could represent Ldb1-positive/cre recombinase-escapee ductal epithelial cells. Furthermore, positive Ldb1 staining is observed in the adipose tissue surrounding the mammary ducts in both wildtype and Ldb1-null mammary glands (**Figure 4.1A-B**). Overall, IHC analysis demonstrates that Ldb1 is expressed within the mammary ductal epithelium and in the surrounding adipocytes in wildtype mice. Ldb1 knockout results in an absence of its expression specifically within the ductal epithelium of Ldb1-null mammary glands.

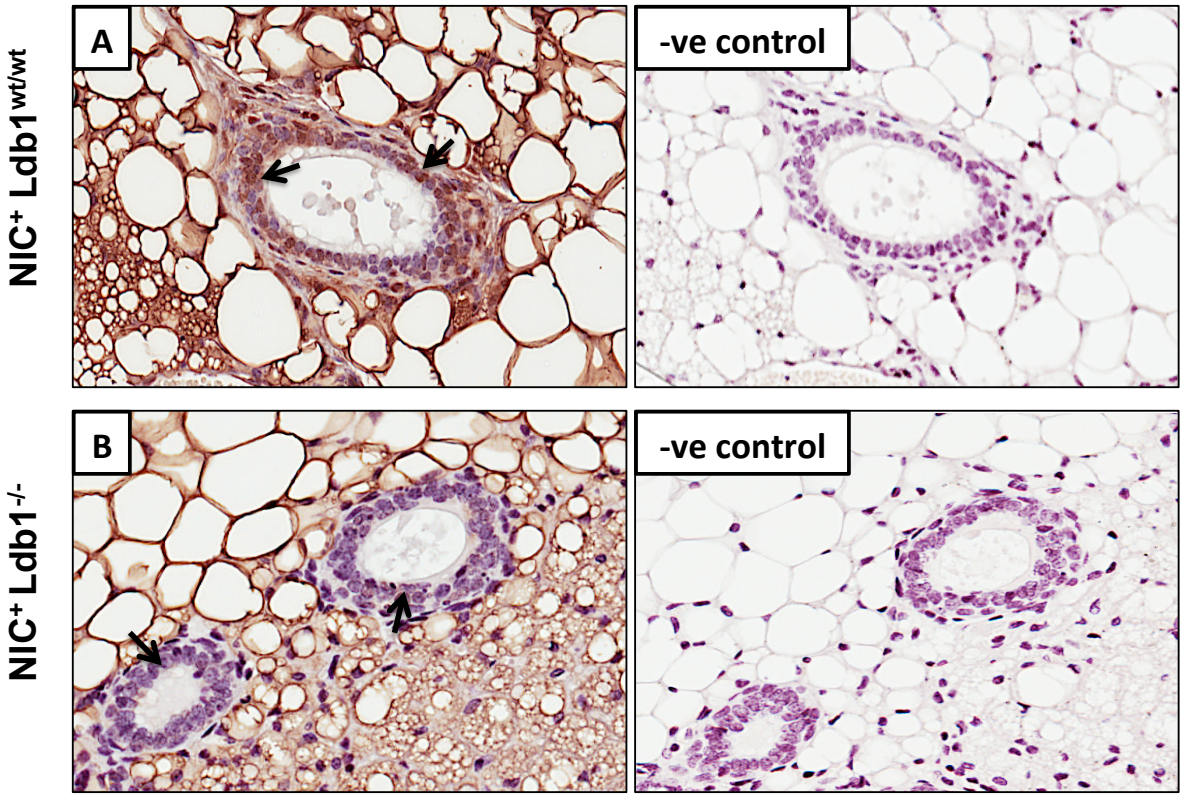

Figure 4.1. Ldb1 expression pattern in the mammary gland. IHC showing Ldb1 expression in mammary gland sections collected from **(A)** wildtype (NIC^{+} $Ldb1^{wt/wt}$) and **(B)** Ldb1-null (NIC^{+} $Ldb1^{-/-}$) virgin adult mice that were 8-12 weeks old. Also, shown is the negative control (-ve control) for the mammary gland sections used for Ldb1 staining; the negative control used is secondary antibody only. **(A)** Ldb1 staining is prominent within the ductal epithelium of wildtype mammary glands (arrows) and in the surrounding adipose tissue. **(B)** Ldb1-null mammary glands lack Ldb1 expression within the ductal epithelium (arrows) but retain Ldb1 expression in the surrounding stroma of the mammary gland.

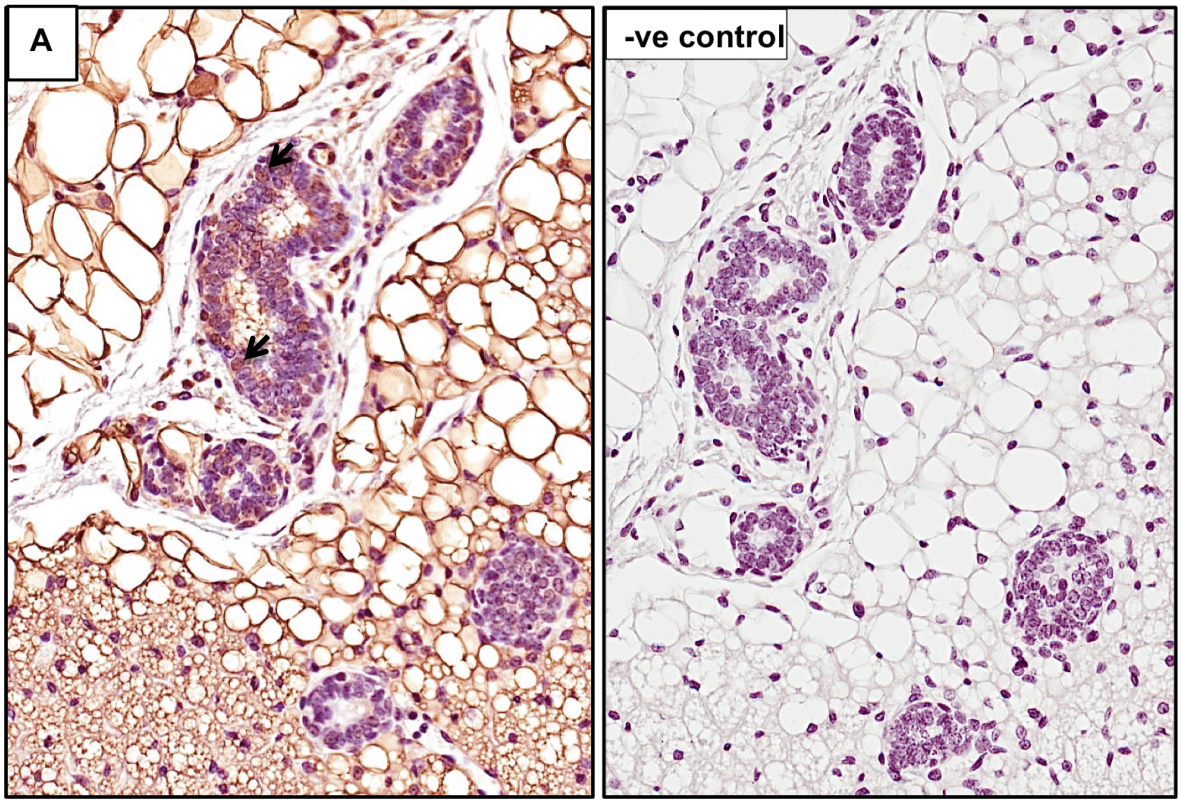

Figure 4.2. Ldb1-positive/cre recombinase-escapee ductal epithelium cells in Ldb1-null mammary glands. **(A)** IHC showing Ldb1 expression in a mammary gland section collected from Ldb1-null (NIC^{+} $Ldb1^{-/-}$) virgin adult mouse (8-12 weeks old). Also, shown is the negative control (-ve control) for the mammary gland section used for Ldb1 staining; the negative control used is secondary antibody only. Nuclear Ldb1 staining is observed within the ductal epithelium in some of the ducts in the mammary gland (arrows); suggesting incomplete cre-mediated deletion of Ldb1 in the mammary gland.

4.2. Ldb1 deletion does not affect the normal organization of mammary epithelial layers and the gross morphology of the mammary gland tissue

Before carrying out tumorigenesis studies, we investigated if Ldb1 deletion in the mammary gland would have adverse effects on the development of the tissue in adult virgin mice. We performed IHC using wildtype (NIC^{+} $Ldb1^{wt/wt}$) and Ldb1-null (NIC^{+} $Ldb1^{-/-}$) mammary glands from adult virgin mice to stain for the luminal epithelial layer marker cytokeratin 8 (CK-8), and the basal epithelial layer marker cytokeratin 14 (CK-14). We found that luminal CK-8 and basal CK-14 are expressed uniformly in both wildtype and Ldb1-null mammary ductal epithelium (**Figure 4.3**). This finding suggests that Ldb1 is not essential for mediating mammary ductal epithelial organization during development. Also, H&E staining was performed and showed that Ldb1 deletion did not affect the microscopic structure of the mammary gland (**Figure 4.4**). Together, these results suggest that Ldb1 deletion does not affect the normal organization of mammary epithelial layers and the gross morphology of the tissue in adult virgin mice.

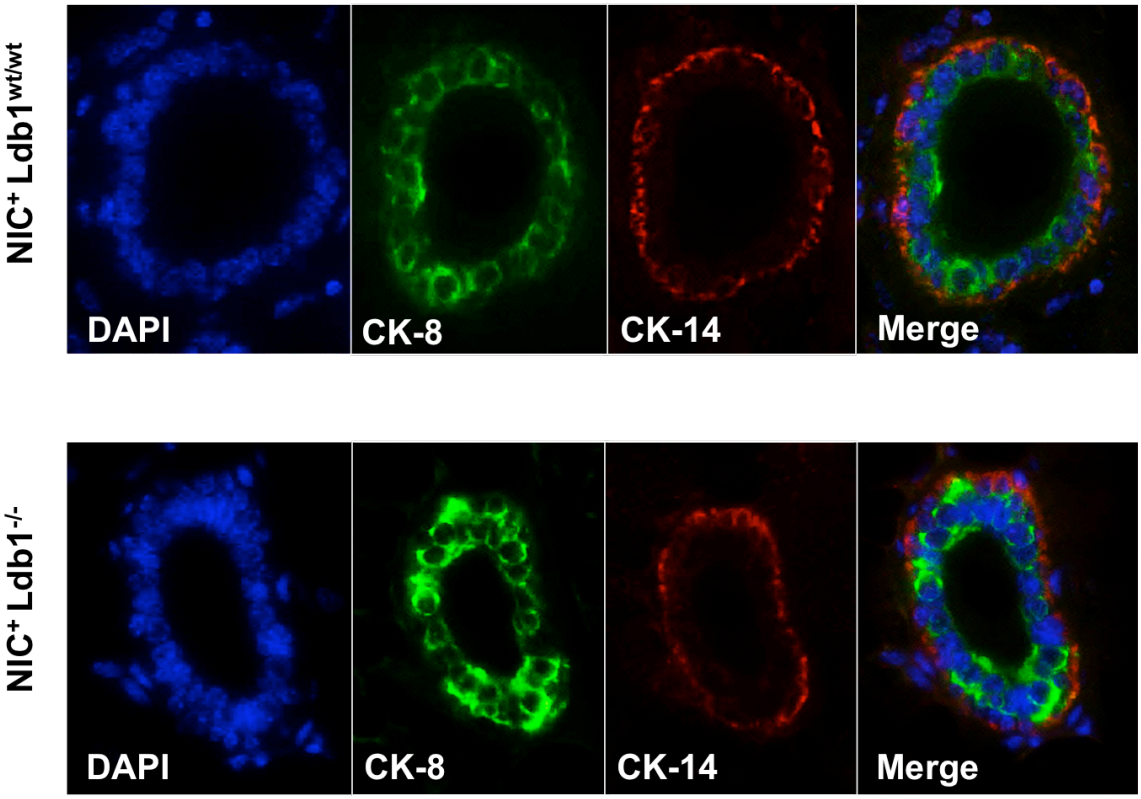

Figure 4.3. Ldb1 deletion does not affect CK8 or CK14 expression within the ductal epithelium in adult virgin mammary glands. To study the impact of Ldb1 deletion on mammary gland development, paraffin-embedded sections of virgin adult mammary glands (8 to 12 weeks old) from wildtype (NIC^+ $Ldb1^{wt/wt}$) and Ldb1-null (NIC^+ $Ldb1^{-/-}$) mice were subjected to double immunofluorescence staining for cytokeratin 8 (CK-8) to mark mammary luminal epithelial cell layer and cytokeratin 14 (CK-14) to mark mammary myoepithelial/basal cells. Ldb1 deletion does not affect CK-8 or CK-14 expression; hence, Ldb1 deletion does not affect the normal organization of mammary epithelial layers in adult virgin mice.

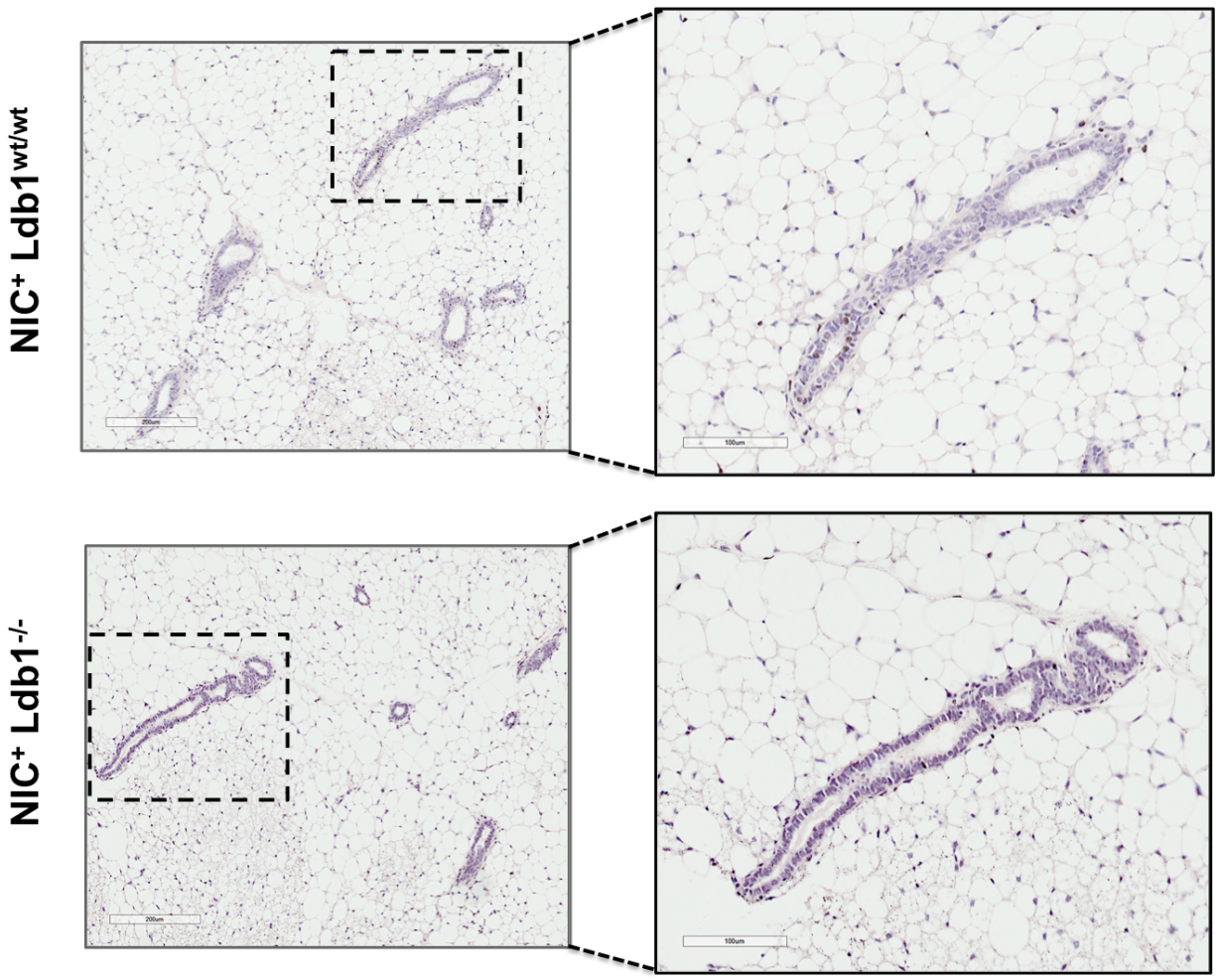

Figure 4.4. Ldb1 deletion does not affect the gross morphology of the mammary gland. H&E staining showing mammary gland sections from wildtype (NIC^{+} $Ldb1^{wt/wt}$) and Ldb1-null (NIC^{+} $Ldb1^{-/-}$) virgin adult mice (8-12 weeks old). H&E stained sections show no difference in the microscopic structure of the mammary gland between wildtype and Ldb1-null mice.

4.3. Ldb1 expression in Neu-induced primary mammary tumors

To assess the role of Ldb1 in Neu-induced mammary tumorigenesis, we interbred Ldb1-floxed mice with MMTV-NIC mice to generate Ldb1-null female mice. MMTV-NIC mice express the Neu mutant (NDL 2-5) and cre recombinase from the same transcript. The expression of the MMTV-NIC transgene results in the formation of invasive mammary ductal carcinomas (Ranger et al. 2009). Three cohorts of mice were generated for this study: wildtype (NIC^{+} $Ldb1^{wt/wt}$), heterozygote (NIC^{+} $Ldb1^{wt/-}$), and Ldb1 null (NIC^{+} $Ldb1^{-/-}$). The expression of Ldb1 in Neu-induced mammary tumors was assessed for the three different cohorts at endpoint by western blot. As shown in **Figure 4.5**, the Cre/loxP system is efficient in the excision of the Ldb1 gene as demonstrated by the absence of Ldb1 expression in mammary tumors isolated from Ldb1-null mice. Also, western blot showed that the expression of Ldb2, SLK and ErbB2 is equivalent among the three different genotypes, suggesting that Ldb1 deletion does not have an impact on the expression of these proteins in Neu-induced mammary tumors (**Figure 4.5**). Overall, the Cre-loxP system efficiently mediated Ldb1-deletion and did not affect the expression of its highly related paralog, Ldb2, in Neu-induced primary tumors.

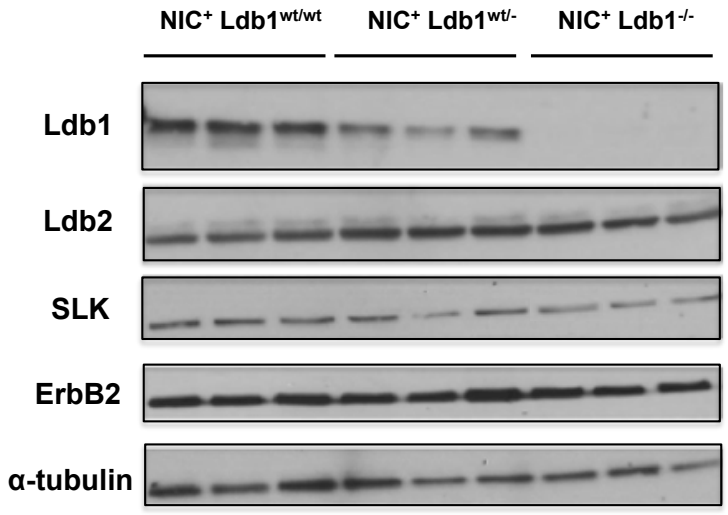

Figure 4.5. Ldb1 expression in Neu-induced mammary tumors. Western blot analysis of whole tumor lysates obtained from wildtype (NIC^+ $Ldb1^{wt/wt}$), heterozygote (NIC^+ $Ldb1^{wt/-}$) and Ldb1-null (NIC^+ $Ldb1^{-/-}$) mice. The expression of Ldb1, Ldb2, SLK and ErbB2 was compared among the three different genotypes. The α-tubulin served as a loading control. Cre-mediated excision of Ldb1 is efficient in Ldb1-null mice. The expression of Ldb1 related paralog, Ldb2, is equivalent among the three different genotypes. This suggests that the Cre-loxP system is specifically targeting the floxed *Ldb1* gene for excision. Also, the expression of SLK and ErbB2 is not affected by Ldb1 deletion in the tumors.

4.4. Mammary-specific Ldb1 deletion does not affect overall survival and tumor growth

To test the role of Ldb1 on the progression of Neu-induced tumors, cohorts of Ldb1 conditional knockout mice were tracked for tumor onset and overall survival. Kaplan-Meier survival curves of mice classified based on Ldb1 expression (wildtype: NIC^{+} $Ldb1^{wt/wt}$, heterozygote NIC^{+} $Ldb1^{wt/-}$, and Ldb1 null NIC^{+} $Ldb1^{-/-}$) were generated. For the three cohorts under study, endpoint was determined when the total tumor volume was about 1.7 cm^3. All mice had a similar overall survival of approximately 160 days. No statistically significant difference was observed when comparing the survival curves of wildtype and Ldb1-null mice (p=0.111), or when comparing wildtype and heterozygote (NIC^{+} $Ldb1^{wt/-}$) overall survival curves (p=0.0911) (**Figure 4.6A)**. The formation of primary mammary tumors was monitored by physical palpations on a biweekly basis. Percentage of tumor-free plots showed that all mice, irrespective of their genotype, developed tumors around the same time point at approximately 144 days. As shown in **Figure 4.6B**, no significant difference was observed when comparing wildtype and Ldb1-null Kaplan Meier tumor free survival curves (p=0.101); or when comparing wildtype and heterozygote (NIC^{+} $Ldb1^{wt/-}$) tumor free survival curves (p=0.208). Moreover, tumors removed at endpoint showed no statistically significant difference in the total tumor volume per mouse between wildtype and Ldb1-null mice (p=0.99) (**Figure 4.7**). We also assessed the proliferation and apoptotic rates of primary tumors isolated from wildtype and Ldb1-null mice by measuring the percentage of ki-67 and active cleaved caspase-3 positive cells among the total number of tumor cells, respectively. As shown in **Figure 4.8A**, Ldb1 deletion had no significant effect on the fraction of Ki-67 positive primary tumor cells (p=0.67). Supporting this, no difference was observed when comparing the

expression level of the proliferative marker *cyclin D1* in the tumor lysates among the three different genotypes under study (**Figure 4.8B**). Furthermore, Ldb1 deletion had no significant effect on the number of active cleaved caspase 3-positive cells in Neu-induced primary tumors (p=0.93) (**Figure 4.9A**). Western blot analysis confirmed this by showing no difference in the expression level of active cleaved caspase-3 in the tumor lysates extracted from the three different cohorts (**Figure 4.9B**). Thus, Ldb1 deletion in primary Neu-overexpressing tumors does not affect proliferation or apoptosis. Taken together, these results suggest that Ldb1 is not required for the progression of Neu-induced tumors; its deletion does not affect overall survival or Neu-mediated tumor growth in an MMTV-NIC mouse model.

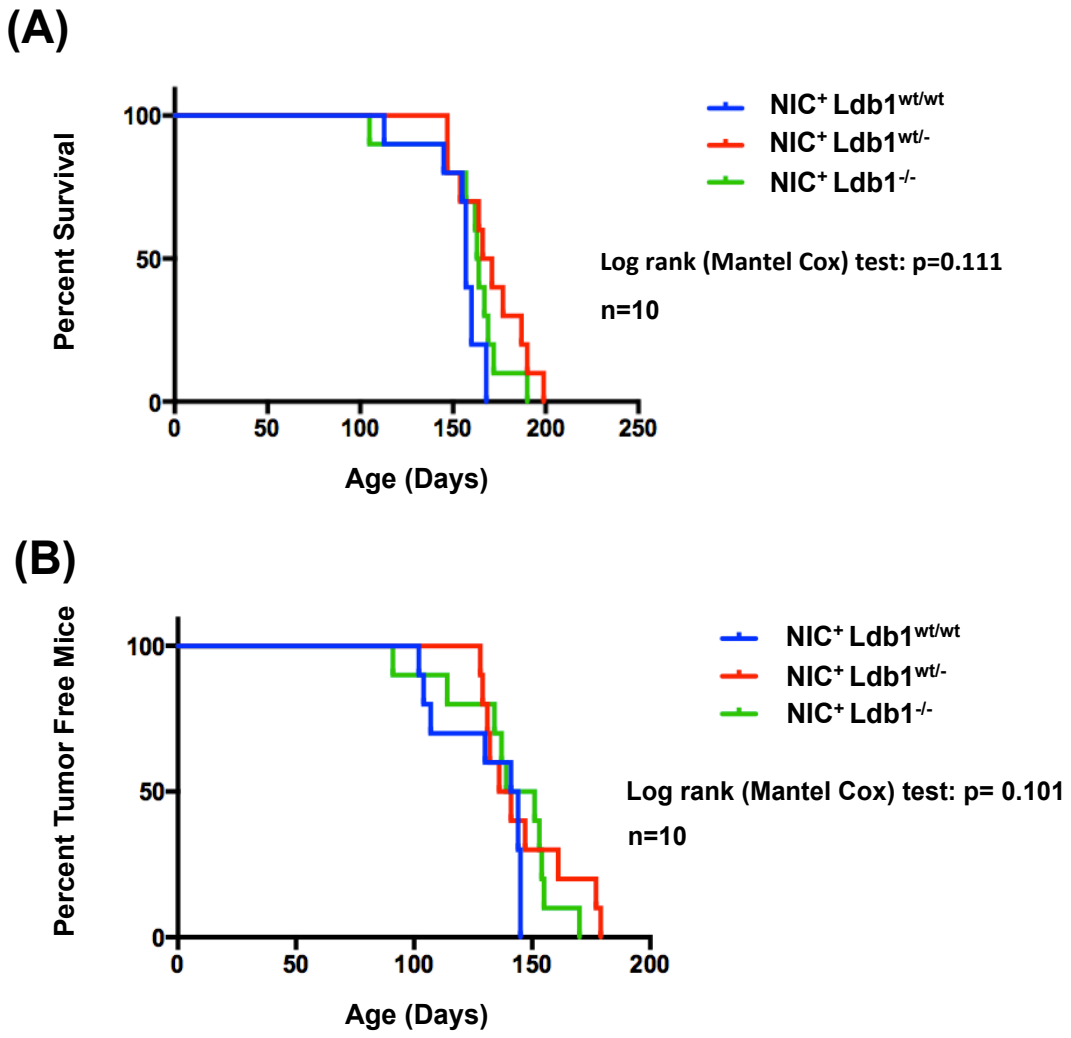

Figure 4.6. Ldb1 deletion does not affect overall survival and tumor onset. Kaplan-Meier curves displaying **(A)** overall survival and **(B)** the percentage of tumor-free mice from date of birth to tumor onset for wildtype (NIC^+ $Ldb1^{wt/wt}$), heterozygote (NIC^+ $Ldb1^{wt/-}$) and Ldb1-null (NIC^+ $Ldb1^{-/-}$) mice. Ten mice (n=10) from each genotype were used to generate the curves. The p-value was determined using the log rank (Mantel Cox) test. The displayed p-values are comparing wildtype and Ldb1-null Kaplan-Meier curves. For overall survival analysis, endpoint was determined when the total tumor volume was about 1.7 cm^3, and for tumor onset analysis, tumor formation was detected by biweekly physical palpations. All mice, irrespective of their genotype developed tumors at approximately 144 days and they all had a similar overall survival of 160 days.

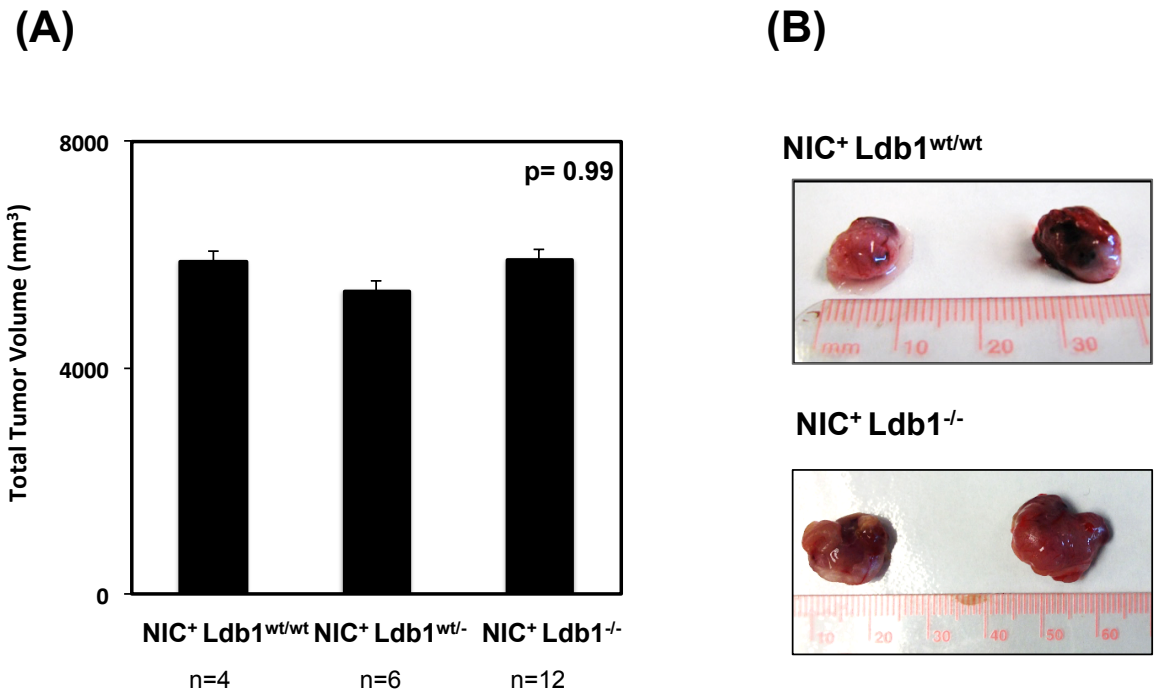

Figure 4.7. Ldb1 deletion does not affect total tumor volume at endpoint. (A) Tumors from 4 wildtype (NIC^+ $Ldb1^{wt/wt}$), 6 heterozygote (NIC^+ $Ldb1^{wt/-}$), and 12 Ldb1-null (NIC^+ $Ldb1^{-/-}$) mice were extracted at endpoint and analyzed using the sphere volume equation ($V= 4/3\ \pi\ r^3$) to determine total tumor volume (TTV) per mouse. The P-value was calculated using a two-tailed student's t-test. The displayed p-value is comparing wildtype and Ldb1-null TTV per mouse (p=0.99). **(B)** Shows tumors at endpoint from wildtype (NIC^+ $Ldb1^{wt/wt}$) and Ldb1-null (NIC^+ $Ldb1^{-/-}$) mice extracted for volume calculation to determine the TTV per mouse.

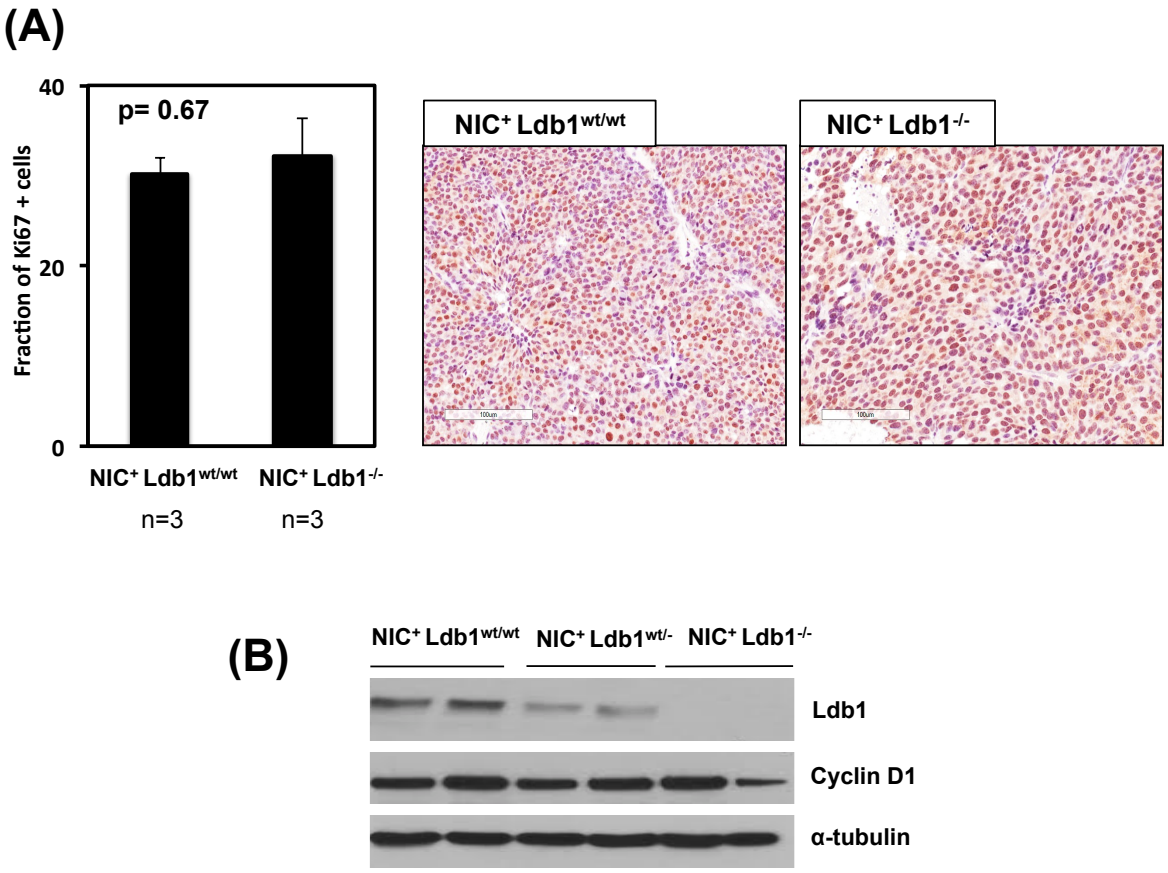

Figure 4.8. Ldb1 deletion does not affect proliferation in Neu-induced primary mammary tumors. (A) IHC showing Ki-67 staining of wildtype (NIC^+ $Ldb1^{wt/wt}$) and Ldb1-null (NIC^+ $Ldb1^{-/-}$) primary Neu-induced tumors. Tumor paraffin-embedded sections from three different wildtype and Ldb1-null mice were compared (n=3); and 5 different section views for each primary tumor section were used for analysis. ImageJ software was used to calculate the number of Ki67+ cells over the total number of tumor cells. No significant difference was observed in the fraction of Ki67 positive cells when comparing wildtype and Ldb1-null primary tumors. The P-value was calculated using a two-tailed student's t-test (p=0.67). **(B)** Western blot showing cyclin D1 expression in whole tumor lysates from wildtype (NIC^+ $Ldb1^{wt/wt}$), heterozygote (NIC^+ $Ldb1^{wt/-}$) and Ldb1-null (NIC^+ $Ldb1^{-/-}$) mice. No difference in cyclin D1 expression level was observed when comparing the three different genotypes under study.

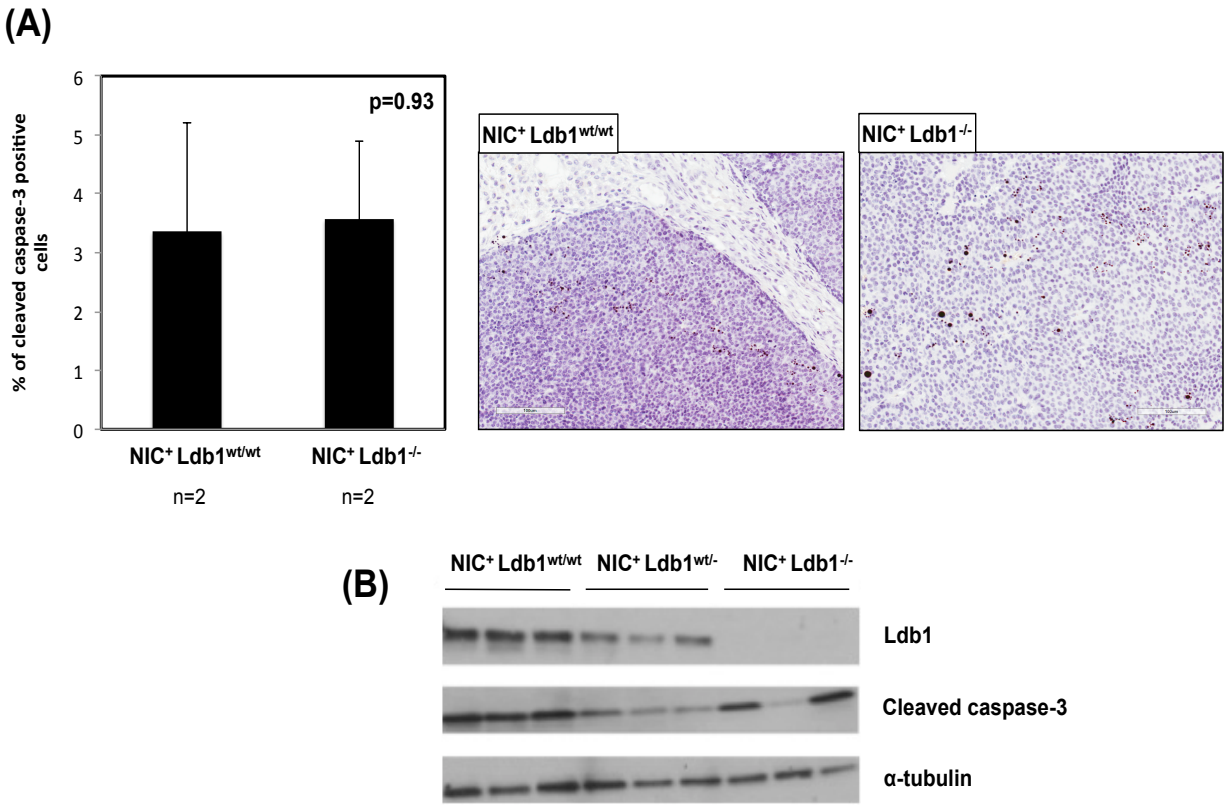

Figure 4.9. Ldb1 deletion does not affect apoptosis in Neu-induced primary mammary tumors. (A) IHC showing cleaved caspase-3 staining of wildtype (NIC^+ $Ldb1^{wt/wt}$) and Ldb1-null (NIC^+ $Ldb1^{-/-}$) primary Neu-induced tumors. ImageJ software was used to calculate the number of active cleaved caspase-3+ cells over the total number of tumor cells. Tumor paraffin-embedded sections from two different wildtype and Ldb1-null mice were compared (n=2). No significant difference was observed in the percentage of active cleaved-caspase positive cells between wildtype and Ldb-1 null primary tumor sections. The P-value was calculated using a two-tailed student's t-test (p=0.93). **(B)** Western blot showing cleaved caspase-3 expression in whole tumor lysates from wildtype (NIC^+ $Ldb1^{wt/wt}$), heterozygote (NIC^+ $Ldb1^{wt/-}$) and Ldb1-null (NIC^+ $Ldb1^{-/-}$) mice. No consistent difference in cleaved caspase-3 expression was observed among the three different genotypes.

4.5. Mammary-specific Ldb1 deletion does not affect SLK autophosphorylation or SLK kinase activity in-vivo

Previously it was shown that Ldb1 knockdown is associated with an increase in SLK kinase activity in MEF3T3 fibroblasts (Storbeck et al. 2009). This led us to examine the effect of Ldb1 deletion on SLK activity in primary tumors. Specifically, we predicted that Ldb1 deletion would result in an upregulation of SLK activity in Ldb1-null tumors. Tumor lysates from wildtype (NIC^{+} $Ldb1^{wt/wt}$) and Ldb1-null (NIC^{+} $Ldb1^{-/-}$) mice were used to perform an in-vitro kinase assay to assess SLK autophosphorylation activity. Also, a Histone H1 kinase assay was performed to assess SLK kinase activity in the tumor lysates. Surprisingly, Ldb1 deletion did not have a significant effect on SLK activity as measured by its autophosphorylation ($p=0.95$) (**Figure 4.10**), or by the phosphorylation of its substrate Histone H1 ($p=0.24$) (**Figure 4.11**). Taken together, these data suggest that Ldb1 does not regulate SLK activity in Neu-transformed primary tumors.

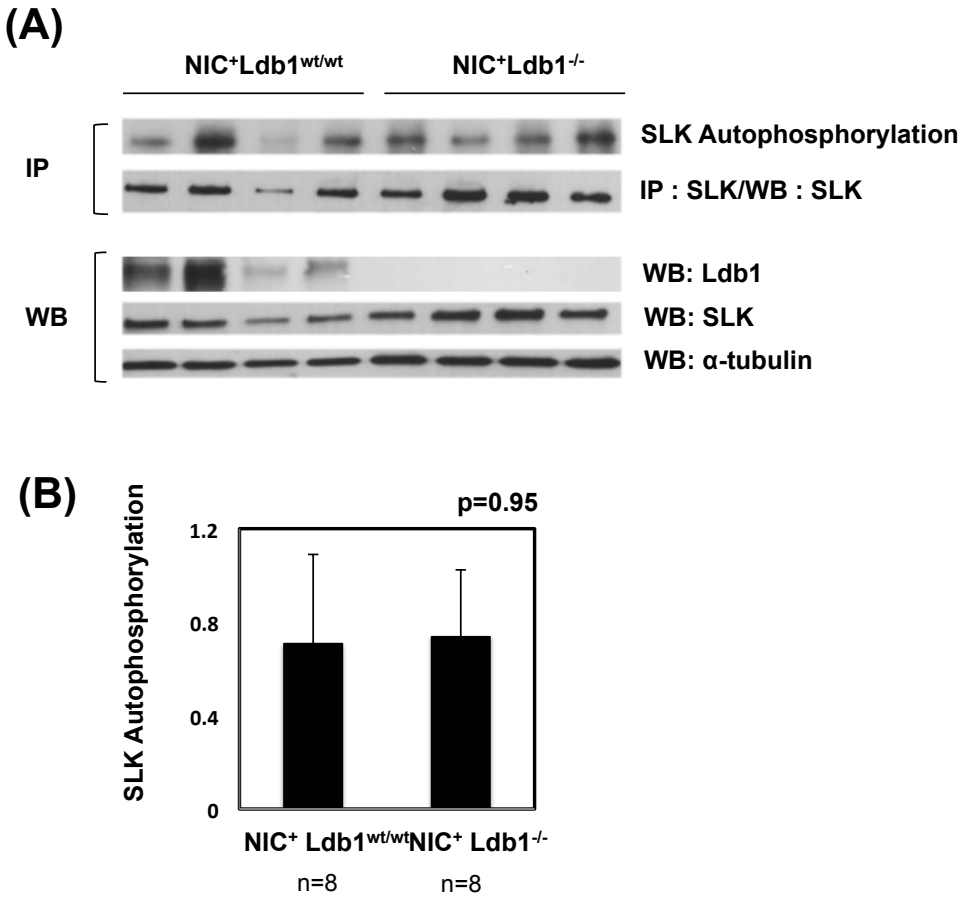

Figure 4.10. Conditional Ldb1 knockout in the mammary gland does not affect SLK autophosphorylation level. (A) In-vitro kinase assay was performed using whole tumor lysates from wildtype (NIC^+ $Ldb1^{wt/wt}$) and Ldb1-null (NIC^+ $Ldb1^{-/-}$) mice to assess SLK autophosphorylation level. A total of 8 different tumors were used for analysis from each genotype. **(B)** Shows densitometric quantification of the in-vitro kinase assay data after normalization to immunoprecipitated SLK. No significant difference was observed in SLK autophosphorylation level between wildtype and Ldb1-null primary tumor lysates. The P-value was calculated using a two-tailed student's t-test (p=0.95).

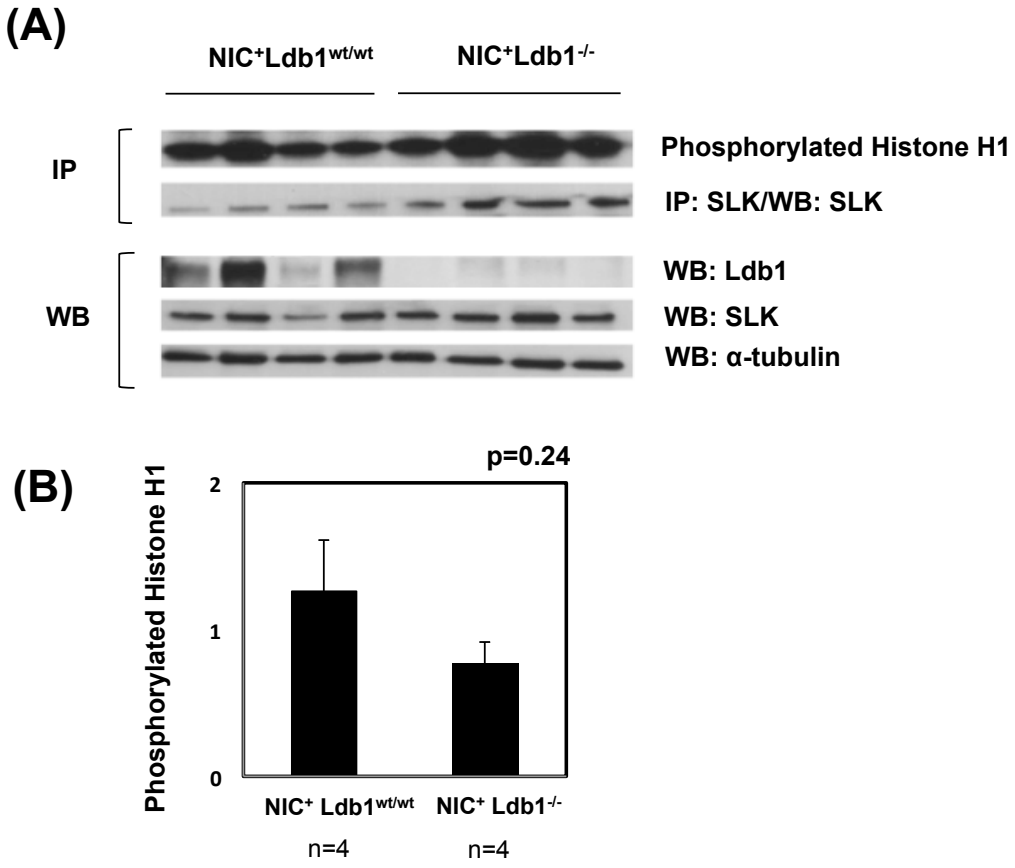

Figure 4.11. Conditional Ldb1 knockout in the mammary gland does not affect SLK kinase activity. (A) In-vitro Histone H1- Kinase assay was performed using whole tumor lysates from wildtype (NIC^+ $Ldb1^{wt/wt}$) and Ldb1-null (NIC^+ $Ldb1^{-/-}$) mice to assess SLK kinase activity level. A total of 4 different tumors were used for analysis from each genotype. **(B)** Shows densitometric quantification of the in-vitro kinase assay data after normalization to immunoprecipitated SLK. No significant difference was observed in SLK kinase activity between wildtype and Ldb1-null primary tumor lysates. The P-value was calculated using a two-tailed student's t-test (p=0.24).

4.6. Ldb1 and SLK do not co-localize in migrating tumor cells

Previously, in-vitro direct binding assays showed that Ldb1 binds directly to the ATH domain of SLK in MEF3T3 fibroblasts to negatively regulate its activity (Storbeck et al. 2009). For this reason, we initially sought to investigate if Ldb1 and SLK interact in-vivo. In the current study, we could not co-immunoprecipitate SLK and Ldb1 in primary tumor lysates and in the established tumor cells (exponentially growing or migrating tumor cells), suggesting that both proteins may not interact in-vivo. An earlier study provided evidence for Ldb1 and SLK colocalization during cellular migration (Storbeck et al. 2009, Baron et al. 2015). Accordingly, we investigated the distribution of Ldb1 and SLK by immunofluorescence (IF) in migrating tumor cells that we established from wildtype mice. Prior to this experiment however, we assayed the specificity of the Ldb1 antibody used for IF analysis. IF was performed to stain for Ldb1 in the established wildtype and Ldb1-null tumor cells, which served as positive and negative controls for Ldb1 expression, respectively. IF analysis showed that in exponentially growing wildtype tumor cells, Ldb1 is expressed in the nucleus and the cytoplasm, however, Ldb1-null tumor cells showed no Ldb1 expression (**Figure 4.12A**). Supporting this, we detected very low levels of Ldb1 in the Ldb1-null tumor cell population by western blot analysis. This residual Ldb1 expression could be due to fibroblast cell contamination in the established tumor cells in culture (**Figure 4.12B**). Taken together, these data confirm the specificity of the Ldb1 antibody and validate its use for IF analysis.

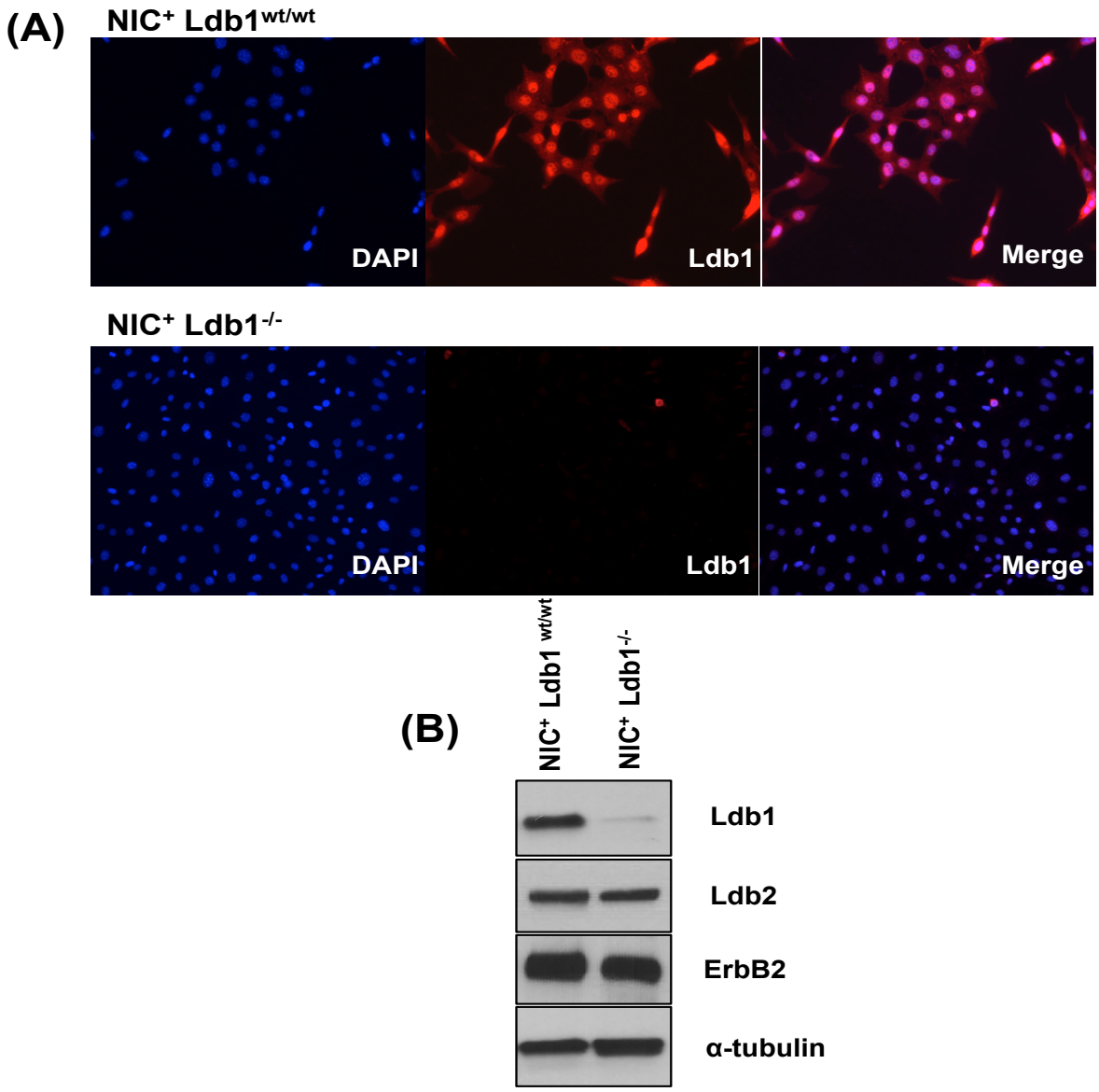

Figure 4.12. Validation of the Ldb1 antibody. (A) IF staining for Ldb1 in exponentially growing wildtype (NIC^+ $Ldb1^{wt/wt}$) (top panel) and Ldb1-null (NIC^+ $Ldb1^{-/-}$) (bottom panel) primary tumor cells. No Ldb1 expression is detected in the Ldb1-null primary tumor cells. **(B)** Western blot analysis using lysates from the established primary tumor cells in culture showed an absence of Ldb1 expression in the tumor cells extracted from Ldb1-null mice when compared to the high Ldb1 expression level in the primary tumor cells extracted from wildtype mice. Overall, these data support the specificity of the Ldb1 antibody.

To determine the localization of Ldb1 and SLK during migration, scratch-wound assays followed by IF were performed using wildtype tumor cells**.** Our lab has previously shown that Ldb1 and SLK colocalize at the leading edge of migrating MEF3T3 fibroblasts within 60 minutes post wounding (Baron et al. 2015). In this study, IF was performed separately for Ldb1 and SLK since they both require anti-rabbit secondary antibody. At 60 minutes post-wounding, SLK staining is strong in the cytoplasm and is more defined at the leading edge of migrating cells, whereas Ldb1 shows prominent nuclear staining in migrating tumor cells (**Figure 4.13**). Interestingly, the staining observed at the 60 minutes time point for Ldb1 and SLK occurs within 15 minutes post wounding (**Figure 4.14**), suggesting that Ldb1 mediates migration primarily by its transcriptional cofactor function. Since Ldb1 and SLK do not colocalize, hence Ldb1 does not regulate SLK activity by direct interaction in migrating Neu-induced tumor cells. Interestingly in the same experiment, we observed that both Ldb1 and SLK show strong cytoplasmic staining at 0 minutes (**Figure 4.15C**). Accordingly, we performed in-vitro kinase assays to assess SLK activity at the 0 and 60 minutes time points, when Ldb1 and SLK are expressed in the same and different cellular compartments, respectively (**Figure 4.15C**). Kinase assays show that SLK activity at the 0 minute time point is comparable to its activity at 60 minutes post wounding (**Figure 4.15B**); suggesting that Ldb1 does not regulate SLK activity in migrating tumor cells. Taken together, our data show that Ldb1 does not colocalize with SLK and does not regulate SLK activity in migrating tumor cells.

Western analysis for Ldb1 during wounding-induced migration showed that Ldb1 is expressed at high levels at 0 minutes; however, a dramatic decrease in Ldb1 expression level occurred at 15 minutes post wounding and this decrease was retained from 15 to 60 minutes post wounding (**Figure 4.15A**). The observed decrease in Ldb1 expression level might be a mechanism used by the primary tumor cells to activate migration.

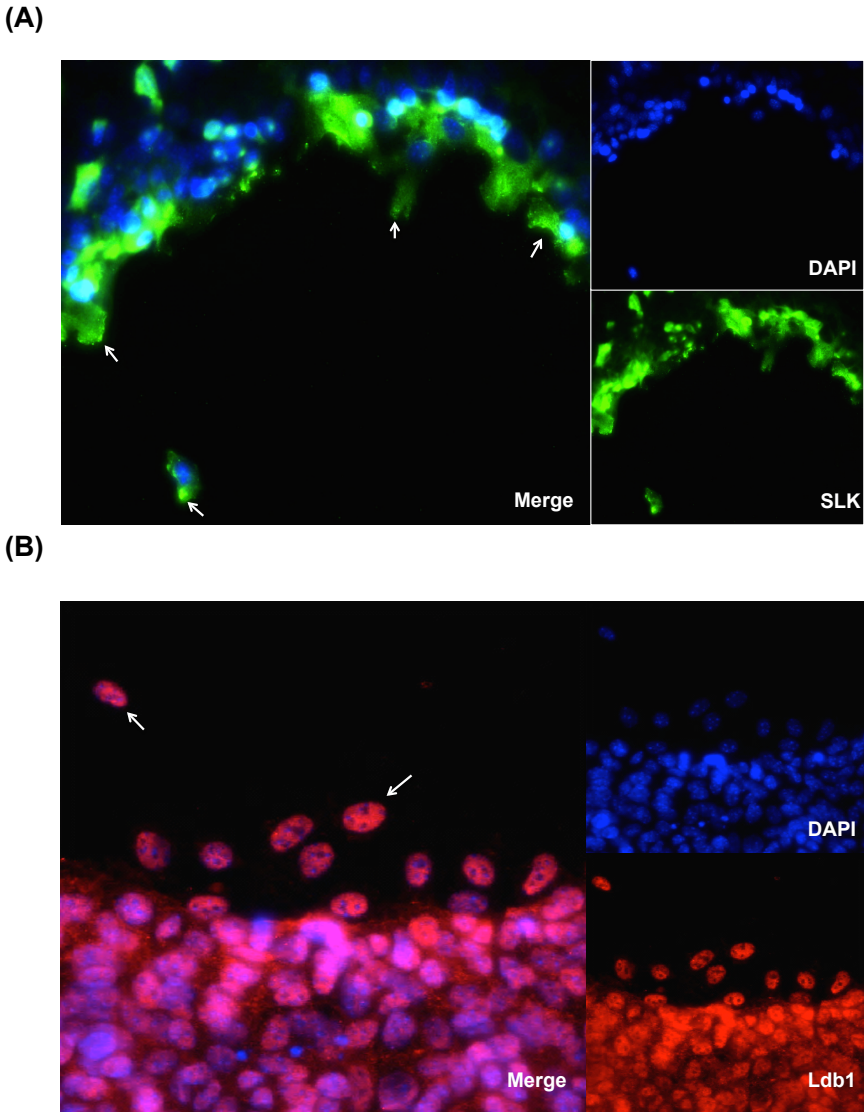

Figure 4.13. Ldb1 and SLK do not colocalize during scratch wound-induced cellular migration of tumor cells. Confluent monolayer of wildtype Ldb1-expressing primary tumor cells (NIC^{+} Ldb1 $^{wt/wt}$) was grown on coverslips coated with fibronectin. The cells were serum starved overnight and scratched the following day with a pipette tip. Cells were then refed with the addition of tumor growth media and collected at 60 minutes post wounding for IF analysis using anti-Ldb1 and anti-SLK antibodies as previously described in *Materials and Methods*. **(A)** Shows SLK staining and **(B)** Ldb1 staining at the wound site at 60 minutes post wounding. The arrows indicate regions of positive SLK and Ldb1 staining.

(C)

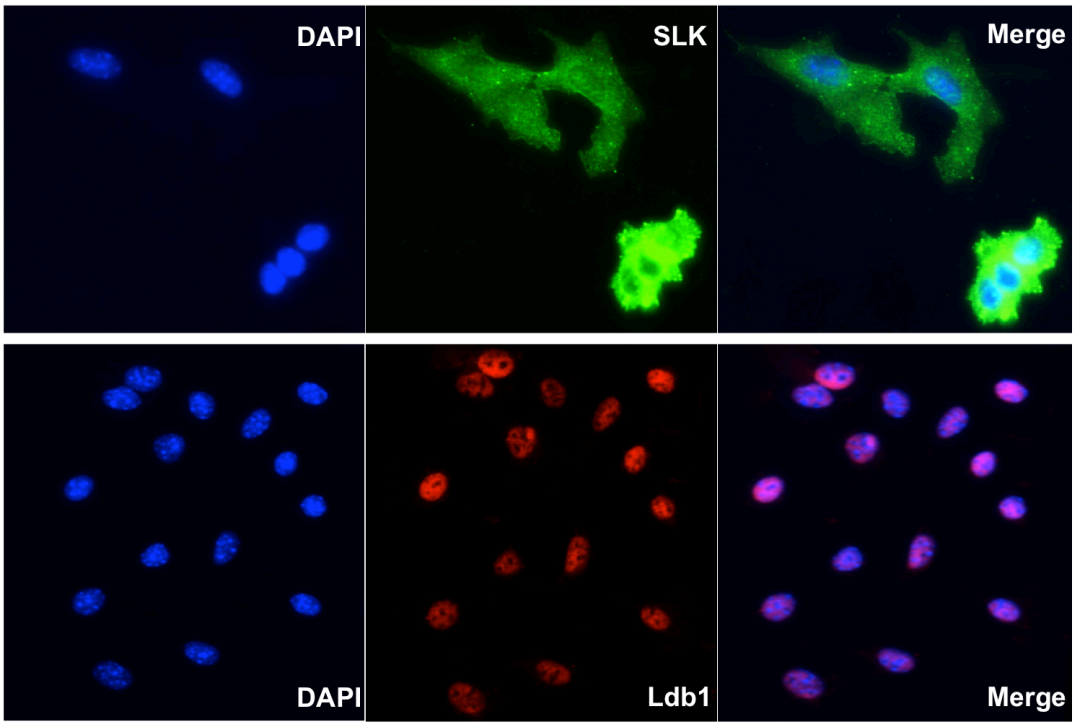

Figure 4.13. Ldb1 and SLK do not colocalize during scratch wound-induced cellular migration of tumor cells. (C) Shows a close up image of tumor cells that have migrated into the wound. In a scratch-wound induced migration model, at 60 minutes post wounding SLK staining is cytoplasmic whereas Ldb1 staining is exclusively nuclear in the migrating primary tumor cells as shown by IF analysis using anti-Ldb1 and anti-SLK antibodies.

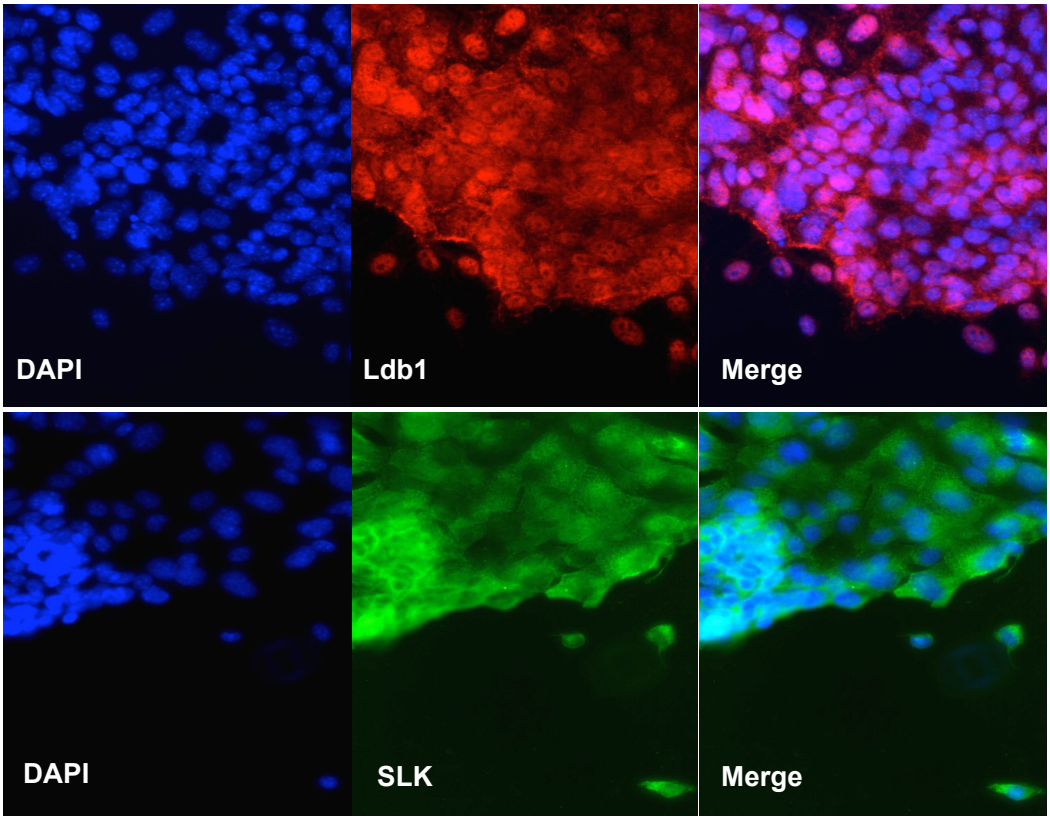

Figure 4.14. Ldb1 and SLK distribution during scratch wound-induced cellular migration of tumor cells at 15 minutes post wounding. At 15 minutes post wounding, Ldb1 staining is nuclear whereas SLK staining is cytoplasmic in the tumor cells that have migrated into the wound.

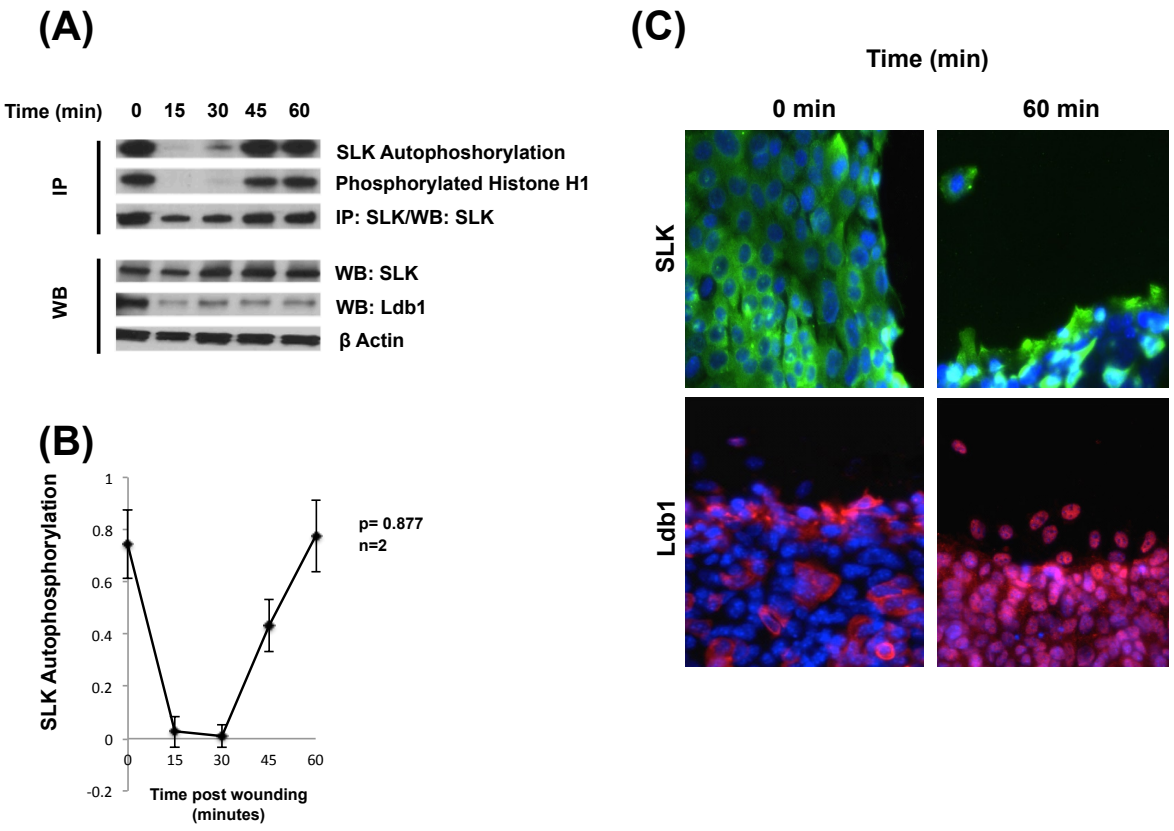

Figure 4.15. Ldb1 does not regulate SLK activity in migrating Neu-overexpressing tumor cells. (A) In-vitro kinase assay was performed to assess SLK autophosphorylation level and SLK kinase activity (phosphorylated Histone H1) in wildtype (NIC^{+} Ldb1 $^{wt/wt}$) tumor cells at different time points from 0 to 60 minutes post wounding **(B)** Shows densitometric analysis of SLK autophosphorylation activity at the different time points (0, 15, 30, 45, and 60 minutes post wounding) after normalization to immunoprecipitated SLK (n=2). **(C)** Representative IF images showing SLK (top panel) and Ldb1 (bottom panel) staining at 0 and 60 minutes post wounding. At 0 minutes, both SLK and Ldb1 show cytoplasmic staining in the tumor cells at the wound site. At 60 minutes post wounding, SLK staining is cytoplasmic and Ldb1 staining is exclusively nuclear in migrating tumor cells. According to densitometric analysis of SLK autophosphorylation activity as shown in **(B)**, no statistically significant difference was observed when comparing SLK activity at the 0 and 60 minutes time points post wounding (p=0.877). The P-value was calculated using a two-tailed student's t-test. This suggests that Ldb1 does not regulate SLK activity in migrating tumor cells.

4.7. Ldb1 deletion increases the migration and invasive capabilities of Neu-induced primary tumor cells in-vitro

Previously it was shown that si-RNA-mediated Ldb1 knockdown in MEF3T3 fibroblasts resulted in a significant increase in their migration capacity (Storbeck et al. 2009). To assess the role of Ldb1 in cell motility, in-vitro Boyden Chamber Chemotaxis and Haptotaxis migration assays were performed using the established wildtype (NIC^{+} $Ldb1^{+/+}$) and Ldb1-null (NIC^{+} $Ldb1^{-/-}$) primary tumor cells. Chemotaxis and Haptotaxis migration assays showed a four-fold increase in the migration capacity of Ldb1-null primary tumor cells when compared to wildtype tumor cells ($p=0.003$ and $p=0.015$, respectively) (**Figure 4.16A,B**). We also performed Matrigel invasion assay using wildtype and Ldb1-null primary tumor cells. We observed a significant 5-fold increase ($p=0.005$) in the invasion potential of Ldb1-null primary tumor cells when compared to wildtype tumor cells (**Figure 4.16C**). Overall, Ldb1 deletion enhances the migratory and invasive capabilities of Neu-induced primary tumor cells in-vitro.

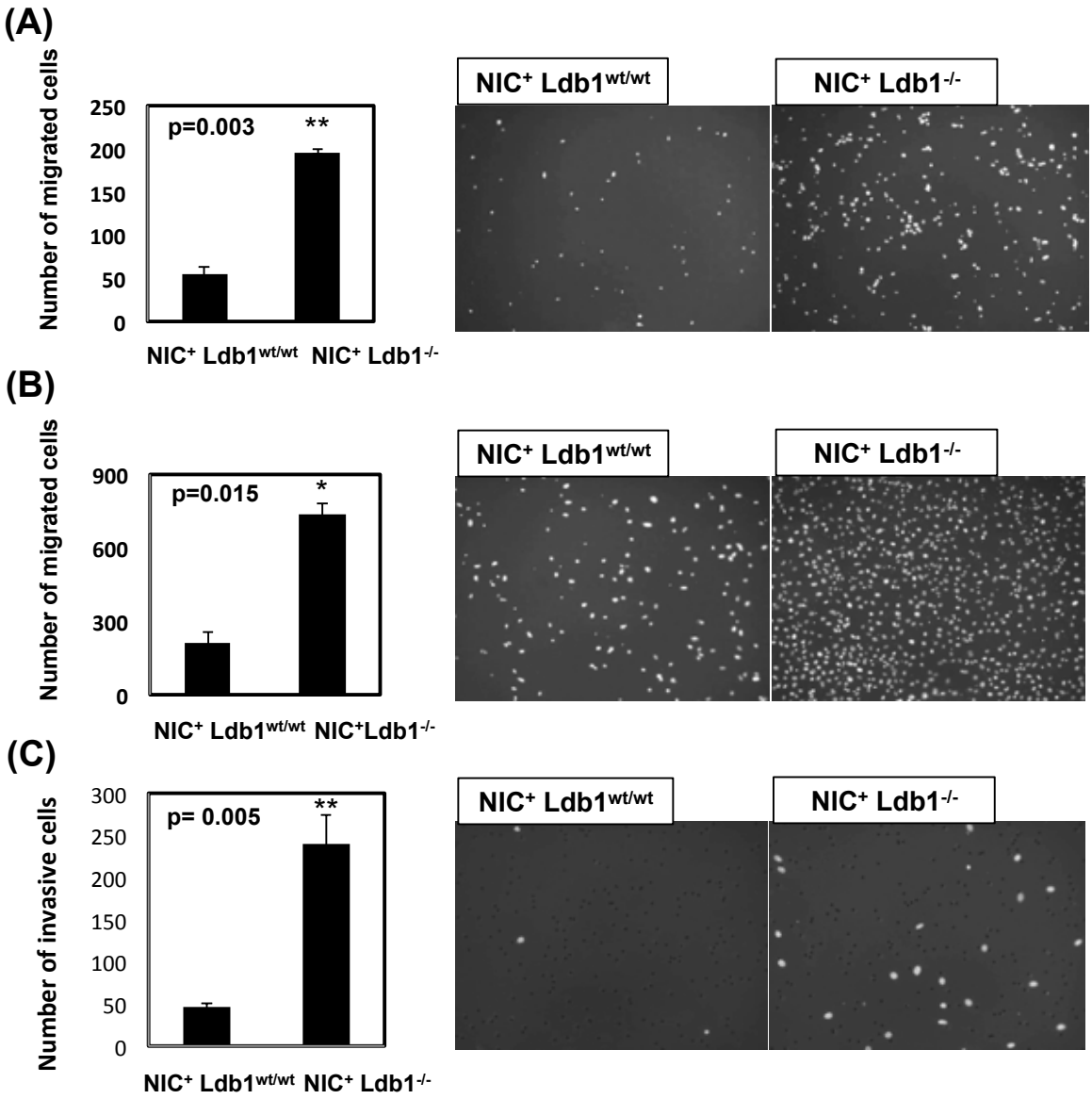

Figure. 4.16. Ldb1 deletion enhances the migration and invasion potential of Neu-induced tumor cells. (A) Boyden chamber chemotaxis and **(B)** haptotaxis migration assays were performed for 17 hours. **(C)** Matrigel invasion assay performed for 24 hours. A single cell-line from a wildtype (NIC^+ Ldb1 $^{wt/wt}$) and an Ldb1-null (NIC^+ $Ldb1^{-/-}$) background was used for both migration and invasion assays. Cell counts were performed in triplicates for wildtype and Ldb1-null tumor cells (n=3). The P-value was calculated using a two-tailed student's t-test (p=0.003 for the chemotaxis migration assay, p=0.015 for the haptotaxis migration assay, and p=0.005 for the invasion assay).

We next attempted to delineate the molecular mechanisms by which Ldb1 deletion enhances the migration and invasive capabilities of Neu-induced tumor cells in-vitro. Interestingly, we observed differences in the morphology of the established tumor cells in culture. Ldb1-null tumor cells displayed a fibroblast-like (mesenchymal) morphology, whereas wildtype Ldb1-expressing cells displayed an epithelial morphology in culture (**Figure 4.17A**). We then assessed the expression level of the epithelial marker E-cadherin and the invasive marker N-cadherin by western blot. Our data showed that Ldb1 deletion is associated with a loss of E-cadherin expression and an upregulation in N-cadherin expression in-vitro. In contrast, wildtype tumor cells expressed high levels of E-cadherin and low levels of N-cadherin (**Figure 4.17B**). Therefore, the upregulation of N-cadherin and downregulation of E-cadherin expressions could likely account for the observed enhanced migration and invasion capacity of Ldb1-null tumor cells in-vitro (**Figure 4.16**). In-vitro kinase assays on exponentially growing tumor cells show that Ldb1 deletion does not affect SLK activity. Therefore, the observed increase in the migration and invasion potential of Ldb1-null tumor cells in-vitro occurs in an SLK independent manner (**Figure 4.17B**)

We then analyzed E-cadherin and N-cadherin expression levels in wildtype and Ldb1-null primary mammary tumors. Although we explanted the tumor cells in culture from primary tumors, we observed a different expression pattern for the two markers. Ldb1-null primary tumors showed an upregulation in E-cadherin expression level and no difference in N-cadherin expression when compared to wildtype primary tumors (**Figure 4.18**). This finding suggests that E-cadherin expression might be tightly regulated by the tumor microenvironment that is markedly different in-vitro.

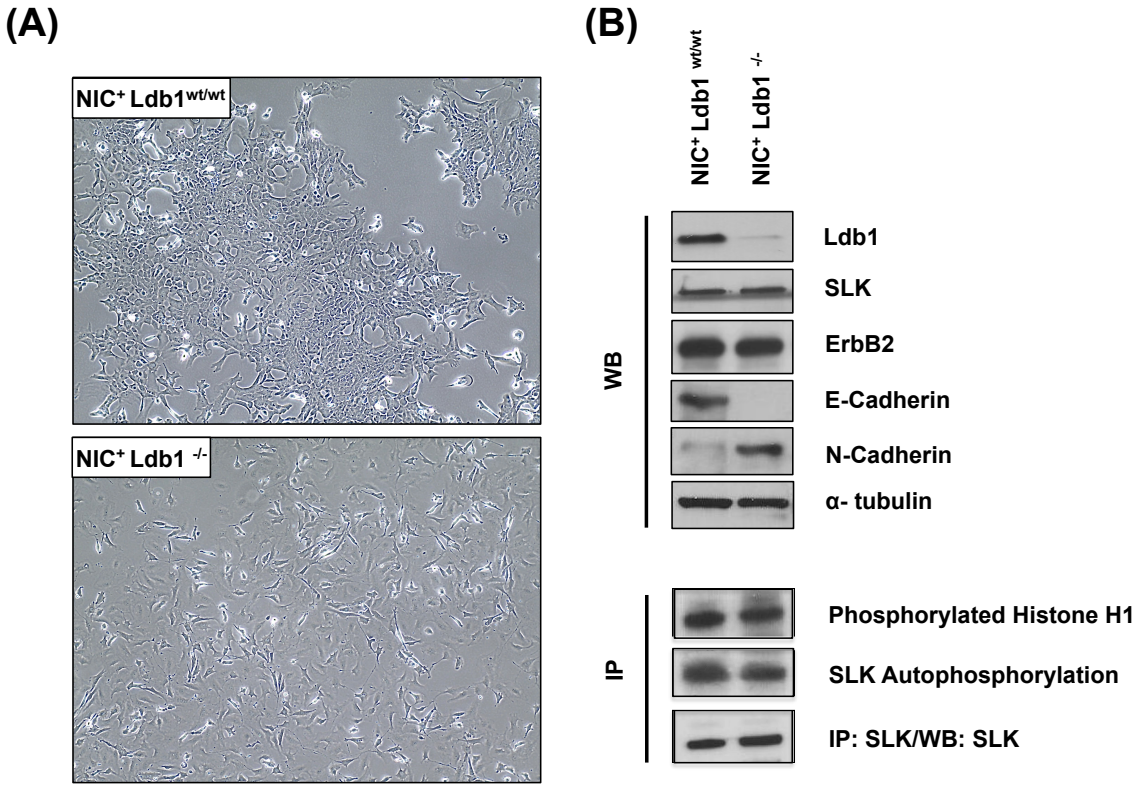

Figure 4.17. Ldb1-null primary tumor cells show an upregulation in N-cadherin expression and a downregulation in E-cadherin expression in-vitro. (A) Phase contrast images showing the morphology of tumor cells in culture under digital inverted microscopy. Wildtype Ldb1-expressing tumor cells (NIC^{+} $Ldb1^{wt/wt}$) display an epithelial-like morphology and Ldb1-null tumor cells (NIC^{+} $Ldb1^{-/-}$) display a mesenchymal-like morphology. **(B)** Western analysis (WB) show that tumor cells from Ldb1-null mice (NIC^{+} $Ldb1^{-/-}$) do not express the cell-adhesion marker E-cadherin but they express high levels of N-cadherin, whereas Ldb1-expressing tumor cells (NIC^{+} $Ldb1^{wt/wt}$) showed an exact opposite trend in the expression of both adhesion markers. In-vitro kinase assay analysis on exponentially growing tumor cells (IP) showed no difference in either SLK autophosphorylation level or SLK kinase activity (phosphorylated histone H1) between wildtype and Ldb1-null primary tumor cells after normalization to immunoprecipitated SLK (IP: SLK, WB: SLK). This suggests that Ldb1-null tumor cells enhance their migration and invasion capacity in an SLK independent manner.

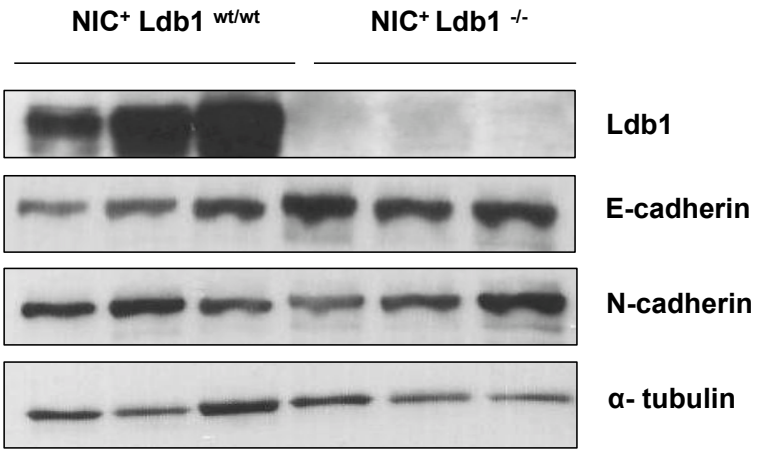

Figure 4.18. Mammary-specific Ldb1 deletion upregulates E-cadherin expression in primary mammary tumors. Whole tumor lysates obtained from wildtype (NIC^+ $Ldb1^{wt/wt}$) and Ldb1-null (NIC^+ $Ldb1^{-/-}$) mice were used for western analysis to assess the expression of E-cadherin and N-cadherin in primary mammary tumors. Ldb1 deletion increases E-cadherin expression in primary tumors; however, no difference was observed in N-cadherin expression level between wildtype and Ldb1-null tumors.

4.8. Ldb1 deletion effect on the spontaneous metastasis of Neu-overexpressing tumors

To study the effect of Ldb1 deletion on Neu-induced metastasis, serial sectioning of lung paraffin-embedded blocks followed by hematoxylin and eosin (H&E) staining of the sections was performed. Examination of H&E stained lung tissue sections revealed that 2 out of 6 wildtype mice (33%) and 1 out of 5 Ldb1-null mice (20%) developed lung metastases (**Table 2, Figure 4.19**). When analyzing lung blocks positive for metastasis, we observed that the average number of established metastases in the lung parenchyma of Ldb1-null mice was lower when compared to control animals, 9 vs. 23 metastatic foci, respectively (**Table 2**). In addition, although lung metastatic lesions were predominantly extravascular in the Ldb1-null mice, some were confined to the lung vasculature. On the contrary, 100% of lung metastases observed in wildtype mice were extravascular (**Figure 4.19**). Overall, these findings suggest that Ldb1 deletion results in a delay in the development of lung metastases in MMTV-NIC mice. However, due to the low incidence of spontaneous metastases observed in this model we cannot confidently draw this conclusion.

$NIC^+ Ldb1^{wt/wt}$

Mouse Tag Number	# Of metastatic foci/lung
6728	11
7258	0
6729	35
NIC B	0
6620	0
7259	0

$NIC^+ Ldb1^{-/-}$

Mouse Tag Number	# Of metastatic foci/lung
7423	0
6739	9
7425	0
8117	0
8530	0

Table 2. A comparison of the number of metastatic foci per lung between wildtype and Ldb1-null mice. We performed serial sectioning of lung paraffin-embedded blocks of wildtype (NIC^+ $Ldb1^{+/+}$) and Ldb1-null (NIC^+ $Ldb1^{-/-}$) mice. Six wildtype vs. five Ldb1-null lung blocks were sectioned and analyzed by H&E to determine the number of metastatic foci per lung. We observed a low incidence of metastasis in the MMTV-NIC animal model. For the lung blocks that were positive for metastasis (highlighted in red), the average number of metastatic foci/lung in wildtype mice, (11+35)/2=23, was higher when compared to Ldb1-null mice, 9.

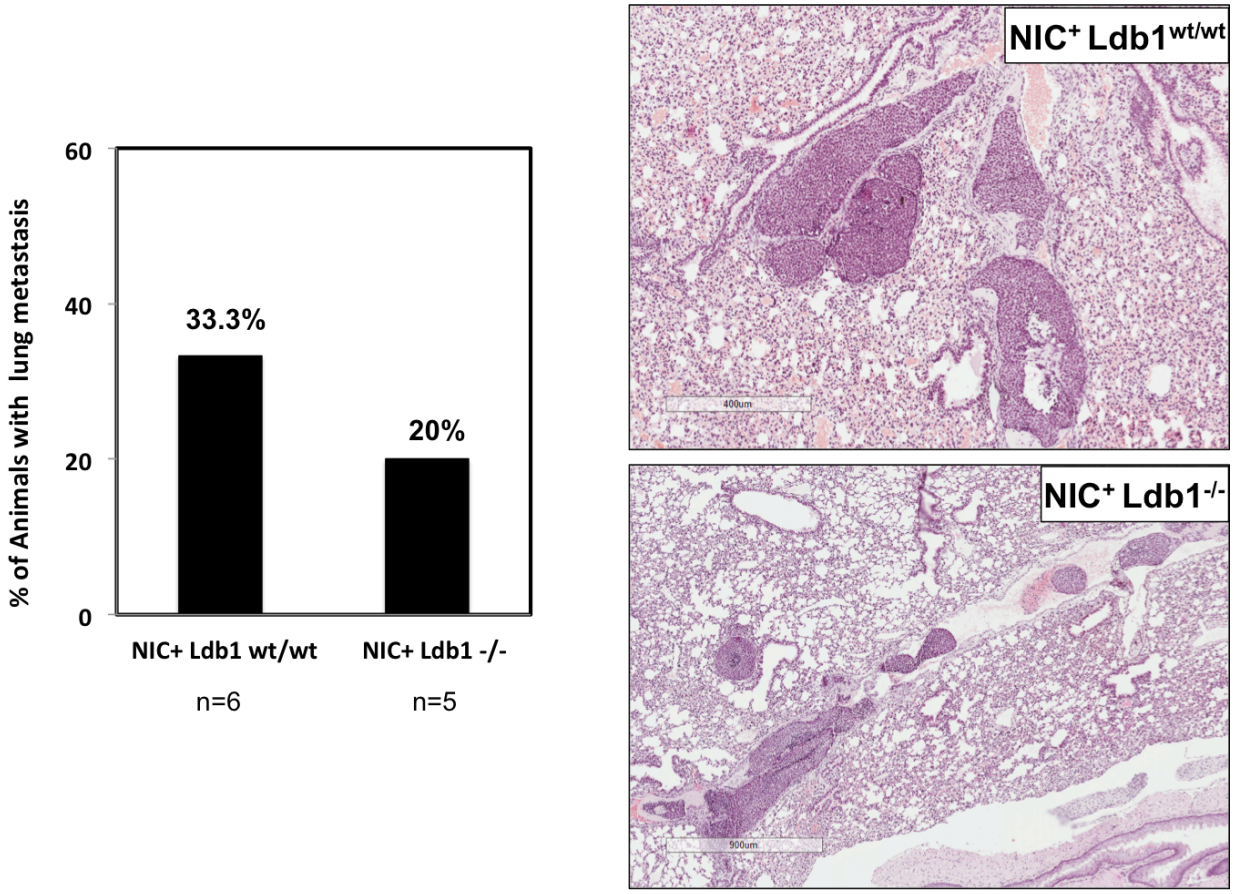

Figure 4.19. The MMTV-NIC animals showed a low incidence of lung metastasis. Serial sectioning of lung paraffin blocks from six wildtype (NIC^{+} $Ldb1^{wt/wt}$) and five Ldb1-null (NIC^{+} $Ldb1^{-/-}$) animals was performed and the sections were subjected to H&E analysis. Percentage of animals harboring metastatic lesions in the lung was determined. Also shown are representative H&E figures of metastatic lesions in the lung from wildtype and Ldb1-null animals that are positive for lung metastases.

4.9. Ldb1 deletion suppresses lung colonization

Due to the low incidence of metastasis in the MMTV-NIC animals, we decided to assess whether Ldb1 deletion would affect the ability of established tumor cells to colonize the lung by performing tail-vein assays. Wildtype or Ldb1-null tumor cells were injected into the lateral tail vein of nude CD1 mice (5 mice per group). Specifically, 5 x 10^5 cells/100μL were injected and pulmonary metastatic lesions on the lung surface were analyzed 6 weeks post injection by inflation with Indian ink. Two and three lungs were analyzed from mice injected with wildtype and Ldb1 null tumor cells, respectively. Surprisingly, wildtype Ldb1 expressing tumor cells exhibited a significantly increased capacity for lung colonization when compared to Ldb1-null tumor cells (**Figure. 4.20C**). On average, 140 pulmonary metastases were detected in mice injected with wildtype tumor cells. In contrast, only 1 visible pulmonary tumor was detected in the mice injected with Ldb1-null tumor cells. In addition, lungs were collected from the two groups for histological analysis. H&E staining showed no evidence for the establishment of lung metastatic lesions in lungs collected from nude mice injected with Ldb1-null tumor cells (**Figure 4.20B**), whereas, lungs collected from mice injected with wildtype tumor cells developed lesions that covered almost 100% of the lung area (**Figure. 4.20A**). As Ldb1-null cells do not show any defect in proliferation (**Figure 4.20D**), the impaired lung colonization capability of Ldb1-null tumor cells is unlikely due to an intrinsic inability to proliferate at the colonization site. Overall, these data suggest that Ldb1 is necessary for the colonization of the lung tissue and may be important for Neu-positive breast cancer metastasis.

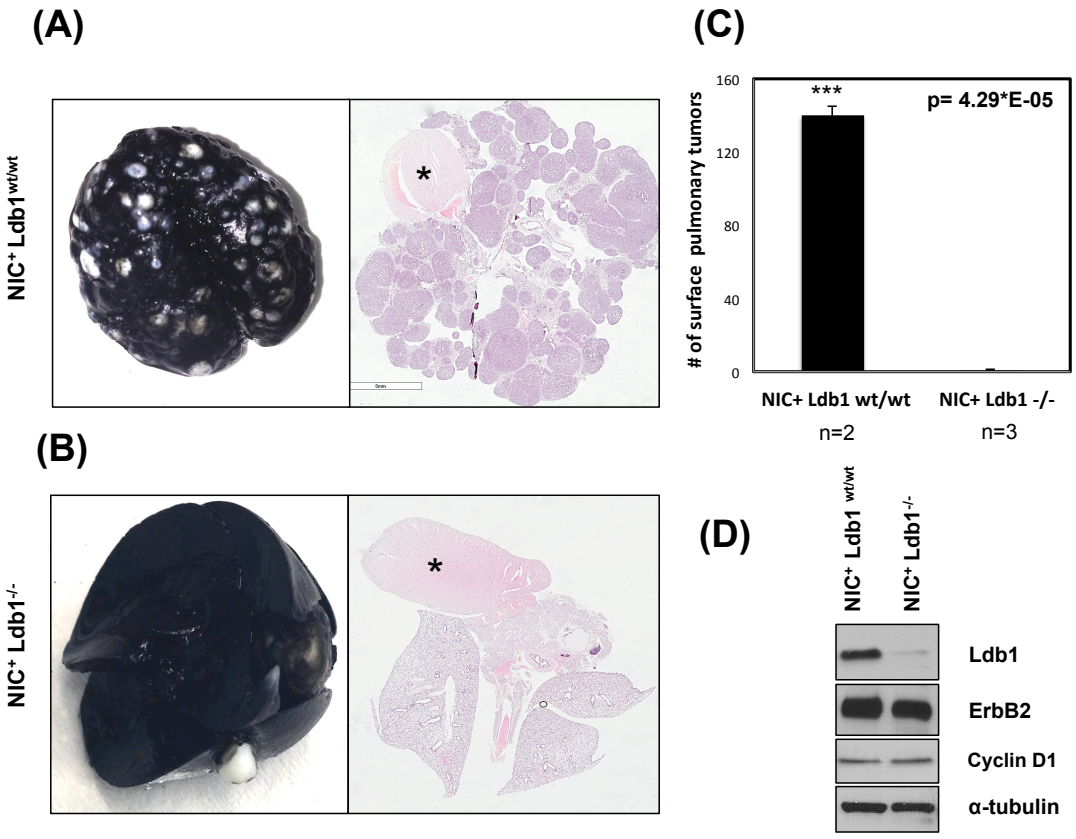

Figure 4.20. Ldb1 is necessary for lung colonization of MMTV-NIC tumor cells. Lung colonization assay was performed as described in *Materials and Methods*. In brief, 5 x 10^5 tumor cells/100µL were injected into the lateral tail vein of nude CD1 mice (five mice per genotype). The mice were sacrificed 6 weeks post injection and the lungs were collected for analysis. Pulmonary metastatic lesions on the lung surface of mice injected with **(A)** wildtype (NIC^+ $Ldb1^{wt/wt}$) and **(B)** Ldb1-null (NIC^+ $Ldb1^{-/-}$) tumor cells were analyzed by inflation with Indian ink. Also, H&E staining was performed to detect lung metastatic foci in mice injected with wildtype (NIC^+ $Ldb1^{wt/wt}$) and Ldb1-null (NIC^+ $Ldb1^{-/-}$) tumor cells. **(C)** Ldb1 deletion significantly inhibits the lung colonization capability of injected Neu-induced tumor cells. The P-value was calculated using a two-tailed student's t-test (p=4.29*E-05). **(D)** Shows western blot analysis on the tumor cells used for the lung colonization assay. No difference was observed in the expression of the proliferative marker, cyclin D1, between wildtype and Ldb1-null tumor cells. Therefore, the defective lung colonization capability of Ldb1-null tumors is unlikely due to an intrinsic defect in proliferation. Shown in asterisks (*) is the heart.

5. DISCUSSION

5.1. Conditional Ldb1 deletion in the mammary epithelium does not impair mammary gland development

We initially investigated the Ldb1 expression pattern in wildtype and Ldb1-null mammary gland tissues of adult virgin mice. Specifically, immunohistochemical analysis was used to confirm mammary gland-specific Ldb1 deletion in Ldb1-null mice. It was previously reported that Ldb1 is expressed in the luminal and basal ductal epithelial cells of the mammary gland (Salmans et al. 2014). In the current study we observed a similar expression pattern for Ldb1 in wildtype mammary glands. Wagner et al. previously established the MMTV-Cre transgene spatial expression pattern by crossing MMTV-Cre mice with ROSA26-lox-stop-lox LacZ reporter mice. The expression of the MMTV-Cre transgene was detected in the epithelial and myoepithelial cells; however, its expression was absent from the stroma of the mammary gland that includes fibroblasts and adipocytes. This supports both the absence of Ldb1 expression within the ductal epithelium and the positive Ldb1 staining observed in the surrounding adipocytes in Ldb1-null mammary glands.

We then assessed the effect of Ldb1 deletion on normal mammary gland development in adult virgin mice. This was important to address prior to elucidating the role of Ldb1 in Neu-induced tumorigenesis, as defects in the tissue may affect the interpretation of the tumorigenesis studies. Previously, Salmans et al. generated a transgenic mouse model in which they directed the expression of a dominant negative Ldb (DN-Ldb) mutant in the basal cell population of the mammary gland using the Keratin 14 (K14) promoter. Ldbs-mediated transcriptional regulation in the basal

mammary epithelial cells was found to promote ductal outgrowth and branching morphogenesis by maintaining the stem cell population in the basal cell compartment of the mammary gland (Salmans et al. 2014). Branching morphogenesis was impaired in K14-DN-Ldb mammary glands by 4 weeks of age and the branching defect persisted throughout adulthood and late pregnancy. Specifically, K14-DN-Ldb mammary glands showed a delay in ductal elongation, a reduction in branching frequency, and the development of smaller terminal end buds (Salmans et al. 2014). In this study, whole mount analysis of mammary glands was not performed; hence, the effect of Ldb1 deletion on the early stages of ductal outgrowth and development is not reported herein. In the current study, we investigated the effect of Ldb1 deletion on the expression of mammary ductal epithelial layer markers in virgin mammary glands. We specifically focused on analyzing mammary gland development in virgin mice as this study investigates the effect of Ldb1 deletion on Neu-induced tumor development in virgin mice. Ldb1 deletion did not affect the expression of the luminal epithelial layer marker CK-8 or the basal epithelial layer marker CK-14. Also, no discernible differences in mammary gland histology were observed between wildtype and Ldb1-null mammary gland sections as demonstrated by H&E analysis. These results argue that Ldb1 does not play a critical role in the morphological organization of the mammary epithelial layers or in the gross morphology of the tissue. Overall, our results show that mammary gland-specific Ldb1 knockout does not affect mammary gland development in adult virgin mice.

A previous study demonstrated that the other Ldb family member, Ldb2, is also expressed in the mammary gland, however, at a significantly lower level when compared to Ldb1 (Salmans et al. 2014). According to the Mouse Genome Informatics website, germline deletion of the *Ldb2* gene did not result in developmental defects (MGI

database/Lexicon Genetics). In contrast, Ldb1 global knockout is embryonic lethal and resulted in a pleiotropic phenotype (Mukhopadhyay et al. 2003). These studies suggest that Ldb1 compensates for Ldb2 functional loss and not vice versa. The lack of Ldb2 compensation in the Ldb1 knockout embryos could be attributed to a different pattern of expression for both proteins (Agulnick et al. 1995; Bach et al. 1997; Visvader et al. 1997; Tran et al. 2006; Ingolf et al. 1997), or the finding that each Ldb factor has a unique oligomerization mode leading to distinct multiprotein transcriptional complexes with different biological functions (Cross et al. 2010). Therefore, in the current study we speculate that the observed lack of developmental defect in the Ldb1-null mammary glands is unlikely due to Ldb2 compensating for Ldb1 functional loss.

A population of Ldb1-positive/cre recombinase-escapee ductal epithelium cells was detected in mammary gland sections from virgin Ldb1-null mice. This observation led us to hypothesize that cre-mediated excision of Ldb1 in the mammary gland is not complete and that Ldb1 function is preserved in a small population of ductal epithelial cells that is sufficient for normal mammary gland development in Ldb1-null mice. In a bicistronic IRES-containing mRNA system such as the MMTV-NIC transgene, 5' cap-independent translation downstream of the IRES has been previously reported to occur at a lower level under normal growth conditions when compared to canonical cap-dependent translation of genes upstream of the IRES (Macejak and Sarnow, 1991; Dirks et al. 1993; Houdebine and Attal, 1999). In the current study, the existence of Ldb1-positive/cre recombinase-escapee ductal epithelial cells suggests that cre-recombinase expression downstream of the IRES may occur at a lower level in-vivo. In support of this hypothesis, some tumors derived from an Ldb1-null genotype background were found to express Ldb1 at levels comparable to wildtype tumors, suggesting that these tumors originated

from cells in which Ldb1 was not efficiently deleted. A different study reported a similar observation of positive hexokinase/cre-recombinase escapee mammary tumor cells in an MMTV-NIC mouse animal model (Patra et al. 2014). Taken together, we hypothesize that Ldb1-null mice show no defect in mammary gland development because of the incomplete cre-mediated deletion of Ldb1 in the mammary gland.

5.2. Ldb1 deletion does not affect primary tumorigenesis in MMTV-NIC mice

SLK kinase activity is required for cell cycle progression through the G2/M phase in MEF3T3 fibroblasts. Expressing an inactive SLK mutant into MEF3T3 fibroblasts inhibited proliferation (O'Reilly et al. 2005). Our lab has previously identified Ldb1 as a negative regulator of SLK kinase activity in MEF3T3 fibroblasts (Storbeck et al. 2009). We therefore hypothesized that Ldb1 knockout would stimulate SLK kinase activity in-vivo to increase proliferation of Neu-induced primary mammary tumors. In this study, we showed that Ldb1 knockout did not affect SLK activity in-vivo. This suggests that Ldb1 does not regulate SLK kinase activity in Neu-overexpressing mammary tumors. Thus the effects of Ldb1 deletion on Neu-induced tumorigenesis in our model are primarily due to Ldb1 knockout and are not attributed to SLK overactivation.

Ldb1 expression level was previously shown to predict prognosis in human breast cancer patients. Specifically, high Ldb1 expression in human breast tumors conferred poor prognosis, whereas low Ldb1 expression was correlated with prolonged survival (Salmans et al. 2014). Here we showed that mammary gland-specific Ldb1 deletion did not affect overall survival of MMTV-NIC animals; all mice from the three different cohorts under study had similar endpoints of approximately 160 days at a total tumor volume of 1.7 cm^3. Previous studies have shown that wildtype MMTV-NIC mice develop tumors with a latency of 146 days (Ursini-Siegel et al. 2008). Our Kaplan–Meier

analysis showed that all mice, irrespective of their genotype, developed mammary tumors at a similar latency of 144 days. Also, no differences were observed in the total tumor volume at endpoint when comparing the three different cohorts under study. Accordingly, mammary-specific Ldb1 deletion did not affect proliferation or apoptosis in the primary tumors. These findings suggest that Ldb1 does not contribute to Neu-mediated tumor growth in an MMTV-NIC mouse model. In contrast, a previous study reported that the inhibition of the transcriptional activities of both Ldb factors in the basal cell compartment of the mammary gland resulted in a significant delay in tumor onset and decreased tumor growth rate in an MMTV-Polyoma Middle T (PyMT) breast cancer mouse model (Salmans et al. 2014). Herein, we only deleted the *Ldb1* gene and we verified the expression of Ldb2 in Ldb1-null tumors. This raises the possibility of a potential compensation by Ldb2 in primary tumor growth in Ldb1-null mice. Nonetheless, Ldb1 deletion affected the migration, invasion and lung colonization capabilities of Neu-overexpressing tumor cells. Therefore, the later findings do not support the hypothesis of Ldb2 compensating for Ldb1 functional loss in Neu-induced primary tumors. The differences in the findings between the two models, the MMTV-NIC and the MMTV-PyMT, suggest that the role of Ldb factors on breast tumorigenesis is context-dependent.

Previous reports have established a role for Ldb1-mediated transcriptional regulation in suppressing cellular proliferation. Ldb1 deletion in the epithelial and mesenchymal cells of the stem cell niche of the small intestine significantly enhanced proliferation in the intestinal crypt epithelium (Dey-Guha et al. 2009). Moreover, Teufel et al. have shown that in a hepatocellular carcinoma (HCC) mouse model, Ldb1 conditional knockout in the liver enhances tumor development by increasing

proliferation. Microarray analysis on Ldb1-null livers demonstrated that the observed increase in proliferation and HCC tumor development is a result of an increase in the expression level of the proliferation marker, cyclin D1, and a decrease in the expression level of the proliferation inhibitor marker, cyclin-dependent kinase inhibitor p21 (Teufel et al. 2010). In the current study, no difference was observed in cyclin D1 expression level between wildtype and Ldb1-null primary tumors. Also, no difference was observed in the proportion of Ki67 positive cells between wildtype and Ldb1-null primary mammary tumors. These findings suggest that Ldb1 deletion in the mammary gland does not impair proliferation of breast carcinomas in an MMTV-NIC mouse model.

Reports from the literature also support a role for Ldb1 in mediating apoptosis. Ldb1 conditional deletion in the stem cell niche of the small intestine resulted in Wnt signaling activation that enhanced apoptosis in Ldb1-null intestinal crypts (Dey-Guha et al. 2009). With respect to tumorigenesis however, Teufel et al. reported that Ldb1 conditional deletion in the liver increased the resistance of HCC tumors to apoptosis. In breast cancer, expressing a dominant negative Ldb1 mutant in MCF-7 breast cancer cells increased LMO4-induced apoptosis (Wang et al. 2007). In this study, we observed no difference in the expression level of the apoptotic marker, active cleaved caspase-3, when comparing wildtype and Ldb1-null Neu-induced primary tumors. This suggests that Ldb1 does not mediate apoptosis in an MMTV-NIC mouse model.

5.3. Ldb1-null tumor cells display an invasive phenotype in-vitro

Our lab has previously established a role for Ldb1 in the negative regulation of cellular motility in MEF3T3 fibroblasts (Storbeck et al. 2009). Efficient Ldb1 knockdown in MEF3T3 fibroblasts resulted in a significant SLK activation that enhanced the migration potential of these cells (Storbeck et al. 2009). In the current study, we

hypothesized that Ldb1 knockout would increase SLK activity and consequently enhance the migration potential of tumor cells. Herein, analysis of primary tumor cell migration by the in-vitro scratch assay showed that the induction of motility in wildtype tumor cells leads to a downregulation of Ldb1 expression within 15 minutes post wounding. This finding suggests that Ldb1 downregulation is required for enhancing tumor cell migration for wound closure. Supporting this, results from Boyden chamber assays showed that Ldb1 deletion increases the migration and invasion potential of tumor derived cells in-vitro. We then assessed if the enhanced migration and invasion potential of Ldb1-null tumor cells is due to SLK activation. We observed no difference in SLK activity between wildtype and Ldb1-null tumor cells, which suggests that Ldb1 does not regulate SLK activity in Neu-transformed tumor cells. Overall, our data show that the observed increase in the migration and invasion capabilities of Neu-induced tumor cells is a specific effect of Ldb1 knockout and is not due to SLK overactivation.

The loss of Ldb1-mediated regulation of SLK activity in Neu-transformed tumor cells raised the question whether these two proteins physically interact in tumor cells. Storbeck et al. provided the first evidence for direct interaction between Ldb1 and SLK through co-immunoprecipitation in MEF3T3 cells that were subjected to wound-induced migration. Also, evidence for colocalization of Ldb1 and SLK at the leading edge of migrating cells was previously shown in migrating MEF3T3 fibroblasts (Baron et al. 2015; Storbeck et al. 2009). In the current study, we were unsuccessful in showing co-immunoprecipitation of both Ldb1 and SLK in migrating tumor cells, suggesting that both proteins may not interact in these cells. Supporting this, we found that Ldb1 and SLK do not colocalize, and therefore they do not interact directly in migrating tumor cells. Specifically, IF analysis showed that SLK staining is cytoplasmic, whereas Ldb1 is

exclusively expressed in the nucleus of migrating tumor cells. Overall, our data show that the distribution of Ldb1 and SLK in migrating tumor cells markedly differed from migrating fibroblasts. The observed nuclear localization of Ldb1 during tumor cell migration suggests that it mediates migration by its transcriptional cofactor function.

The expression profile of E-cadherin and N-cadherin in Ldb1-null primary tumor cells in-vitro suggests that Ldb1-deletion promotes an invasive phenotype. A hallmark of this invasive phenotype is the loss of E-cadherin expression and the upregulation of the mesenchymal marker N-cadherin. This was observed in the established Ldb1-null tumor cells and could contribute to the mesenchymal morphology exhibited by these cells in culture. Cadherins are transmembrane glycoproteins that mediate calcium-dependent cell-cell adhesion. E-cadherin has a tumor invasion suppressor role. Forced expression of E-cadherin into E-cadherin negative carcinoma cells decreases the invasion capacity of these cells by promoting cell-cell adhesion (Mareel et al. 1994). On the other hand, N-cadherin expression promotes cellular motility and invasion by facilitating the interaction between N-cadherin expressing- breast cancer cells and N-cadherin expressing- stromal cells (Hazan et al. 1997). Nieman et al. demonstrated that N-cadherin expression level, but not E-cadherin, correlates with increased motility and invasion of human breast carcinoma cells. Therefore, the observed upregulation of N-cadherin in Ldb1-null tumor cells could account for the observed increase in their migration and invasion potential in-vitro.

As we were unsuccessful in establishing additional cell lines in culture, one potential limitation to our in-vitro analysis is that we only compared a single cell-line from a wildtype and an Ldb1-null background. Although a clear motility phenotype has been observed, additional lines need to be surveyed. Moreover, Ldb1 nuclear localization

in migrating Neu-induced tumor cells suggests that the effect of Ldb1 on cellular migration is mediated primarily by its transcriptional cofactor function. For this reason, microarray analysis using wildtype (NIC x $Ldb1^{+/+}$) and Ldb1-null (NIC x $Ldb1^{fl/fl}$) tumors needs to be performed in the future. This will verify if the effect on the expression of E- and N-cadherins is at the transcriptional levels. It will also uncover additional de-regulated genes in the Ldb1-null tumors that might be involved in mediating cellular motility and invasion.

5.5. The role of Ldb1 in Neu-induced metastasis

We observed a low incidence of spontaneous metastasis in the MMTV-NIC animals, which can be attributed to the early endpoint for this study. According to the literature, wildtype MMTV-NIC mice are assessed for the presence of metastatic lung lesions 6 weeks following the initial palpation and they develop lung metastases with an incidence of 62.5% (Ranger et al. 2009). In this study however, mice were sacrificed 2 weeks following initial palpation as per Animal Care and Veterinary Services (ACVS) guidelines and only 33.3% of wildtype MMTV-NIC mice developed lung metastases. Serial sectioning analysis of lung blocks from Ldb1-null mice provides evidence for the establishment of lung metastatic foci in these animals; which suggests that disseminated Ldb1-null primary tumor cells are capable of metastasizing to the lung. Interestingly, when analyzing blocks positive for metastases we found that Ldb1 deletion results in a delay in the development of pulmonary metastasis as evidenced by the decreased average number of established metastases per lung and the detection of intravascular pulmonary tumor emboli in the Ldb1-null mice. Due to the low incidence of metastases in the MMTV-NIC mouse model, we cannot statistically verify that the phenotype observed in Ldb1-null mice is due to Ldb1 deletion. Orthotropic implantation of wildtype and Ldb1-

null primary tumor cells into the mammary fat pad will have to be performed to assess the effect of Ldb1 deletion on the metastatic potential of Neu-induced primary tumor cells.

Ldb1 deletion was consistently correlated with an upregulation in E-cadherin expression in Neu-induced primary tumors in-vivo. This might contribute to the potential delay in the development of pulmonary metastases in the Ldb1-null mice. E-cadherin loss of expression is thought to loosen intercellular connections thereby facilitating the dissemination of tumor cells from their primary site. E-cadherin expression loss has been reported in many aggressive tumors including that of gastric cancer (Oka et al. 1992; Matsuura et al. 1992), breast cancer (Oka et al. 1993), prostate cancer (Umbas et al. 1992), and squamous carcinomas of the head and neck (Schipper et al. 1991). The MMTV-NIC breast cancer mouse model used in the current study recapitulates invasive ductal carcinomas (IDCs). In the context of IDCs, no complete loss of E-cadherin expression has been previously reported; however, a reduction in E-cadherin expression level has been noted. Specifically, 52% of IDC cases were reported to show a reduction in E-cadherin expression level (Jiang and Mansel, 2000). Reduced E-cadherin expression in IDCs frequently results from epigenetic silencing through promoter hypermethylation of the E-cadherin gene (CDH1). Specifically, CDH1 promoter hypermethylation occurs in 30% of ductal carcinomas in-situ and the incidence increases to 60% in IDCs (Nass et al. 2000). This suggests that transcriptional repression of E-cadherin expression through epigenetic mechanisms has a role in IDC progression.

Data from the literature are controversial regarding the correlation between reduced E-cadherin expression level and tumor spread in IDCs (Parker et al. 2001). E-cadherin expression loss has been reported to serve as a marker for nodal metastasis development in breast carcinomas (Madhavan et al. 2001). This was supported in the IDC

type of breast cancer by the Jeschke et al. group who observed a significantly low E-cadherin expression level in human IDCs with lymph node and distant metastases, in comparison to a strong E-cadherin expression level in human mammary in-situ ductal carcinomas. Moreover, the loss of E-cadherin expression in IDCs was correlated with poor differentiation and high tumor grade (Gamallo et al. 1993). Ectopic expression of E-cadherin into the mesenchymal-like MDA-MB-231 breast cancer cells resulted in the acquisition of an epithelial phenotype and the consequent suppression of their migration and invasion potential (Chao et al. 2010). These results suggest that E-cadherin expression is important for maintaining the differentiated noninvasive state of tumor cells.

Reports from the literature support a role for Ldb1 in tumor dedifferentiation. Ldb1 and its partner LMO4 are expressed at the invasive front of less differentiated oral squamous carcinomas and their expression is upregulated in carcinoma cells that metastasize to the lymph nodes (Mizunuma et al. 2003). Also, Ldb1 and LMO4 expression in invasive breast carcinoma cells is essential in maintaining their undifferentiated state. In the current study, we showed that Ldb1-deletion increases E-cadherin level in Neu-induced primary tumors. We therefore speculate that Ldb1 deletion promotes the development of well-differentiated tumors with less metastatic potential in the MMTV-NIC model. Performing microarray analysis using wildtype and Ldb1-null tumors will provide information about the expression profile of epithelial differentiation markers and a measure of the differentiation grade of the tumors under study.

In a recent study, Zhang et al. performed mass spectrometry using the mouse pituitary tumor cell line AtT-20 and identified members of the Mi2/nucleosome remodeling and deacetylase (Mi2/NuRD) complex as Ldb1-interacting proteins. The Mi2/NuRD complex consists of multiple protein subunits with either enzymatic or non-

enzymatic activities. The enzymatic subunits of the Mi2/NuRD complex are the histone deacetylase (HDAC) subunit, and the Mi-2α/Mi-2β subunit (also known as CHD3/CHD4, chromo domain/helicase/DNA-binding), which catalyze histone deacetylation and ATP-dependent chromatin remodeling, respectively. The Mi2/NuRD complex also consists of multiple functional components with non-enzymatic activities including the metastasis-associated protein family members (MTAs). In vertebrates, there are three MTA family members: MTA-1, -2 and -3. In AtT-20 cells, MTA2 interacts directly with Ldb1 to form a complex that occupies enhancers upstream of target genes for transcriptional regulation (Zhang et al. 2015). Ldb1 regulates MTA2 recruitment to enhancers of target genes co-regulated by the Ldb1/MTA2 complex. CHIP-Seq analysis showed that Ldb1 knockdown significantly reduces MTA2 recruitment on Ldb1-dependent regulated genes (Zhang et al. 2015).

In the context of breast cancer, MTA2-containing Mi2/NuRD complex is critical for TWIST-mediated E-cadherin gene transcriptional repression (Fu et al. 2011). TWIST is a member of the class II basic helix-loop-helix (bHLH) transcription factor family that binds to conserved E-box DNA elements in promoter regions of target genes. TWIST is overexpressed in high-grade/invasive breast cancers. TWIST up-regulation results in the downregulation of E-cadherin expression and the subsequent induction of epithelial to mesenchymal transition (Mironchik et al. 2005). TWIST negatively regulates the expression of E-cadherin by directly interacting with E-boxes 1 and 2 on the promoter of the E-cadherin gene (Vesuna et al. 2007). Mass spectrometry and Co-IP analyses have identified TWIST as an MTA2-interacting protein in breast cancer cells (Fu et al. 2011). Specifically, TWIST interacts with MTA2 to form a complex that is required to target the Mi2/NuRD complex to the E-cadherin promoter for transcriptional repression. Lentivirus-

based knockdown of MTA2 released the inhibition on the E-cadherin promoter activity and upregulated E-cadherin expression (Fu et al. 2011). In the current study, we hypothesize that the observed up-regulation in E-cadherin expression in the Ldb1-null Neu-induced primary tumors can be attributed to reduced MTA2 recruitment to the E-cadherin promoter, consequently impairing MTA2 dependent TWIST-mediated E-cadherin transcriptional repression. This proposes that Ldb1 deletion might interrupt TWIST-mediated EMT-induction in Ldb1-null primary tumors resulting in a delay in metastasis development in Ldb1-null mice. Ldb1 (Johnsen et al. 2009) and MTA2-containing TWIST/NuRD complex (Fu et al. 2012) are involved in the repression of estrogen receptor α (ER α) expression in breast cancer cell lines and in IDCs. This provides strong evidence that Ldb1 is a component of the MTA2-containing TWIST/NuRD complex and supports the hypothesis of the involvement of Ldb1 in MTA2 dependent TWIST-mediated E-cadherin transcriptional repression.

5.5. Ldb1 deletion suppresses the lung colonization capability of Neu-overexpressing tumor cells

We finally assessed the effect of Ldb1 loss on the ability of Neu-overexpressing tumor cells to colonize the lungs of nude mice. Metastatic colonization is defined as the initial formation of micrometastases, their survival, and subsequent growth into macroscopic metastases at distant organ sites. Previous studies that performed lung colonization assays using wildtype MMTV-NIC cells collected lungs 4 weeks post injection and the total lung area occupied by metastatic lesions was approximately 53% (Ranger et al. 2009). In this study however, lungs were collected 6 weeks post injection of tumor cells into the lateral tail vein and the wildtype tumor cells developed metastatic lesions that covered almost 100% of the lung area. The more motile and invasive Ldb1-

null tumor cells were predicted to colonize the lung more efficiently than wildtype tumor cells. Surprisingly, Ldb1-null tumor cells exhibited a significant decreased capacity to colonize the lungs when compared to wildtype tumor cells. H&E analysis revealed no evidence for the development of lung lesions in the mice that were intravenously injected with Ldb1-null tumor cells. This indicates that Ldb1 expression is necessary in promoting lung colonization. It will be of interest to test a sh-RNA-mediated knockdown approach for stable Ldb1 knockdown in wildtype primary tumor cells in our experimental lung colonization assay. This will determine if the effect on lung colonization is due to a tumor intrinsic defect of the Ldb1 knockdown in the Neu-induced tumor cells. Based on results reported herein, we expect to observe a significant inhibition in the lung colonization capability of the stable Ldb1-knockdown tumor cells.

Ldb1-null tumor cells display increased invasive capability in-vitro; however, they are defective in their ability to colonize the lung in-vivo. The defect in the lung colonization of Ldb1-null tumor cells is not due to a defect in their proliferative capacity as western analysis showed no difference in cyclin D1 expression level between Ldb1-null tumor cells and their wildtype counterparts. In the current study we observed a difference in E-cadherin expression between in-vitro and in-vivo conditions. Ldb1-null primary tumors express high levels of E-cadherin when compared to wildtype tumors; however, when Ldb1-null tumors are explanted and cultured in-vitro they lose E-cadherin expression. This suggests that the microenvironment in which the cells reside modulates E-cadherin expression. As shown in this study, the variability introduced by the surrounding microenvironment can cause differences in the behavior of these cells between in-vitro and in-vivo conditions. We therefore speculate that the results from the

in-vitro Boyden chamber migration and Matrigel invasion assays do not mimic the in-vivo migratory and invasive behavior of Neu-transformed Ldb1-null tumor cells.

Cancer stem cells (CSCs) constitute a small population within a tumor and possess self-renewal abilities essential for the development and maintenance of the tumor. CSCs are identified in several solid cancers including breast cancer and have been shown to express specific cell-surface markers. Al-Hajj et al identified tumor-initiating ESA+ $CD44^{+}CD24^{-/low}$ breast cancer stem cells and showed that they can form heterogeneous tumors in mice when xenotransplanted into nude mice. According to the cancer stem cell hypothesis, CSCs are necessary for successful colonization of metastatic niches as they primarily function to reinitiate and sustain aggressive tumor growth at secondary metastatic sites (Velasco-Velázquez et al. 2011). The implantation of CD44+ breast cancer stem cells into the mammary fat pad of nude mice resulted in the development of lung metastatic cells that were CD44+. This finding suggests that the CSCs that disseminate from primary tumors are essential for colonization during metastasis (Liu et al. 2010). Moreover, CSCs mediate the metastatic capacity of breast cancer cells (Charafe-Jauffret et al. 2009). The inoculation of aldehyde dehydrogenase (ALDH) positive breast cancer stem cells into nude mice via intracardiac injection resulted in the development of multiple metastases in different secondary sites including the bone and the lung. In contrast, ALDH negative tumor cells displayed limited metastatic potential to local lymph nodes (Charafe-Jauffret et al. 2009). These studies provide strong evidence that CSCs presence within tumors is linked with the establishment of distant metastases in breast cancer. Furthermore, CSCs are postulated to be involved in tumor invasion and in the development of metastases. Breast cancer stem cells with the surface profile $CD44^{high}/CD24^{low}$ were shown to express high levels of mesenchymal markers involved

in the induction of EMT including N-cadherin, vimentin, Snail1/2 and TWIST1/2 (Mani et al. 2008). Overall, these studies suggest a role for CSCs in breast cancer cell invasion, dissemination from primary tumors and colonization in distant metastatic sites.

The suppression in the lung colonization capability of Ldb1-null tumor cells could be attributed to the loss of CSC subpopulation within the Ldb1-null primary tumors. Ldb1 is highly expressed in the less differentiated Claudin-low breast cancer tumors, which are enriched with stem cells characterized by the gene signature $CD44^{+}/CD24^{-/low}$ (Hennessy et al. 2009). This proposes a possible functional role for Ldb1 in Claudin-low breast cancer development. Furthermore, several studies have addressed the important role of Ldb1 in maintaining stem cell population necessary for the homeostasis of several epithelial tissues such as the hair follicle (Xu et al. 2007), the adult intestinal crypt (Dey-Guha et al. 2009), and the mammary gland (Salmans et al. 2014). In the K14-DN-Ldb mouse model, the deletion of both Ldb factors significantly reduced the number of stem cells in the basal compartment of the mammary gland. This suggests that Ldb1 function is required for the maintenance of the stem cell population in the mammary gland. In an MMTV-NIC mouse model, cre-mediated Ldb1 deletion occurs primarily in the mammary ductal epithelium (Wagner et al. 2001), from which primary tumors arise (Ursini-Siegel et al. 2008). Therefore, one possibility is that mammary gland-specific cre-mediated Ldb1 deletion reduces the number of stem cells in the established Ldb1-null primary tumors contributing to their impaired lung colonization capability. To test this hypothesis, in-vitro colonogenic assays need to be performed to compare the capability of primary tumor cells isolated from wildtype and Ldb1-null tumors in forming colonies. We speculate that Ldb1 deletion will abrogate the ability of Neu-induced primary tumor cells to grow as mammospheres in-vitro.

6. General conclusion

This in-vivo study is novel as it is the first to address the effect of Ldb1-deletion on Neu-driven tumorigenesis in a mammary gland specific Ldb1-knockout mouse model. We found that Ldb1 does not regulate SLK activity in Neu-transformed primary tumors. Therefore, the effects of Ldb1 deletion on Neu-induced tumorigenesis in the MMTV-NIC animal model are not due to an increase in SLK activity as a result of the loss of Ldb1-mediated negative regulation of SLK activity, which does not support our initial hypothesis. Although it could have a subtle role, Ldb1 is not required for the development of a functional mammary gland. Also, mammary gland-specific Ldb1 deletion does not affect Neu-mediated tumor growth or overall survival in an MMTV-NIC mouse model. An important finding in the current study is the inhibitory effect that Ldb1 deletion imparts on the lung colonization capability of Neu-induced primary tumor cells. Future assessment of gene expression profiling of Ldb1-null tumors by microarray analysis will help identify deregulated genes that may contribute to the suppression of the lung colonization capability of Neu-transformed Ldb1-null tumor cells. Furthermore, future characterization of the effect of Ldb1-deletion on metastasis might offer therapeutic opportunity to limit the spread of metastatic Neu-induced breast cancers.

7. REFERENCES

1. Agulnick, A. D., M. Taira, J. J. Breen, T. Tanaka et al. 1995. Interactions of the LIM-domain binding factor Ldb1 with LIM homeodomain proteins. *Nature* **384** (6606): 270-2.
2. Al-Zahrani, K. N., K. D. Baron, and L. A. Sabourin. 2013. Ste20-like kinase SLK, at the crossroads: a matter of life and death. *Cell Adh Migr* **7** (1): 1-10.
3. Al-Zahrani, K. N., P. Sekhon, D. R. Tessier, J. Yockell-Lelievre et al. 2014. Essential role for the SLK protein kinase in embryogenesis and placental tissue development. *Dev Dyn* **243** (5): 640-51.
4. Ali, I. U., G. Campbell, R. Lidereau, and R. Callahan. 1988. Lack of evidence for the prognostic significance of c-erbB-2 amplification in human breast carcinoma. *Oncogene Res* **3**: 139-146.
5. Aranda, V., T. Haire, M. E. Nolan et al. 2006. Par6-aPKC uncouples ErbB2 induced disruption of polarized epithelial organization from proliferation control. *Nat Cell Biol* **8** (11): 1235-45.
6. Bach, I., C. Carriere, H. P. Ostendorff, B. Anderson et al. 1997. A family of LIM domain-associated cofactors confer transcriptional synergism between LIM and Otx homeodomain proteins. *Genes Dev* **11** (11): 1370-80.
7. Banin Hirata, B. K., J. M. Oda, R. Losi Guembarovski et al. 2014. Molecular Markers for Breast Cancer: Prediction on Tumor Behavior. *Dis Markers* doi: 10.1155/2014/513158
8. Baron, K.D., K. Al-Zahrani, J. Conway et al. 2015. Recruitment and activation of SLK at the leading edge of migrating cells requires Src family kinase activity and

the LIM-only protein 4. *Biochim Biophys Acta* **1853** (7): 1683-92.

9. Benlimame, N., Q. He, S. Jie, D. Xiao, Y. J. Xu et al. 2005. FAK signaling is critical for ErbB-2/ErbB-3 receptor cooperation for oncogenic transformation and invasion. *J Cell Biol* **171** (3): 505-516.
10. Berger, M. S., G. W. Locher, S. Saurer et al. 1988. Correlation of c-erbB2 gene amplification and protein expression in human breast carcinoma with nodal status and nuclear grading. *Cancer Res* **48**:1238-1243.
11. Bertos, N. R., and M. Park. 2011. Breast cancer- one term, many entities?. *J Clin Invest* **121** (10): 3789-96.
12. Bertucci, F., P. Finetti, and D. Birnbaum. 2012. Basal breast cancer: a complex and deadly molecular subtype. *Curr Mol Med* **12** (1): 96-110.
13. Bouchard, L., L. Lamarre, P. J. Tremblay, and P. Jolicoeur. 1989. Stochastic appearance of mammary tumors in transgenic mice carrying the MMTV/c-neu oncogene. *Cell* **57** (6): 931-6.
14. Breen, J. J., A. D. Agulnick, H. Westphal, and I. B. Dawid. 1998. Interactions between LIM domains and the LIM domain-binding protein Ldb1. *J Biol Chem* **273**: 4712-4717.
15. Carraway, K. L., M. X. Sliwkowski, R. Akita, J. V. Platko et al. 1994. The erbB3 gene product is a receptor for heregulin. *J Biol Chem* **269** (19): 14303-6.
16. Chao, Y. L., C. R. Shepard, and A. Wells. 2010. Breast carcinoma cells re-express E-cadherin during mesenchymal to epithelial reverting transition. *Mol Cancer* 9:179 doi: 10.1186/1476-4598-9-179.
17. Charafe-Jauffret, E., C. Ginestier, F. Iovino et al. 2009. Breast cancer cell lines contain functional cancer stem cells with metastatic capacity and a distinct

molecular signature. *Cancer Res* **69** (4): 1302-13.

18. Cybulsky A. V., T. Takano, J. Papillon, A. Khadir, K. Bijian, C. C. Chien, C. E. Alpers, and H. Rabb. 2004. Renal expression and activity of the germinal center kinase SK2. *Am. J. Physiol. Renal Physiol* **286**: F16–F25.
19. Cybulsky, A. V., T. Takano, J. Guillemette, J. Papillon, R. A. Volpini, and J. A. Di Battista. 2009. The Ste20-like kinase SLK promotes p53 transactivation and apoptosis. *Am J Physiol Renal Physiol* 297 (4): F971-80.
20. Dan, I., N. M. Watanabe, and A. Kusumi. 2001. The Ste20 group kinases as regulators of MAP kinase cascades. *Trends Cell Biol* **11** (5): 220-30.
21. Dankort, D. L., N. Jeyabalan, N. Jones et al. 2001. Multiple ErbB-2/Neu Phosphorylation Sites Mediate Transformation through Distinct Effector Proteins. *J Biol Chem* **276** (42): 38921-8.
22. Dankort, D. L., Z. Wang, V. Blackmore, M. F. Moran, and W. J. Muller. 1997. Distinct tyrosine autophosphorylation sites negatively and positively modulate neu-mediated transformation. *Mol Cell Biol* 17 (9): 5410-25.
23. Dey-Guha, I., M. Mukhopadhyay, M. Phillips, and H. Westphal. 2009. Role of ldb1 in adult intestinal homeostasis. *Int J Biol Sci* **5** (7): 686-94.
24. Falck, V. G., and W. J. Gullick. 1989. *c-erbB-2* oncogene product staining in gastric adenocarcinoma. An immunohistochemical study. *J Pathol* 159: 107-11.
25. Fu, J., L. Qiu, T. He et al. 2011. The TWIST/Mi2/NuRD protein complex and its essential role in cancer metastasis. *Cell Res* **21** (2): 275-89.
26. Fu, J., L. Zhang, T. He, X. Xiao et al. 2012. TWIST represses estrogen receptor-alpha expression by recruiting the NuRD protein complex in breast cancer cells. *Int J Biol Sci* 8 (4): 522-32.

27. Gamallo, C., J. Palacios, A. Suarez et al. 1993. Correlation of E-cadherin expression with differentiation grade and histological type in breast carcinoma. *Am J Pathol* **142** (4): 987-93.

28. Garrett, T.P., N. M. McKern, M. Lou et al. 2003. The crystal structure of a truncated ErbB2 ectodomain reveals an active conformation, poised to interact with other ErbB receptors. *Mol Cell* 11(2): 495-505.

29. Graus-Porta, D., R. R. Beerli, J. M. Daly, and N. E. Hynes. 1997. ErbB-2, the preferred heterodimerization partner of all ErbB receptors, is a mediator of lateral signaling. *EMBO J* 16: 1647–1655.

30. Guilluy, C., M. Rolli-Derkinderen, L. Loufrani, A. Bourge et al. 2008. Ste20-Related Kinase SLK Phosphorylates Ser188 of RhoA to Induce Vasodilation in Response to Angiotensin II Type 2 Receptor Activation. *Circ Res* **102** (10): 1265-74.

31. Guo, W., and F. G. Giancotti. 2004. Integrin signalling during tumour progression. *Nat Rev Mol Cell Biol* 5 (10): 816-26.

32. Guy, C. T., M. A. Webster, M. Schaller, T. J. Parsons, R. D. Cardiff, and W. J. Muller. 1992. Expression of the neu protooncogene in the mammary epithelium of transgenic mice induces metastatic disease. *Proc Natl Acad Sci USA* 89 (22): 10578-82.

33. Hao, W., T. Takano, J. Guillemette, J. Papillon, G. Ren, and A. V. Cybulsky. 2006. Induction of apoptosis by the Ste20-like kinase SLK, a germinal center kinase that activates apoptosis signal-regulating kinase and p38. *J Biol Chem* **281** (6): 3075-84.

34. Holbro, T., R. R. Beerli, F. Maurer, M. Koziczak et al. 2003. The ErbB2/ErbB3 heterodimer functions as an oncogenic unit: ErbB2 requires ErbB3 to drive breast tumor cell proliferation. *PNAS* 100 (15): 8933-8938.

35. Huck, L., S. M. Pontier, D. M. Zuo and W. J. Muller. 2010. β1-integrin is dispensable for the induction of ErbB2 mammary tumors but plays a critical role in the metastatic phase of tumor progression. *Proc Natl Acad Sci USA* 107 (35): 15559-15564.

36. Itoh, S., Y. Kameda, E. Yamada, K. Tsujikawa et al (1997). Molecular cloning and characterization of a novel putative STE20-like kinase in guinea pigs. *Arch Biochem Biophys* 340 (2): 201-7.

37. Jeschke, U., I. Mylonas, C. Kuhn, N. Shabani et al. 2007. Expression of E-cadherin in human ductal breast cancer carcinoma in situ, invasive carcinomas, their lymph node metastases, their distant metastases, carcinomas with recurrence and in recurrence. *Anticancer Res* 27 (4A): 1969-74.

38. Jiang, W. G., and R. E. Mansel. 2000. E-cadherin complex and its abnormalities in human breast cancer. *Surg Oncol* **9** (4): 151-71.

39. Johnsen, S. A. C. Gungor, T. Prenzel et al. 2009. Regulation of estrogen-dependent transcription by the LIM cofactors CLIM and RLIM in breast cancer. *Cancer Res* **69** (1): 128-36.

40. Jurata, L. W., and G. N. Gill. 1997. Functional analysis of the nuclear LIM domain interactor. NLI. *Mol Cell Biol* **17**: 5688-5698.

41. Jurata, L. W., D. A. Kenny, and G. N. Gill. 1996. Nuclear LIM interactor, a rhombotin and LIM homeodomain interacting protein, is expressed early in neuronal development. *Proc Natl Acad Sci USA* 93 (21): 11693-8.

42. Jurata, L. W., S. L. Pfaff, and G. N. Gill. 1998. The nuclear LIM domain interactor NLI mediates homo- and heterodimerization of LIM domain transcription factors. *J Biol Chem* 273 (6): 3152-7.

43. Kallioniemi, O. P., A. Kallioniemi, W. Kurisu et al. 1992. ERBB2 amplification in breast cancer analyzed by fluorescence in situ hybridization. *Proc Natl Acad Sci U S A* **89**:5321–5325.

44. Kimberly, A. H. 2012. Molecular Pathology of Breast Cancer. What a Pathologist Needs to Know. *Am J Clin Pathol* **138** (6): 770-80.

45. King, C. R., M. H. Kraus, and S. A. Aaronson. 1985. Amplification of a novel v-erbB-related gene in a human mammary carcinoma. *Science* 229 (4717): 974-6.

46. Lemoine, N. R., S. Staddon, C. Dickson, D. M. Barnes, and W. J. Gullick. 1990. Absence of activating transmembrane mutations in the c-erbB-2 proto-oncogene in human breast cancer. *Oncogene* 5 (2): 237-9.

47. Liu, H., M. R. Patel, J. A. Prescher, A. Patsialou et al. 2010. Cancer stem cells from human breast tumors are involved in spontaneous metastases in orthotopic mouse models. *Proc Natl Acad Sci USA* 107 (42): 18115-20.

48. Lohrisch, C., and M. Piccart. 2001. An overview of HER2. *Semin Oncol* 28:3–11

49. Luhovy, A. Y., A. Jaberi, J. Papillon, J. Guillemette, and A. V. Cybulsky. 2012. Regulation of the Ste20-like kinase, SLK: involvement of activation segment phosphorylation. *J Biol Chem* 287 (8): 5446-58.

50. Madhavan, M., P. Srinivas, E. Abraham et al. 2001. Cadherins as predictive markers of nodal metastasis in breast cancer. *Mod Pathol* **14** (5): 423-7.

51. Malhotra, G. K., X Zhao, H. Band, and V. Band. 2010. Histological, molecular and functional subtypes of breast cancers. *Cancer Biol Ther* 10 (10): 955-60.

52. Mareel, M., Bracke, M., and F. Van Roy (1994). Invasion promoter versus invasion suppressor molecules: the paradigm of E-cadherin. *Mol Biol Rep* 19: 45-67.

53. Matsuura K., J. Kawanishi, S. Fujii, M. Imamura et al. 1992. Altered expression of E-cadherin in gastric cancer tissues and carcinomatous fluid. *Br J Cancer* 66 (6): 1122-30

54. Mironchik, Y., P. T. Winnard, F. Vesuna et al. 2005. Twist overexpression induces in vivo angiogenesis and correlates with chromosomal instability in breast cancer. *Cancer Res* **65** (23): 10801-9.

55. Mizunuma, H., J. Miyazawa, K. Sanada, and K. Imai. 2003. "The LIM-only protein, LMO4, and the LIM domain-binding protein, LDB1, expression in squamous cell carcinomas of the oral cavity". *Br J Cancer* 88 (10): 1543-8.

56. Moasser, M.M. 2007. The oncogene HER2: its signaling and transforming functions and its role in human cancer pathogenesis. *Oncogene* **26** (45): 6469-87.

57. Mukhopadhyay, M., A. Teufel, T. Yamashita, A. D. Agulnick et al. 2003. Functional ablation of the mouse Ldb1 gene results in severe patterning defects during gastrulation. *Development* 130 (3): 495-505.

58. Muller, W. J., E. Sinn, P. K. Pattengale, R. Wallace, and P. Leder. 1988. Single-step induction of mammary adenocarcinoma in transgenic mice bearing the activated c-neu oncogene. *Cell* 54 (1): 105-15.

59. Nass, S.J., J. G. Herman, E. Gabrielson, P. W. Iversen, F. F. Parl, N. E. Davidson, and J.R. Graff. 2000. Aberrant methylation of the estrogen receptor and E-cadherin 5'CpG islands increases with malignant progression in breast cancer. *Cancer Res* 60: 4346-8.

60. Nieman, M. T., R. S. Prudoff, K. R. Johnson, and M. J. Wheelock. 1999. N-cadherin promotes motility in human breast cancer cells regardless of their E-cadherin expression. *J Cell Biol* 147 (3): 631-44.

61. O'Reilly, P. G., S. Wagner, D. J. Franks, K. Cailliau et al. 2005. The Ste20-like kinase SLK is required for cell cycle progression through G2. *J Biol Chem* **280**: 42383–42390.

62. Oka, H., H. Shiozaki, K. Kobayashi et al. 1993. Expression of E-cadherin cell adhesion molecules in human breast cancer tissues and its relationship to metastasis. *Cancer Res* **53** (7): 1696-701.

63. Oka, H., H. Shiozaki, K. Kobayashi, H. Tahara et al. 1992. Immunohistochemical evaluation of E-cadherin adhesion molecule expression in human gastric cancer. *Virchows Arch A Pathol Anat Histopathol* 421 (2): 149-56

64. Otten, A. D., M. M. Sanders, and G. S. McKnight. 1988. The MMTV LTR promoter is induced by progesterone and dihydrotestosterone but not by estrogen. *Mol Endocrinol* 2 (2): 143-7.

65. Pytowski, B., D. J. Hicklin, G. Kornhaber, D. V. Dellaratta, and L. Witte. 1998. Identification and initial characterization of mSLK, a murine member of the STE20 family of kinases. *Arch Biochem Biophys* **359** (2): 310-9.

66. Quizi, J. L., K. Baron, K. N. Al-Zahrani, P. O'Reilly et al. 2013. SLK-mediated phosphorylation of paxillin is required for focal adhesion turnover and cell migration. *Oncogene* **32** (39): 4656-63.

67. Roovers, K., S. Wagner, C. J. Storbeck, P. O'Reilly et al. 2009. The Ste20-like kinase SLK is required for ErbB2-driven breast cancer cell motility. *Oncogene* **28**: 2839-2848.

68. Roskoski, J. R. 2014. The ErbB/HER family of protein-tyrosine kinases and cancer. *Pharmacol Res* **79**: 34-74.

69. Sabourin, L. A., and M. A. Rudnicki. 1999. Induction of apoptosis by SLK, a ste20-related kinase. *Oncogene* **18** (52): 7566-7575.

70. Sabourin, L. A., K. Tamai, P. Seale, J. Wagner, and M. A. Rudnicki. 2000. Caspase 3 cleavage of the ste20-Related kinase SLK releases and activates an apoptosis-inducing kinase domain and an actin-dissembling region. *Mol Cell Biol* 20 (2): 684-96.

71. Salmans, M. L., Z. Yu, K. Watanabe, E. Cam et al. 2014. The Co-factor of LIM Domains (CLIM/LDB/NLI) Maintains Basal Mammary Epithelial Stem Cells and Promotes Breast Tumorigenesis. *Plos Genet* **10** (7): e1004520. doi: 10.1371/journal.pgen.

72. Schade, B., R. Lesurf, V. Sanguin-Gendreau, T. Bui et al. 2013. β-Catenin Signaling Is a Critical Event in ErbB2-Mediated Mammary Tumor Progression. *Cancer Res* **73** (14): 4474-87.

73. Schipper, J. H., U. H. Frixen, J. Behrens et al. 1991. E-cadherin expression in squamous cell carcinomas of head and neck: inverse correlation with tumor dedifferentiation and lymph node metastasis. *Cancer Res* **51** (23 Pt 1): 6328-37.

74. Sells, M. A., and J. Chernoff. 1997. Emerging from the Pak: the p21-activated protein kinase family. *Trends Cell Biol* **7**: 162-7.

75. Shih, C., L. C. Padhy, M. Murray, and R. A. Weinberg. 1981. Transforming genes of carcinomas and neuroblastomas introduced into mouse fibroblasts. *Nature* 290 (5803): 261-4.

76. Siegel, P M., D. L. Dankort, W. R. Hardy, and W. L. Muller. 1994. Novel activating mutations in the neu proto-oncogene involved in induction of mammary tumors. *Mol Cell Biol* **14** (11): 7068-77.

77. Siegel, P. M., and W. J. Muller. 1996. Mutations affecting conserved cysteine residues within the extracellular domain of Neu promote receptor dimerization and activation. *Proc Natl Acad Sci U S A* 93 (17): 8878-83.

78. Siegel, P. M., E. D. Ryan, R. D. Cardiff, and W. J. Muller. 1999. Elevated expression of activated forms of Neu/ErbB-2 and ErbB-3 are involved in the induction of mammary tumors in transgenic mice: implications for human breast cancer. *EMBO J* **18** (8): 2149-64.

79. Slamon, D. J., W. Godolphin, L. A. Jones et al. 1989. Studies of the HER2/neu proto-oncogene in human breast and ovarian cancer. *Science* 244: 707-12.

80. Song, S. H., C. Hou, and A. Dean. 2007. A positive role for NLI/Ldb1 in long-range beta-globin locus control region function. *Mol Cell* 28 (5): 810-22.

81. Sotiriou, C., and L. Pusztai. 2009. Gene-expression signatures in breast cancer. *N Engl J Med* 360(8): 790-800.

82. Spurr, N. K., E. Solomon, M. Jansson, D. Sheer et al. 1984. Chromosomal localization of the human homologues to the oncogenes erbA and B. *EMBO J* **3**: 159-163.

83. Stenman, G., J. Sandros, A. Nordkvist et al. 1991. Expression of the ERBB2 protein in benign and malignant salivary gland tumors. *Genes Chromosomes Cancer* 3 (2): 128-135.

84. Taira, M., M. Jamrich, P.J. Good, and I.B. Dawid. 1992. The LIM domain-containing homeobox gene Xlim-1 is expressed specifically in the organizer

region of Xenopus gastrula embryos. *Genes & Dev* 6: 356-366.

85. Teufel, A., T. Maass, S. Strand, S. Kanzler et al. 2010. Liver-specific Ldb1 deletion results in enhanced liver cancer development. *J Hepatol* 53 (6): 1078-84.
86. Torre, L. A., F. Bray, R. L. Siegel, J. Ferlay et al. 2012. Global Cancer Statistics. *CA Cancer J Clin* 65: 87-108.
87. Tzahar, E., H. Waterman, H., X. Chen, G. Levkowitz et al. 1996. A hierarchical network of interreceptor interactions determines signal transduction by Neu differentiation factor/neuregulin and epidermal growth factor. *Mol ell Biol* 16 (10): 5276-87.
88. Umbas, R., J. A. Schalken, T. W. Aalders et al. 1992. Expression of the cellular adhesion molecule E-cadherin is reduced or absent in high-grade prostate cancer. *Cancer Res* **52** (18): 5104-9.
89. Ursini-Siegel, J., B. Schade, R. D. Cardiff, and W. J. Muller. 2007. Insights from transgenic mouse models of ERBB2-induced breast cancer. *Nat Rev Cancer* **7** (5): 389-97.
90. Ursini-Siegel, J., W. R. Hardy, D. Zuo, S. H. Lam, V. Sanguin-Gendreau et al. 2008. ShcA signalling is essential for tumour progression in mouse models of human breast cancer. *EMBO J* 27 (6): 910-20.
91. Vallejos, C. S., H. L. Gomez, W. R. Cruz et al. 2010. Breast cancer classification according to immunohistochemistry markers: subtypes and association with clinicopathologic variables in a peruvian hospital database. *Clin Breast Cancer* **10** (4): 294-300.
92. Van Meyel, D. J., J. B. Thomas, and A. D. Agulnick. 2003. Ssdp proteins bind to LIM-interacting co-factors and regulate the activity of LIM-homeodomain protein

complexes in vivo. *Development* 130 (9): 1915-25.

93. Velasco-Velazquez, M. A., V. M. Popov, M. P. Lisanti et al. 2011. The role of breast cancer stem cells in metastasis and therapeutic implications. *Am J Pathol* 179 (1): 2-11.
94. Venter, D.J., N. L. Tuzi, S. Kumar, and W. J. Gullick. 1987. Overexpression of the c-erbB-2 oncoprotein in human breast carcinomas: immunohistological assessment correlates with gene amplification. Lancet **2**:69–72.
95. Vesuna, F., P. Van Diest, J. H. Chen, and V. Raman. 2007. Twist is a transcriptional repressor of *E-cadherin* gene expression in breast cancer. *Biochem Biophys Res Commun* 367 (2): 235-41.
96. Visvader, J. E., D. Venter, K. Hahm, M. Santamaria et al. 2001. The LIM domain gene LMO4 inhibits differentiation of mammary epithelial cells in vitro and is overexpressed in breast cancer. *Proc Natl Acad Sci USA* 98 (25): 14452-7.
97. Visvader, J. E., X. Mao, Y. Fujiwara, K. Hahm, and S. H. Orkin. 1997. The LIM-domain binding protein Ldb1 and its partner LMO2 act as negative regulators of erythroid differentiation. *Proc Natl Acad Sci U S A* **94** (25): 13707-12.
98. Wagner, K. U., K. McAllister, T. Ward, B. Davis, R. Wiseman, and L. Hennighausen. 2001. Spatial and temporal expression of the Cre gene under the control of the MMTV-LTR in different lines of transgenic mice. *Transgenic Research* 10: 545-553.
99. Wagner, M. J., M. M. Stacey, B. A. Liu and T. Pawson. 2013. Molecular Mechanisms of SH2- and PTB- Domain-Containing Proteins in Receptor Tyrosine Kinase Signaling. *Cold Spring Harb Perspect Biol* **5** (12): a008987. doi: 10.1101/cshperspect.a008987.

100. Wagner, S., C. J. Storbeck, K. Roovers, Z. Y. Chaar et al. 2008. FAK/src-family dependent activation of the Ste20-like kinase SLK is required for microtubule-dependent focal adhesion turnover and cell migration. *PloS One* **3** (4): e1868. doi: 10.1371/journal.pone.0001868.

101. Wagner, S., T. A. Flood, P. O'Reilly, K. Hume, and L. A. Sabourin. 2002. Association of the Ste20-like kinase (SLK) with the microtubule. Role in Rac1-mediated regulation of actin dynamics during cell adhesion and spreading. *J Biol Chem* 277 (40): 37685-92.

102. Wallasch, C., F. U. Weiss, G. Niederfellner et al. 1995. Heregulin-dependent regulation of HER2/neu oncogenic signaling by heterodimerization with HER3. *EMBO J* 14 (17): 4267-75.

103. Wang, N., K. K. Lin, Z. Lu, K. S. Lam et al. 2007. The LIM-only factor LMO4 regulates expression of the BMP7 gene through an HDAC2-dependent mechanism, and controls cell proliferation and apoptosis of mammary epithelial cells. *Oncogene* 26 (44): 6431-41.

104. Xu, X., J. Mannik, E. Kudryavtseva et al. 2007. Co-factors of LIM domains (Clims/Ldb/Nli) regulate corneal homeostasis and maintenance of hair follicle stem cells. *Dev Biol* **312**:484–500

105. Xu, Z., S. Huang, L. Chang, A. D. Agulnick, and S. J. Brandt. 2003. Identification of a TAL1 Target Gene Reveals a Positive Role for the LIM Domain-Binding Protein Ldb1 in Erythroid Gene Expression and Differentiation. *Mol Cell Biol* 23 (21): 7585-7599.

106. Yarden, Y. 2001. Biology of HER2 and its importance in breast cancer. *Oncology* 61 (2): 1-13.

107. Yarden, Y. and M.X. Sliwkowski. 2001. Untangling the ErbB signalling network. *Nat Rev Mol Cell Biol* 2 (2): 127-37.

108. Zhang, F., B. Tanasa, D. Merkurjev, C. Lin et al. 2015. Enhancer-bound LDB1 regulates a corticotrope promoter-pausing repression program. *Proc Natl Acad Sci USA* 112 (5): 1380-5.

109. Zhang, Y. H., K. Hume, R. Cadonic, C. Thompson et al. 2002. Expression of the Ste20-like kinase SLK during embryonic development and in the murine adult central nervous system. *Brain Res Dev Brain Res* 139 (2): 205-15.

110. Zhao, Y., K. M. Kwan, C. M. Mailloux, W. K. Lee, A. Grinberg et al. 2007. LIM-homeodomain proteins Lhx1 and Lhx5, and their cofactor Ldb1, control Purkinje cell differentiation in the developing cerebellum. *Proc Natl Acad Sci USA* 104 (32): 13182-6.